The influence of fixation and cryopreservation of cerebrospinal fluid on antigen expression and cell percentages by flow cytometric analysis

by

Gabriela Singh

SNGGAB002

SUBMITTED TO THE UNIVERSITY OF CAPE TOWN

In fulfilment of the requirements for the degree

MSc (Med) in Neuroscience

Supervisor:

Dr Ursula Rohlwink

Department of Surgery

Faculty of Health Science

University of Cape Town

December 2021

DECLARATION

I, Gabriela Singh, hereby declare that the work on which this dissertation is based is my original work (except where acknowledgements indicate otherwise) and that neither the whole work nor any part of it has been, is being, or is to be submitted for another degree in this or any other university.

I empower the university to reproduce for the purpose of research either the whole or any portion of the contents in any manner whatsoever.

Signature: Signed by candidate

Date: _____09/12/2021_____

ACKNOWLEDGEMENTS

To my supervisor, Dr Ursula Rohlwink, your passion for neuroscience and your research is an inspiration- you have set the example of the kind of scientist I aspire to be. Thank you for your mentorship and support in my development as a young researcher over the years, I wish every student could have a supervisor as amazing as you.

I would like to acknowledge Prof Figaji, as Head of Paediatric Neurosurgery and our research enterprise at Red Cross War Memorial Children's Hospital. Thank you to all the neurosurgeons for assisting in the timely collection of these samples, which was ultimately the most important aspect of this study. Your efforts and all the hard work that you do "behind the scenes" are much appreciated.

To Rozanne Adams, thank you for passing on your knowledge of flow cytometry and for being patient and kind during my training.

To Dr Arjan van Laarhoven, Dr Catherine Riou, Dr Tim Reid, Dr Jill Combrinck, and members of the Francis Crick Flow cytometry STP, thank you all for your input and advice throughout this study.

To my parents, your unconditional support has made this journey possible. Mom, thank you for always believing in me and reassuring me on my days of doubt. Your influence has moulded me into the person I am today. I love you.

A special thanks to Claudia and Heidi, even from afar you both have offered endless support. I appreciate you.

The financial assistance of the National Research Foundation (NRF) towards this research is hereby acknowledged. Opinions expressed and conclusions arrived at, are those of the author and are not necessarily to be attributed to the NRF.

ABSTRACT

Introduction: Infections of the central nervous system (CNS) remain a major burden of disease. Cerebrospinal fluid (CSF) is an essential sample for the investigation of CNS pathologies and flow cytometry enables detailed immunophenotyping of cells present in CSF. However, the pauci-cellular nature of CSF, and the rapid cell death following sampling, incumbers the use of flow cytometric analysis of these samples. Immediate processing and analysis of CSF for flow cytometry is not feasible in busy clinical environments where sample collection is unpredictable, and flow cytometers are not readily available. Therefore, developing a method to easily store CSF samples is highly desirable for clinically relevant research on CNS pathologies. Thus, the objective of this study was to examine 2 methods of long-term storage of CSF samples which ensured reliable measurement of cell percentages and relative proportion of cell subsets using flow cytometry.

Aims: To examine percentages and relative proportion of subsets of selected peripheral leukocytes and brain derived cells in 1) cryopreserved CSF in comparison to freshly processed CSF, and 2) Transfix-treated CSF in comparison to freshly processed CSF.

Method: CSF samples were prospectively collected and processed as follows 1) Fresh- within 24 hours (the current gold standard); 2) Cryopreserved- analysed after 1 month storage at -80°C; 3) Transfix- analysed after 2 week storage at 2-8°C. Percentages of numerous white blood cell populations and brain-derived immune cells were analysed using flow cytometry and compared across these methods. The median fluorescent intensity of select markers was also compared across these methods.

Results: The majority of cell percentages were not statistically significantly different between Fresh and Cryopreserved CSF, and cell proportions were comparable. Conversely, loss of marker expression of various lymphocyte sub-populations was observed in Transfix-treated CSF compared to Fresh, and certain cell populations could not be clearly distinguished in Transfix-treated CSF.

Conclusion: Cryopreservation is a feasible option for long-term storage of CSF and allows quantification of cell percentages and immunophenotyping of peripheral and brain-derived cell populations by flow cytometry. This offers valuable opportunities for clinical research across a broad spectrum of CNS conditions (infectious and non-infectious). Further, this work highlights the potential to cryopreserve other surgical specimens for which the application of flow cytometry is currently limited by resource constraints and low cell counts.

TABLE OF CONTENTS

LIST OF TABLES

LIST OF FIGURES

LIST OF ABBREVIATIONS

APC	Allophycocyanin
APC-H7	Allophycocyanin hillite 7
BB	Brilliant blue
BBB	Blood brain barrier
BD	Becton Dickinson
BV	Brilliant violet
CD	Cluster of differentiation
CI	Confidence interval
CMI	Cell-mediated immunity
CT	Computed tomography
DC	Dendritic cells
DMSO	Dimethyl sulfoxide
EDTA	Ethylenediaminetetraacetic acid
EVD	External ventricular drain
FBS	Foetal bovine serum
FCS	Foetal calf serum
FSC	Forward scatter
GFAP	Glial fibrillary acidic protein
HIV	Human immunodeficiency virus
HLA	Human leukocyte antigen
HREC	Human resources ethics committee
IFN	Interferon
LOA	Limits of agreement
MAIT	Mucosal associated invariant T cells
MFI	Median fluorescent intensity
MHC	Major histocompatibility complex
MMP	Matrix metalloproteinase
NET	Neutrophil extracellular trap
NHLS	National Health Laboratory service
NK	Natural killer
NKT	Natural killer T cells
NO	Nitric oxide
NSE	Neuron-specific enolase
PAMP	Pathogen-associated molecular pattern
PBMC	Peripheral blood mononuclear cell
PBS	Phosphate buffered saline
PE	Phycoerythrin
PMT	Photomultiplier tube
PRR	Pathogen recognition receptors
RCWMCH	Red Cross War Memorial Children's
ROS	Reactive oxygen species
RPMI	Roswell Park Memorial Institute

SD	Standard deviation
SSC	Side scatter
TB	Tuberculosis
TBM	Tuberculous meningitis
TCR	T cell receptor
TH	T helper
TLR	Toll like receptor
TMEM	Transmembrane protein
TNF	Tumour necrosis factor
USA	United States of America
VPS	Ventriculoperitoneal shunt
WBC	White blood cell

CHAPTER 1: INTRODUCTION

The analysis of inflammatory mediators within cerebrospinal fluid (CSF) can provide valuable information pertaining to ongoing disease processes in central nervous system (CNS) conditions[1, 2]. This remains increasingly important for developing countries faced with a high disease burden of CNS infections, which in most instances, predominantly affect vulnerable populations such as young children, and are accompanied by high morbidity and mortality rates[3-5]. Immunophenotypic characterisation of CSF by flow cytometry has become a popular technique for the study of neurological and other neuro-inflammatory conditions[6-9]. Unfortunately, CSF samples have low cellularity and are prone to rapid cellular degradation *ex vivo*, all of which is not ideal for flow cytometric analysis[10]. It is therefore recommended to immediately process CSF samples intended for flow cytometric analysis; however, this is often impractical and logistically challenging for many institutions. Currently, cell stabilizing reagents are used to prolong cell viability in CSF, showing promising results as options for short-term storage of CSF samples. Great advances have been made in developing long-term preservation protocols for specimens including whole blood[11], stem cells[12], embryos[13], and hepatocytes[14]. However, similar advances have not been matched for CSF samples.

This thesis will highlight the burden of CNS infections, discuss the role of immune cells in the defence against them; and finally, summarize the challenges associated with flow cytometric analysis of CSF samples and potential solutions to this problem. Thereafter, the data of this project examining 2 methods of long-term CSF storage for flow cytometric analysis are presented.

CHAPTER 2: CENTRAL NERVOUS SYSTEM INFECTIONS

1. Background

Infections of the CNS pose a unique clinical challenge given the various disease entities, heterogenous and non-specific presentation, and the different CNS compartments that are affected[15, 16]. These compartments include the ventricles, meninges, brain matter and spinal cord; and infections may be of viral, bacterial, parasitic, or fungal aetiology[5]. The long-term complications of CNS infections include neurobehavioral disorders, neurological deficits, and cognitive impairments[17], and the long term implications of these outcomes is particularly troubling in children. The associated high morbidity and mortality rates emphasize the need for rapid diagnosis and improved treatment strategies[16]. CNS infections in developing countries have been relatively neglected, which is paradoxical seeing as the disease prevalence is greatest in these regions[3]. This chapter highlights the high disease burden of CNS infections by briefly describing a selection of CNS infections that occur commonly, particularly in the developing world.

Bacterial infections: Tuberculous meningitis (TBM) is the most severe manifestation of extrapulmonary tuberculosis (TB) disease and is predominantly reported in developing countries in which TB is endemic[18]. Studies investigating the incidence rates of TBM in the Western Cape, South Africa, reported TBM to be the commonest cause of meningitis occurring largely in young children with more than 60% of cases under the age of 5 years and 25.2% under the age of 1 year[19, 20]. Primary infection in the lung precedes TBM and the progression of the disease and clinical manifestation thereof differ in children compared to adults[21]. The high rate of extra-pulmonary dissemination is observed more frequently in children than in adults, with peak incidences of TBM occurring between the ages of two and four years[22]. Moreover, individuals with human immunodeficiency virus (HIV) are also a vulnerable group predisposed to higher rates of TB dissemination, particularly TBM, and higher fatality rates during co-infection[18]. Despite great advances that have been made to understand the pathogenesis of TBM, relevant clinical and scientific challenges remain. For instance, TBM poses a challenge both diagnostically and in terms of patient management. The non-specific presentation of clinical symptoms often leads to a delay in diagnosis, a consequent delay in treatment, and increased risk of poor outcome[23]. Despite adequate anti-mycobacterial drugs, mortality rates remain high and the majority of those affected suffer long-term neurological sequelae[24, 25]. The pathological and injury cascades that lead to poor

outcome are a consequence of the dysregulated immune response[2]. A characteristic clinical feature of TBM is the presence of inflammatory exudate in the basal cisterns and ventricles. Consequently, this causes vascular pathology which may further lead to the development of infarcts; hydrocephalus, by obstructing the flow of CSF; and cranial nerve palsies through compression of cranial nerves in the vicinity[26]. However, much still remains unknown regarding the local immune response occurring in the brain as well as vulnerabilities in the systemic response which enables dissemination in young children.

Healthcare-acquired infections: Shunt infections are one of the major complications associated with surgical interventions used for the treatment of hydrocephalus and can manifest in ventriculitis. Ventriculoperitoneal shunts (VPS) are permanent catheters that are used for CSF diversion from the ventricles to the peritoneal cavity[1, 27], whereas external ventricular drains (EVDs) temporarily divert CSF from the ventricles to an external bag at the bedside[1]. Despite being an effective means at resolving excessive accumulation of CSF in the brain, the invasiveness of these neurosurgical procedures expose the brain to various microorganisms that are either situated within the operative environment or colonize the skin of the scalp, consequently resulting in infection[1]. Microorganisms from the *Staphylococcus* genus are reported to be the major contributors of infection with *Staphylococcus aureus* causing 10-30% of infections, whereas *Staphylococcus epidermis* causes over 50% of infections[1]. Briefly, these organisms form biofilms, a structure composed of thick polysaccharide layers and several cellular constituents, on the surface of catheters. Following the formation of a biofilm, an optimal niche is created wherein the bacteria can proliferate and eventually detach in order to perpetuate the spread of infection[27, 28]. Shunt infection incidence rates vary worldwide, with rates of 4.1-17.4% reported in the United States, whereas developing countries such as Saudi Arabia had incidence rates of 32%[29]. Significantly higher rates are reported in neonates and infants, with pre-term neonates and infants with low birth weights identified as a vulnerable group for high risk of shunt infection and adverse complications[27, 28]. Furthermore, this particular subgroup of young patients are prone to recurring infections, require multiple revisions, and have higher mortality rates[27]. The varying clinical symptoms of shunt infections often leads to a delay in diagnosis and subsequently a delay in treatment. The role of the peripheral immune response against biofilm infection has been well established; however, there is a paucity of data on the local immune response occurring in the CNS. Given the neurological disabilities (>20% incidence

rates of seizures) associated with shunt infections[30, 31], understanding the underlying pathogenesis and the contribution of the neuroimmune response is of great necessity[27, 28].

Fungal infections: Fungal infections of the CNS are caused by a broad spectrum of microorganisms originating from the *Blastomyces species*, known to infect immunocompetent hosts, and the *Candida* and *Cryptococcal species* which cause opportunistic infections in immune-compromised individuals[32]. Fungal infections of the CNS resulting from the *Candida* species are a cause of significant morbidity and mortality among children with hematologic malignancy[33]. Whereas the *Cryptococcal species* have significantly contributed to the mortality rates of individuals with AIDS, with more than 500 000 patients per year succumbing to cryptococcal meningitis in Sub-Saharan Africa[34]. Initial entry of these pathogens occurs through the respiratory tract, followed by haematogenous spread to the CNS[1]. Several studies have shown that certain mycotoxins produced by fungi exhibit immunosuppressive functions, inhibit phagocytosis, and cause significant damage to microglia (resident immune cells in the brain) resulting in axonal demyelination[35-38]. Timely diagnosis of fungal infections remains a challenge as clinical presentation is non-specific, and patients are often asymptomatic during the early stages of infection[39]. The use of molecular imaging (e.g., antibody targeted against specific receptors) instead of computed tomography (CT) scans, may enhance the sensitivity and specificity of diagnostic imaging[40].

Viral infections: Incidences of viral CNS infections per year are far greater (20-30/100.000 per year) compared to the aforementioned infections, signifying a significant public health burden worldwide[41, 42]. The vast number of neurotropic viruses, viral tropism, the different ways in which the CNS barriers are exploited, and the broad geographic range, enhance the complexity of this particular group of infections[41]. For instance, viral encephalitis signifies a medical crisis given its expansive geographic locations, with herpes simplex encephalitis being the most common form of viral encephalitis found worldwide, whereas Japanese encephalitis virus, West Nile virus, and Dengue virus predominate in the tropics and Asian continent[1]. A characteristic feature of viral CNS infections is the rapid onset of neuro-inflammation which consequently causes severe brain damage and may even result in death[43]. Immuno-compromised individuals and young children are groups that are particularly vulnerable to viral CNS infections[44]. The need for improved vaccine development, given the emergence of new viruses, is ever-growing.

Parasitic infections: Parasitic CNS infections are a major health burden in developing countries. Of the estimated 500 million cases of *Plasmodium falciparum* infection recorded in 2002, more than 70% of these cases were reported in sub-Saharan Africa[45]. The pleomorphic nature as well as the numerous pathological lesions triggered by these microorganisms gives rise to unpredictable host-immune responses[1]. *Plasmodium falciparum* is the leading cause of cerebral malaria which is the most severe complication of human malaria parasite infection[1, 3]. It is predominantly reported on the African continent in malaria-endemic countries, particularly among young children, with an incidence of 1-12 cases/1 000 children per year[46]. In a large cohort of Kenyan adolescents, mortality rates were reported to exceed 20%[47]. The exact mechanism(s) leading to the development of cerebral malaria and why certain individuals are more prone to CNS invasion, have yet to be elucidated[3].

The current treatment strategies for most CNS infections are targeted against the pathogen itself; however, directing focus towards understanding host immunity better, and subsequent investigation into the interactions between the host-immune response and the pathogen are necessary given that immunopathology is an inherent property of CNS infections.

CHAPTER 3: IMMUNE RESPONSE TO CNS INFECTIONS

Although once perceived as an immune-privileged site, the CNS is capable of initiating immune responses through resident immune cells, such as microglia and astrocytes, in conjunction with infiltrating cells from the periphery[48, 49]. Neuro-inflammation is inherent in all CNS infections and can perpetuate damage[48, 49]. Post-infection neurological sequela are common and may be as a consequence of the invading pathogen or the host inflammatory response[50]. Both innate and adaptive immune responses play significant roles during the acute phase of neuro-infection as well as contributing to the neurological damage during infection[50]. Table 1 summarises the characteristics of both peripheral- and resident immune cells of the CNS.

Table 1: Summary of peripheral- and brain derived immune cell characteristics

Peripheral immune cells	Cell Characteristics	Cell surface receptor characteristics
NK cells	Comprise >10% of circulating leukocytes; defined by CD56 marker expression. Capable of cell lysis and early production of cytokines & chemokines[51].	CD56 serves as a pathogen recognition receptor during innate immune response[52].
Neutrophils	Most abundant leukocyte; commonly defined by CD16 marker expression. Capable of phagocytosis[53].	CD16 forms part of the immunoglobulin superfamily and participates in antibody-dependent cellular cytotoxicity[54]
Monocytes	Comprise ±10% of circulating leukocytes; defined and differentiated by CD14 and CD16 marker expression. Produce cytokines & possess phagocytic functions[55].	CD14 also serves as a pathogen recognition receptor capable of recognizing bacterial lipopolysaccharide[56]
$CD4^+$ T-cells	Provides essential support for cytotoxic cells and antibody-mediated responses; capable of differentiating into various subsets[57] .	CD4 is a glycoprotein and assists TCR in communicating with antigen presenting cells[58]
$CD8^+$ T-cells	Cytotoxic cells; also capable of differentiating into different subsets with both effector and memory properties[59].	CD8 is a transmembrane glycoprotein and participates in T cell signalling[60]
γδ T-cells	Important for mucosal immunity; mostly found in tissues[61].	γδ receptors are capable of recognizing pathogens in the absence of antigen recognition or the need for antigen-presenting cells[62]
MAIT cells	Highly abundant in liver & mucosal surfaces; defined by co-expression of CD161 & Vα7.2 markers. Capable of producing copious amounts of TNF-α & IFN-γ[9, 54].	CD161 is a C-type lectin-like receptor and can act as a co-stimulatory receptor. Vα7.2 is an evolutionary conserved invariant TCR α-chain[63]
Brain derived immune cells	**Characteristics**	
Microglia	Comprise approximately 10% of resident cells in CNS; broadly defined by co-expression of $CD45^+$ & $CD11b^+$. Promote synaptic remodelling and angiogenesis, can also secrete pro-inflammatory cytokines[64].	CD45 is a type I transmembrane protein and important for T- and B-cell receptor signalling. CD11b is an integrin family member and regulates leukocyte adhesion[65,66]
Astrocytes	Most abundant cell type in the brain;	GFAP is a type III

	expression of GFAP defines astrocyte activation. Involved in synaptogenesis and BBB maintenance[67].	intermediate filament protein[68]

Abbreviations: BBB, blood brain barrier; CD, cluster of differentiation; CNS, central nervous system; GFAP, glial fibrillary acidic protein; MAIT, mucosal associated invariant T cell; NK, natural killer; TCR, T-cell receptor; TNF- α, tumour necrosis factor- α; IFN- γ, interferon- γ.

1. Neuro-immune response

Microglia are the resident immune cells of the brain which play an important role in regulating neuro-inflammation[69, 70]. They respond to local signals in the brain and receive signals from the periphery, establishing a well-controlled bi-directional system[69]. Possessing a vast repertoire of receptors including pathogen recognition receptors (PRRs), scavenger receptors and members of the toll-like receptors (TLRs), microglia can recognize a wide array of infectious pathogens, stemming from fungal, viral, bacterial and parasitic origin[70]. Following pathogenic entry into the CNS and recognition of pathogen-associated molecular patterns (PAMPs), microglia rapidly convert to an activated state taking on an amoeboid shape. In this activated state, microglia act as antigen-presenting cells and are capable of activating naïve T-cells through major histocompatibility complex (MHC) expression and secrete a variety of cytokines including pro-inflammatory cytokines and those required for effector T-cell differentiation, as well as nitric oxide (NO) and reactive oxygen species (ROS)[71]. Furthermore, microglia have anti-bactericidal properties, including the production of cathelicidins. In an experimental model of S*treptococcus pneumoniae*, microglial expression and secretion of rat cathelin-related antimicrobial peptide, a homologue of human cathelicidin LL-37, was observed[72]. In addition, chemokines released from both microglia and astrocytes promote the recruitment of peripheral immune cells, discussed below[49, 73]. Apart from contributing towards the pro-inflammatory milieu, activated microglia aid in resolving inflammation by releasing anti-inflammatory mediators[74, 75]. However, the balance between promoting and regulating the immune response is not always maintained, and activated microglia can promote neuronal damage, as seen in experimental meningitis models[76, 77]. It is evident that microglia possess heterogenous functions that have both beneficial and detrimental roles in pathological contexts.

Although traditionally viewed as playing a supportive role, astrocytes have been implicated in regulating immune responses in the CNS[78]. Similar to microglia, astrocytes also express a variety of receptors involved in innate immunity and secrete cytokines and

chemokines that exert effects on neighbouring cells of the brain and play a part in promoting blood brain barrier (BBB) leakage and subsequent recruitment of peripheral immune cells[79, 80]. Furthermore, their role as antigen presenting cells has also been described. Experimental studies have demonstrated that astrocytes are capable of expressing low levels of MHC enabling them to present myelin protein epitopes to T cells[81, 82]. Different activation states of astrocytes can be induced and are dependent on the CNS inflammatory condition at hand (reviewed by Giovannoni and Quintana, 2020)[83]. The expression of astrocyte reactivity marker, glial fibrillary protein (GFAP), is a common feature seen in most CNS inflammatory conditions. Depending on the location of astrocytes in the CNS and their proximity to the injury site, expression levels of GFAP can vary[83].

2. Immune cell trafficking across the BBB

The BBB is a functional and structural barrier that limits entry of immune cells and pathogens to the brain[48, 84]. In the absence of neuroinflammation, the BBB selectively allows the migration of certain immune cells into the CNS to participate in immune surveillance[84, 85]. Under physiological conditions the CSF contains high percentages of memory $CD4^+$ T cells and very few innate immune cells, suggesting that the former are specifically involved in immune surveillance[86]. In keeping with this, experimental models of multiple sclerosis and autoimmune encephalomyelitis investigating cell migration across the BBB during immune surveillance, reported mostly on memory/effector $CD4^+$ T cells[85, 87]. Moreover, it appears that the migration of $CD4^+$ T cells across the BBB occurs independently of antigen recognition of BBB endothelial cells[88]. Increased BBB permeability is a feature of various CNS infections, however the mechanisms through which infectious pathogens disrupt and compromise BBB integrity, varies. For instance, Japanese encephalitis virus and herpes simplex virus disrupt the BBB through upregulated matrix metalloproteinase (MMP) 9 activity[89]. Whereas *Mycobacterium tuberculo*sis (*Mtb*) has been shown to possess certain virulence factors capable of rearranging the cytoskeleton of the BBB[90]. This in turn creates an optimal niche for trafficking of peripheral immune cells. Although this occurrence is important early on to assist brain-derived immune cells in responding to the infection, exaggerated and prolonged inflammatory responses can trigger a cascade of pathological events leading to significant brain damage. Activated local immune cells of the brain release pro-inflammatory mediators which assists in recruiting peripheral immune cells. These cells in turn produce additional pro-inflammatory cytokines, accumulate in the capillaries of the brain, and release toxic amounts of nitric oxide and reactive oxygen species. The cumulative effect of this

inflammatory milieu include impeded cerebral blood flow leading to brain oedema, ischemic tissue injury and neuronal cell death[91]. Figure 1 provides a schematic summary of the inflammatory response occurring at the BBB.

Figure 1: Schematic diagram of the inflammatory response at the BBB interface

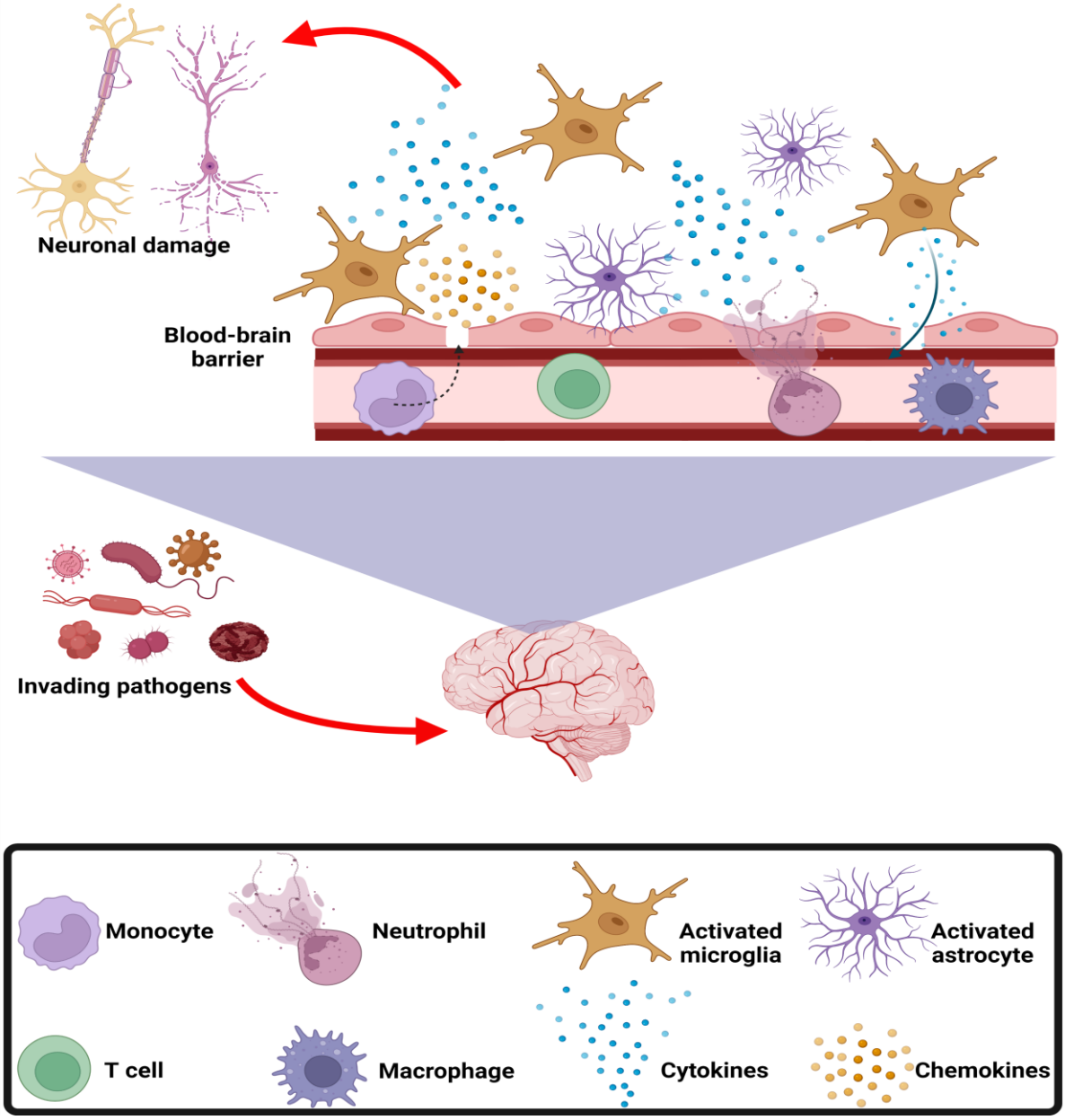

Following entry of infectious pathogens, microglia and astrocytes are activated and subsequently release cytokines and chemokines. These inflammatory mediators take part in promoting BBB leakage and recruiting peripheral immune cells. In turn, peripherally recruited immune cells release their own inflammatory mediators to aid the response which also further activates brain-resident immune cells. Prolonged inflammatory responses can result in significant neuronal damage. Created with Biorender.com

3. Peripherally-recruited innate immune cells

Both innate- and adaptive immune cells are recruited to the CNS to participate in pathogen clearance. Forming part of the innate immune system, natural killer (NK) cells serve an immunomodulatory role through the cytokines that are released and exert cytotoxic-mediated effects[92, 93]. Recruitment of NK cells to the CNS has been reported in several pathological conditions[93, 94]. Increased CSF NK cell numbers and activation were reported among an adult TBM cohort[9]. Conversely, NK cells demonstrated an immature phenotype and functional deficiencies within the CSF and blood of adults with heterogenous neuro-infections[95] and children with herpetic encephalitis[93], respectively. NK cells have been implicated in the direct elimination of cryptococci in both *in vivo* animal and *in vitro* human studies through perforin mediated cytotoxicity. Furthermore, NK cells are also capable of entering the CNS during several inflammatory diseases such as multiple sclerosis[96], with reports of increased CSF NK cell numbers in patients with diverse neuroinflammatory diseases[93].

Neutrophil migration across the BBB has been appreciated in both sterile-(ischemic stroke) and non-sterile conditions[97, 98]. Neutrophils are the most abundant polymorphonuclear cells and exert phagocytic functions. High numbers of mature and activated neutrophils ($CD16^{+}$) were observed in the CSF of adult TBM patients[9], which was associated with worse prognosis[99]. Various mediators released by neutrophils including proteolytic enzymes, oxygen free radicals, and neutrophil extracellular traps (NETs) play a part in BBB breakdown and cause damage to glial cells and surrounding neurons[100].

Monocyte infiltration is a hallmark of inflammation and occurs in various CNS infections. Following entry into the brain, these cells are capable of differentiating into either macrophages or DCs, carrying out further effector functions[101]. For instance, in experimental autoimmune encephalomyelitis models, DC and macrophages originating from Ly6Chi monocytes, the mouse analogue of human classical and intermediate monocytes, exhibit a pro-inflammatory phenotype capable of effectively stimulating TH1 and TH17 mediated immune responses in the CNS. This finding was also substantiated in viral encephalitis models, where macrophages and DCs produced high levels of NO and TNF-α[101]. Adult TBM patients exhibit high numbers of classical monocytes in CSF whereas non-classical and intermediate monocytes, were present at lower numbers[9]. Furthermore, infiltrating monocytes have shown the ability to differentiate into microglia in infectious models of bacterial meningitis[77], and CNS inflammatory models including Parkinson's disease and Alzheimer's disease[102].

4. Peripherally-recruited adaptive immune cells

Two mechanisms constitute the acquired immune response, namely cell mediated immunity and humoral immunity. The former is driven by T cell responses and effector mechanisms, whereas humoral immunity consists of B cell maturation and antibody generation[103]. Cell mediated immunity (CMI) develops within 2-6 weeks following infection, with a rapid influx of lymphocytes and additional activated macrophages. Due to the important role of CMI in the host response against various CNS infections, clinical manifestations and disease outcome may be impacted by the efficacy of CMI[104]. As previously mentioned, CMI is mediated by T cells and the subsequent cytokines that are secreted. There are several conventional and unconventional T cell subsets implicated in CNS infection, with both of these subsets having their own distinct effector functions and phenotypic surface markers[105].

4.1 Conventional T cells

T-helper (T_H) cells, such as $CD4^+$ cells, are of importance in the protective response against infections of various aetiologies[104]. The T_H-driven response is mediated by IFN-γ and TNF-α release, which attract granulocytes and monocytes and promote their anti-microbial functions. In previous studies, it has been shown that T cells possessing multiple effector functions (polyfunctional T cells), are capable of exerting protective immune responses in viral CNS infections[106, 107]. Conventional T cells are found in meagre numbers within the CNS under physiological conditions. The majority of the cells present in CSF include both memory $CD4^+$ (40-50%) and $CD8^+$ (20-30%) T cells[42]. $CD4^+$ T cells are important for both the peripheral activation of $CD8^+$ T cell function and maintaining their antiviral function during CNS infections[108]. Gradual depletion of peripheral $CD4^+$ T cells results in diminished recruitment of $CD4^+$ T cells to the CNS, whereas $CD8^+$ T cell recruitment appears to be only slightly affected. However, increased apoptosis and decreased production of granzyme B and IFN-γ by infiltrating $CD8^+$ T cells are observed in the absence of $CD4^+$ T cells in the CNS during viral encephalitis[108].

4.2 Unconventional T cells

The immune system is conventionally divided into two branches, namely the innate and adaptive immunity. However, certain immune cells exhibit merged properties and bridge the innate-adaptive immunity border. These cells include unconventional αβ and

γδ T cells, each with their respective subset of cells[109]. γδ T cells comprise only 3% of the T-cell population. These cells participate in immune surveillance and play an important role in eliciting responses against pathogens located in peripheral blood and mucosa[110]. Interestingly, γδ T cells have also been found in the CSF of paediatric and adult TBM patients[9, 111]. Unconventional αβ cells also serve as an important factor in mucosal immunity and are capable of 1) immediate cytolysis and cytokine/chemokine secretion following thymic egress; 2) recognizing conserved antigens (modified peptides and glycolipids) seeing as they are not restricted to MHC class I or class II molecules; and 3) possess a relatively conserved T cell receptor (TCR) repertoire[109]. The two major subsets of unconventional αβ T-cells include CD1d-restricted NK T (NKT) cells and MR1-restricted mucosal-associated invariant (MAIT) T -cells[109]. NKT cells are capable of producing a wide array of immune responses to both viral and bacterial infections and play a role in tumour surveillance[112]. The main subpopulation of MR1-restricted T cells are MAIT cells, which are found in both lymphoid tissues and non-lymphoid organs. Additionally, MAIT cells can circulate in the bloodstream, comprising up to 10% of the T cell compartment[113]. Low numbers of both NKT and MAIT cells were found in the CSF of adult TBM patients[9], similarly, low numbers of the latter cell population were also observed in the CSF of multiple sclerosis patients[114].

CHAPTER 4: FLOW CYTOMETRY

1. Overview

Flow cytometry is a technique that allows rapid analysis of single cell suspensions as they intersect with either one or multiple lasers[115]. Both the physical and fluorescent properties of cells are measured through flow cytometry[116]. The physical properties are determined in the manner through which cells scatter light. Light scattering occurs in two different directions (1) the forward direction, also known as forward scatter (FSC), which provides information on the cells' relative size, and (2) 90° direction, also known as side scatter (SSC) which provides information on the granularity or internal complexity of a cell[115]. Light scattering occurs independent of fluorescent emission. The latter results from the binding of a fluorochrome to the cell. The resultant emission is proportional to the amount of fluorochromes bound to the cell. Flow cytometers are defined by three components namely, fluidics, optics, and electronics[115, 116].

Fluidics: The main goal of the fluidic system is to transport the cells within the sample to the laser interrogation point where it can be analysed. The system comprises pressurized sheath fluid, commonly made up of phosphate buffered saline (PBS), that surrounds but does not intermix with the sample stream. The sample is also pressurized once transported to the flow chamber, the pressure difference between the sheath fluid and sample stream creates a laminar flow, forcing the cells into a conical shape. The entire process is known as hydrodynamic focusing and ensures that the cells move in single-file line when intersecting with the excitation lasers, allowing uniform cell illumination[115, 116].

Optics: The optical system consists of excitation lasers, optical filters, and detectors. Excitation lasers produce high intensity monochromatic light needed to analyse the cells within a sample. A single flow cytometer can have a wide range of excitation lasers with the ability to detect physical (SSC and FSC) and multiple fluorescent parameters. Following excitation, the light emitted from the cells is collected by a series of filters that direct the light to detectors that are specific for that particular fluorochrome. The detectors then convert the photons of light emitted from the cell into a relative number of electrons to generate an electrical current. Two types of detectors are used within the optical system: (1) photodiodes which are capable of detecting stronger light signals generated by FSC and (2) photomultiplier tubes (PMT) which are more sensitive compared to photodiodes and can detect weaker light signals generated by SSC and fluorescence[116].

Electronics: The electrical current is converted to a voltage pulse by an amplifier. A further conversion is implemented by an analogue-to-signal converter, which converts the pulse into a digital signal for subsequent computer processing[116].

2. Importance of CSF analysis

CSF serves as an important diagnostic aid and research tool in the evaluation of inflammatory conditions involving the CNS, of an infectious or non-infectious nature[1]. More specifically, white blood cell counts are of particular interest when it comes to the differential diagnosis of neurological diseases[10]. Healthy individuals possess clear CSF with total leukocyte counts of 5 cells/mm^3 or less in infants and adults, whereas preterm infants and 4-8 week old neonates have counts of less than 20 cells/mm^3 and 15 cells/mm^3, respectively[1]. Furthermore, normal CSF does not contain polymorphonuclear cells, erythrocytes, plasma cells or eosinophils. Any change in CSF composition is indicative of pathology[1].

In terms of clinical research, CSF is a precious biological specimen for various CNS pathologies and extremely valuable for cell count analysis and biomarker discovery. Given the close proximity with the brain parenchyma, several brain-derived constituents including proteins, cytokines, and metabolites, are present in the CSF. Analysis of these constituents within CSF is of great interest in clinical research as it can provide valuable information pertaining to ongoing pathological processes in the brain[117]. For instance, elevated concentrations of tissue injury markers including total Tau protein, phosphorylated tau, neuron-specific enolase (NSE), β-amyloid, S100B, and GFAP, have been associated with poorer outcome in conditions such as Alzheimer's disease[118], traumatic brain injury[119], ischaemic stroke[120], and CNS infections[121]. Immunophenotypic characterisation, which is one of the most widely used applications of flow cytometry, has become a popular method for quantitative analysis of immune cells within CSF of neuroinflammatory diseases including multiple sclerosis[85], as well as several CNS infections, allowing better insight into disease immunopathogenesis[9]. Furthermore, CSF immunophenotypic characterisation by flow cytometry is also used for the detection of leptomeningeal localizations of haematological malignancies[122].

3. Challenges associated with flow cytometric CSF analysis

Flow cytometric analysis of white blood cell counts requires sufficient cell numbers within a sample, and given that CSF has low cellularity, it often hinders the use of flow cytometry for CSF analysis[7, 10]. However, Subira *et al* demonstrated that in low volume (1ml) CSF

samples containing cell counts of ≤5 leukocytes/µl, T lymphocytes could still be reliably quantified, whereas reliable absolute counts of B cells required ≥5 leukocytes/µl within a sample[7]. With regards to monocytes, the use of more specific markers such as cluster of differentiation (CD) 14, appeared to be more crucial in identifying these mononuclear cells within CSF samples, as opposed to sample volume and absolute cell counts[7].

The rapid decline in the viability of white blood cells within CSF immediately following sampling is the most challenging obstacle to overcome. A number of studies have reported significant loss of cell numbers in CSF within 30 minutes of sampling as well as varying survival rates among different leukocyte subsets[10, 123, 124]. Steele *et al* attributed this rapid cell loss to hypotonicity, and low concentration of lipids and proteins in CSF. Lipids and proteins serve to provide structural support for leukocyte membranes[125]. More specifically, it has been shown that monocytes and granulocytes, particularly neutrophils, are most susceptible to this rapid decline in cell numbers, as opposed to lymphocytes[123]. Nevertheless, rapid cell loss in CSF samples can result in an underestimation of cell counts which can have grave consequences in clinical practice especially in the differential diagnosis of neuro-pathologies[10]. Furthermore, it also incumbers the application of flow cytometry for clinically relevant research of CNS pathologies.

4. Effectiveness of current cell stabilizing reagents

To address cell viability issues in CSF samples, certain cell stabilizing reagents have been used to limit the rapid cell loss in CSF samples prior to flow cytometric analysis. According to the available literature, only serum-containing media and Transfix® have been used to stabilise CSF.

The addition of serum-containing media, consisting of RPMI 1640 and foetal calf serum (FCS), immediately after CSF sampling, was shown to improve sample quality and prolong cell viability[10]. De Graaf *et al* compared leukocyte counts at varying timepoints in native CSF versus CSF with serum-containing media and observed that serum-containing media prevented cell loss for up to five hours following sampling[10]. Leukocyte counts in native CSF were significantly lower at all timepoints compared to CSF with serum-containing media, with the exception of neutrophil counts, which remained stable at the 30 minute mark. It was further observed that compared to lymphocytes and neutrophils, monocytes were the more vulnerable leukocyte subset, experiencing a dramatic loss in cell counts at the 1h mark[10]. Moreover, Greig *et al* found that CSF stabilised with serum-containing media resulted in

more than 90% of samples having quantifiable cell counts that were suitable for flow cytometric analysis; whereas in native CSF, 70% of samples had inadequate cell counts[126].

Transfix® was originally designed to stabilise whole blood samples for flow cytometric analysis of leukocytes[127]. Soon after, Transfix® in combination with ethylenediaminetetraacetic acid (EDTA) was used to stabilise CSF samples. Several studies have reported on the effectiveness of Transfix® in stabilizing CSF for storage, reducing leukocyte degradation, and decreasing autofluorescence[124, 128-130]. De Jongste *et al* investigated the effect of Transfix® on leukocyte numbers and the detection of leptomeningeal localizations of haematological malignancies in CSF, compared to simultaneously collected native CSF and CSF stabilized with serum-containing media[130]. No significant differences in sample quality were observed in either of the three conditions 30 minutes after withdrawal. However, the ability to detect haematological malignancies in CSF following 18 hours of storage, was significantly greater in Transfix-treated CSF as compared to native CSF and CSF with serum-containing medium. Quantitatively, the median leukocyte counts 30 minutes after CSF withdrawal, was significantly higher in Transfix-treated CSF compared to native CSF, but comparable to CSF with serum-containing media. The median leukocyte count of Transfix-treated CSF was 2.3 times higher than native CSF and 1.8 times higher than CSF with serum-containing media, after 18 hours of storage[130]. However, in terms of marker expression, significant decreases were seen in fluorescence intensity in Transfix-treated CSF for CD45 marker at 30 minutes, and CD19 and CD20 markers at both the 30 minute and 18hr timepoint. Out of the three leukocyte subsets, lymphocytes were best preserved in Transfix-treated CSF, whereas monocytes and granulocytes experienced a greater decline in number over time, with surface antigen labelling being negatively impacted. However, no increases in autofluorescence were observed in either Transfix-treated CSF nor CSF with serum-containing media[130].

5. The need for an alternative method for stabilizing CSF for flow cytometric analysis

It is well documented that CSF samples intended for flow cytometric analysis require rapid processing following withdrawal given the highly perishable nature and low number of cells of this specimen. Despite the encouraging results of Transfix® and serum-containing media, these two reagents do not allow long-term storage (>18 hours) of CSF. Previous studies have observed substantial loss of fluorescence intensity in Transfix-treated CSF, which questions the applicability of this reagent on weakly expressed cell markers. It is also

apparent that Transfix® stabilizes leukocyte subsets with differing efficacy- with lymphocytes being the subset better maintained as opposed to monocytes and granulocytes which decrease in number with prolonged storage in this reagent[130]. This not only incumbers potential cytomorphological testing, but no additional functional assays can be performed in Transfix-treated CSF. Serum-containing media has a short shelf life of three months and has only been shown to preserve CSF cells for a maximum period of 5 hours[10], therefore it does not offer an alternative to Transfix.

Finding an alternative method that allows long-term storage and batched analysis of CSF samples collected over time, is therefore highly desirable in clinical research. This would be beneficial for 1) resource-limited settings where only basic laboratory equipment is available; 2) busy clinical environments where CSF samples are collected at unpredictable times (after hours/over the weekend); 3) field site clinical studies where flow cytometers aren't readily available; and 4) multi-centre studies faced with logistical challenges of collecting samples at different sites and transporting samples between centres within a limited time-period.

Cryopreservation serves as an attractive alternative to running samples fresh and has been implemented and deemed effective in whole blood samples[11] and isolated peripheral blood mononuclear cells[131]. It is a process which involves the use of very low temperatures to preserve biological specimens. This method is advantageous in that cells can be viably stored for a longer period of time (months-years) in cryogenic vials at -80° Celsius (C) or in liquid nitrogen, thus allowing for various types of assays to be performed downstream[132]. To date, there is no literature that reports the effects of cryopreservation on CSF samples. The optimization of this technique will offer valuable opportunities for research in many CNS conditions that currently lack flow cytometry protocols which allow for long term storage while preserving cell viability, deferred (and potentially off-site) analysis, the fixation of cells, and which maximise output from pauci-cellular samples, like CSF. The advantages of cryopreserving CSF samples for flow cytometric analysis would include long-term storage of samples as opposed to running them fresh, batched analysis resulting in better comparability of samples collected at different time points, the option of shipping samples to a central site in multi-centre studies[133], and the potential to conduct flow cytometric samples at sites without an in-house flow cytometer. Cryopreservation of CSF samples could potentially serve as a feasible option for long-term storage.

Therefore, the aim of this study was to examine a method for long-term storage of CSF samples where reliable measurement of cell percentages and relative proportion of cell subsets, is still possible.

CHAPTER 5: AIMS & OBJECTIVE

The objective of this study was to examine 2 methods of long-term storage of CSF samples which ensured reliable measurement of cell percentages and relative proportion of cell subsets using flow cytometry.

Aim 1: To examine percentages and relative proportion of subsets of selected peripheral leukocytes and brain derived cells in cryopreserved CSF in comparison to freshly processed CSF.

Aim 2: To examine percentages and relative proportion of subsets of selected peripheral leukocytes and brain derived cells in Transfix-treated CSF in comparison to freshly processed CSF.

CHAPTER 6: METHODS

1. Study Cohort and Sample Collection

This study prospectively recruited paediatric patients admitted to Red Cross War Memorial Children's Hospital (RCWMCH) between June 2021 and October 2021. Either lumbar or ventricular CSF, and where possible, time-linked and serial samples were collected from patients during clinically indicated neurosurgical procedures that formed part of routine patient management. A volume of ≥3ml of CSF was collected from a cohort with various CNS infections. Given the difficulties surrounding patient recruitment during the ongoing COVID-19 pandemic, an experimental arm was incorporated into the project. The latter involved collecting CSF samples from children who required neurosurgical interventions for conditions unrelated to CNS infections. The CSF samples collected from these patients were spiked with isolated peripheral blood mononuclear cells (PBMCs) from the whole blood of healthy volunteers.

2. Sample processing

A minimum of 3ml of CSF was required in order to divide the sample across the three different protocols 1) "Fresh CSF" serving as the current gold standard; 2) "Transfix-treated CSF" and 3) "Cryopreserved CSF". Patient CSF samples were processed immediately; whereas experimental CSF samples were left in the fridge for a minimum period of one week to ensure the breakdown of any native cells before being spiked with PBMCs. Figure 2 provides an overview of the workflow undertaken with both patient and experimental CSF samples.

Figure 2: Overview of sample processing

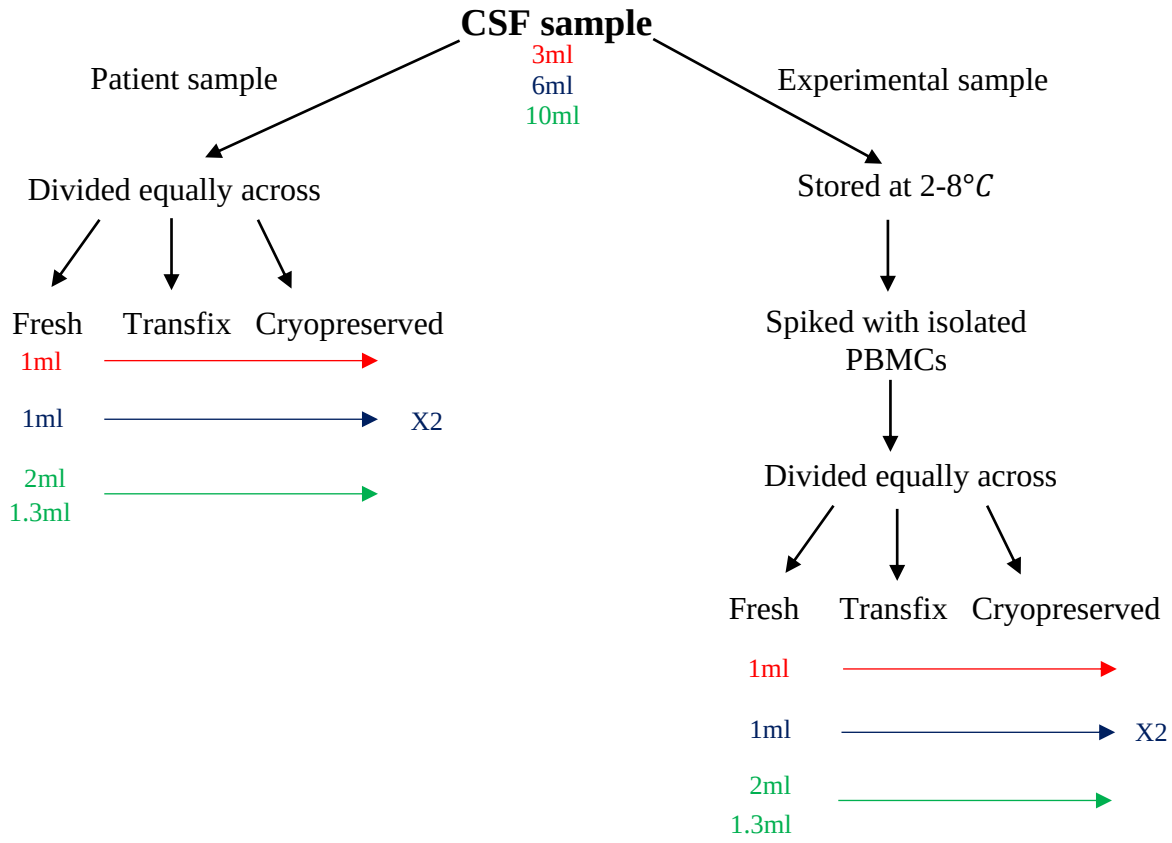

If a total volume of 3ml of CSF was collected, 1ml was distributed across the three protocols. If 6ml of CSF was collected, the same distribution of CSF would take place twice. Whereas, if 10ml of CSF was collected, 2ml of CSF was distributed across the three methods followed by a separate 1.3ml. Therefore, CSF volumes of >3ml resulted in two samples from a single patient.

2.1 Patient CSF samples

Immediately after withdrawal, the CSF samples were divided equally into the three appropriately labelled sterile tubes.

Fresh CSF: CSF was immediately transferred to a tube containing an equal volume of serum-containing media made up of 90% RPMI 1640 and 10% heat inactivated foetal bovine serum (FBS). The CSF with serum-containing media was left in the fridge and processed within an hour. Briefly, the sample was centrifuged at 300g for 5 minutes at 4°C with the break turned off. The supernatant was discarded, and the cell pellet was resuspended in 75µl of antibody cocktail and left to incubate for 30 minutes in the fridge protected from light. Following incubation, 250µl of Becton Deckinson (BD) Cytofix/Cytoperm^{TM} buffer was added to the mixture and incubated for a further 20 minutes in the fridge protected from light. Following the second incubation period, the cell

suspension was washed with 250µl of PermWash buffer. After centrifugation at 610g for 5 minutes, the supernatant was aspirated using a pipette. The cell pellet was resuspended in 100µl of PermWash buffer and stained with 1.25 µl of GFAP antibody and left to incubate for 30 minutes in the fridge protected from light. Following incubation, the cells were washed with 500µl of PermWash buffer. The supernatant was aspirated, and the cell pellet was resuspended in 150µl of R&D Flow Staining buffer and stored at 2-8 °C prior to acquiring on the flow cytometer.

Transfix-treated CSF: CSF was immediately transferred to a Transfix® tube containing 0.2ml of Transfix/EDTA and was stored at 2-8 °C for two weeks. Following the two week storage, CSF was transferred to a 15ml Falcon tube, 5ml of PBS was used to wash the Transfix® tube and thereafter transferred to the 15ml Falcon tube. The sample was centrifuged at 300g for 5 minutes at 4 °C with the break turned off. The supernatant was discarded, and the cell pellet was resuspended in 500µl of PermWash buffer and left to incubate in the fridge for 20 minutes. After the first incubation, the cell suspension was centrifuged at 510g for 5 minutes, the supernatant was aspirated, and the cell pellet was resuspended in 75µl antibody cocktail and left to incubate in the fridge for 30 minutes protected from light. Thereafter, the cells were washed with 500µl of PermWash buffer. The supernatant was aspirated, and the cell pellet was resuspended in 150µl of Flow Staining buffer and stored at 2-8 °C prior to acquiring on the flow cytometer. A fixation step was not required in this protocol seeing as the cells were immediately fixed once added to the Transfix® tube.

Cryopreserved CSF: CSF was immediately centrifuged at 300g for 5 minutes with the break turned off. The supernatant was discarded, and the cell pellet was resuspended in 500µl of cold RPMI. Cryo-solution, made up of 93% of heat inactivated FBS and 7% dimethyl sulfoxide (DMSO), was added drop-wise to the cell suspension and immediately transferred to a cryovial, placed in a Mr Frosty™ freezing container and stored at -80 °C for 1 month. Following the 1 month storage period, cryovials were thawed in a 37 °C water bath by slowly agitating the vial until a block of ice remained. Once partially thawed, 1ml of room temperature RPMI was immediately added to the vial and transferred to a 15ml Falcon tube. An additional 1ml of RPMI was used to wash the cryovial and was also transferred to the 15ml Falcon tube. Thereafter, the sample was centrifuged at 300g for 5 minutes at 4 °C with the break turned off. The same antibody staining process

outlined in the “Fresh” protocol, was used. The cell suspension was stored at 2-8 °C prior to acquiring on the flow cytometer.

2.2 Experimental CSF samples

Isolation of PBMCs: Briefly, 8ml of whole blood was collected in BD Vacutainer CPT Sodium Heparin tubes. The tubes were centrifuged at 1500g for 30 minutes with the break turned off. The plasma was discarded and the layer of PBMCs was carefully isolated and transferred to a 15ml Falcon tube containing 5ml of PBS. Following two wash steps with PBS, the cell pellet was resuspended in 1ml of RPMI and a further 1ml of cryo-solution, consisting of 20% DMSO and 80% heat inactivated FBS, was added drop-wise. The suspension was immediately transferred to cryovials and placed in Mr Frosty^{TM} freezing container for subsequent freezing at -80°C.

Spiking of CSF: The CSF samples were stored at 2-8 °C and spiked with PBMCs within a week following collection. Firstly, the PBMC cryovials were thawed in a 37 °C water bath by slowly agitating the vials until a block of ice remained. Thereafter, 1ml of warmed media, consisting of 90% RPMI and 10% FBS, was added drop-wise and transferred to a 50ml Falcon tube. An additional 19ml of warmed media was added bringing the final volume to 20ml. The suspension was centrifuged at 1800 revolutions per minute (rpm) for 10 minutes, the supernatant was discarded, and the cells underwent a second wash. Following the 2nd wash, the cell pellet was resuspended in 1ml of warmed media, an additional 4ml of media was added bringing the volume to 5ml. To prevent clumping of cells, 20 µl of DNase was added and the sample was left to incubate for 2 hours. During this time, 200 µl of the suspension was aliquoted and sent to the National Health Laboratory Service (NHLS) for a white blood cell count. Following the 2 hour incubation period and cell count, the cells were resuspended in media to have a final concentration of 10 x10^{6} cells/ml. The CSF sample was spiked with a known concentration of cells and the three protocols were immediately carried out as outlined in 2.1.

3. Flow cytometry

Cells were stained with a 16-colour antibody panel (refer to Table 2) for which optimal antibody titres were calculated prior to use (Appendix A). Fluorescence-minus-one controls were used to accurately identify and gate populations of interest (refer to Figure 3 for gating strategy). Sample acquisition was carried out on the BD LSR II flow cytometer, 50 000

events were recorded for patient samples and 1000 000 events were recorded for experimental samples given the higher cell count. Immunophenotyping of major cell populations of interest in this study, are listed in Table 3. Major cell populations were identified using distinct lineage markers. The choice of sub-populations investigated were based on available data in adult TBM and paediatric studies of disseminated TB[9, 134].

Daily Cytometer Setup (CS) and Tracking (T) beads (BD™ Lot 23861) were run to assess cytometer performance. Standardization of the flow experiment was completed at the start of the study as follows. Firstly, application settings were optimized for this particular antibody panel in order to ensure that consistent fluorescence intensity values were obtained with each sample run over the course of the study. Secondly, Sphero™ Rainbow calibration particles (catalogue no. 559123) were acquired under the optimized instrument settings and a set of target values were established. For subsequent sample runs, the optimized application settings were applied to the experiment, and the Rainbow calibration particles were acquired thereafter. Voltages were adjusted if necessary to ensure that bead peaks were within a ±10% range of the target values set during the previous sample run. This standardization ensured that day-to-day variations within the instrument, changes such as instrument maintenance and laser alignment, were accounted for. Single stained BD™ Compensation beads were run after voltages were adjusted and before samples were acquired; 10 000 events were recorded, and a compensation matrix was calculated.

Table 2: List of fluorochrome-conjugated antibodies

Fluorochrome	Marker	Specificity	Reagent description
APC-H7	CD3	T cells	BD Pharmigen™
BV510	CD4	T cells	BD Horizon™
PerCP-Cy5.5	CD8	T cells	BD Pharmigen™
APC-R700	CD69	Activation	BD Horizon™
BB515	CD19	B cells	BD Horizon™
BV605	CD14	Monocytes	BD Horizon™
PE-Cy7	CD16	NK & Monocytes	BD Pharmigen™
BV786	HLA-DR	Activation	BD Horizon™
APC	CD56	NK cells	BD Pharmigen™
PE-Cy5	CD161	MAIT cells	BD Pharmigen™
BV711	Vα7.2	MAIT cells	BD OptiBuild™
BV650	γδ TCR	γδ cells	BD OptiBuild™
PE-CF594	CD11b	Monocytes/macrophages & Microglia	BD Horizon™
V450	CD45	Early differentiation	BD Horizon™
PE	GFAP	Astrocyte activation	BD Pharmigen™
BV570	Live/Dead	Viability	BD Horizon™

Abbreviations: APC, allophycocyanin hillite 7; BB, brilliant blue 515; BD, Becton Dickinson; BV, brilliant violet; CD, cluster of differentiation; GFAP, glial fibrillary acidic protein; HLA-DR, human leukocyte antigen-DR isotype; MAIT, mucosal associated invariant T cell; NK, natural killer; PE, phycoerythrin; PerCP, peridinin-chlorophyll-protein complex.

Table 3: Immunophenotypic characterisation of cell populations

Cell population	Immunophenotypic definition
Leukocytes	$CD45^+$
Microglia	$CD45^+$ $CD11b^{++}$
Non-microglia	$CD45^+$ $CD11b^+$
T cells	$CD3^+$
T-helper cells	$CD3^+CD4^+$
Cytotoxic T cells	$CD3^+CD8^+$
MAIT cells	$CD3^+$ $CD161^+$ $V\alpha7.2^+$
B cells	$CD3^-$ $CD19^+$
NK cells	$CD16^+$ $CD56^+$
Classical monocytes	$CD14^+$ $CD16^-$
Non classical monocytes	$CD14^-$ $CD16^+$
Astrocytes	$CD45^-$ $GFAP^+$

Abbreviations: CD, cluster of differentiation; GFAP, glial fibrillary acidic protein; MAIT, mucosal associated invariant T cell; NK, natural killer.

4. Sample analyses

Percentages of both brain-derived immune cells and peripheral immune cells (T cells, B cells, NK cells and monocytes) were obtained by flow cytometric analysis and compared between the three methods. The Transfix and Cryopreservation methods were each compared separately to the Fresh method, which served as the gold standard. To evaluate the potential loss of cells following cryopreservation, a viability marker was included in the panel and percentage viable cells were only compared between Fresh and Cryopreserved CSF.

The effects of the duration of storage time on cell percentages in Transfix-treated CSF was determined by flow cytometric analysis in experimental CSF samples following 24 hours, 1 week, and 2 week storage in Transfix. Results were compared to the Fresh method which remained the gold standard.

The influence of Transfix and Cryopreservation methods on fluorescent signal was assessed by obtaining the median fluorescent intensity (MFI) of the positive population of certain markers ($CD45^+$, $CD11b^{++}$, $CD3^+$, B cells, $GFAP^+$) and comparing it to the Fresh method in patient and experimental samples.

Case illustrations showing flow data in lumbar and ventricular CSF as well as in serial samples are shown.

5. Data and Statistical analysis

Exported flow cytometry standard (FCS) files were analysed, and gating was performed on FlowJo software (version 10.7.2). Statistical analyses were performed using IBM SPSS Statistics version 27 (IBM Corp, Armonk, New York, USA). Descriptive statistics were performed to determine the distribution of the data, abnormally distributed data were reported as median and interquartile range or minimum-maximum range. The Mann-Whitney test was used to compare percentages of different cell populations and MFI values between the methods. The Bland-Altman test was used to evaluate the level of agreement between the Fresh and Cryopreservation, and Fresh and Transfix methods in patient and experimental samples. Briefly, the difference in cell percentages measured by the paired methods are plotted against the mean value of the two methods. The limits of agreement describe the range in which 95% of the data points should fall within ±2 standard deviations of the mean difference. A Spearman's correlation was also performed on cell percentages between Fresh and the Cryopreservation/Transfix methods. The designated level of statistical significance was set at 0.05.

6. Ethics statement

Informed consent was obtained from the parents/guardians. This project has received the necessary scientific, ethical (HREC 368/202) and hospital approval. Assent was requested in children over the age of 8 years with a Glasgow Coma Scale score of 15 (fully conscious).

CHAPTER 7: RESULTS

A total of 30 CSF samples were collected, of which 10 were from the patient cohort and 20 were from the experimental cohort. The patient cohort comprised 3 patients with clinically diagnosed TBM, 2 with ventriculitis and 1 with bacterial meningitis. Of the 10 CSF samples collected from the patient cohort, one sample was excluded from the statistical analyses due to the abundance of pus present within the sample, resulting in very few cells isolated for flow cytometric analysis. Routine diagnostic cell counts could also not be performed on this sample however, flow cytometric data of this sample are included in the Appendix B. Demographic and clinical characteristics of the cohorts are included in Table 4.

Table 4: Demographic and clinical characteristics of study cohort

Variable	Patient cohort	Experimental cohort
Number		
Patients	5	13
Samples	9	20
Demographics		
Age (years)	1.6 (0.5-1.7)	1.6 (0.6-9.3)
Sex (Male)	3 (60)	7 (54)
Clinical characteristics		
Pathology		
TBM	3	
Ventriculitis	1	
Bacterial meningitis	2	
Total WBC count (cells/µl)	127 (11-535)[a]	743 (260-1250)[b]

Values reported as median (interquartile range), number (percent).

[a] White blood cell (WBC) counts is the sum of lymphocytes and polymorphonuclear cells. Note: The NHLS only reports lymphocytes and polymorphonuclear cells, other cell types are not routinely reported.

[b] Cell count after spiking CSF of experimental samples.

Abbreviations: CSF, cerebrospinal fluid; WBC, white blood cell count.

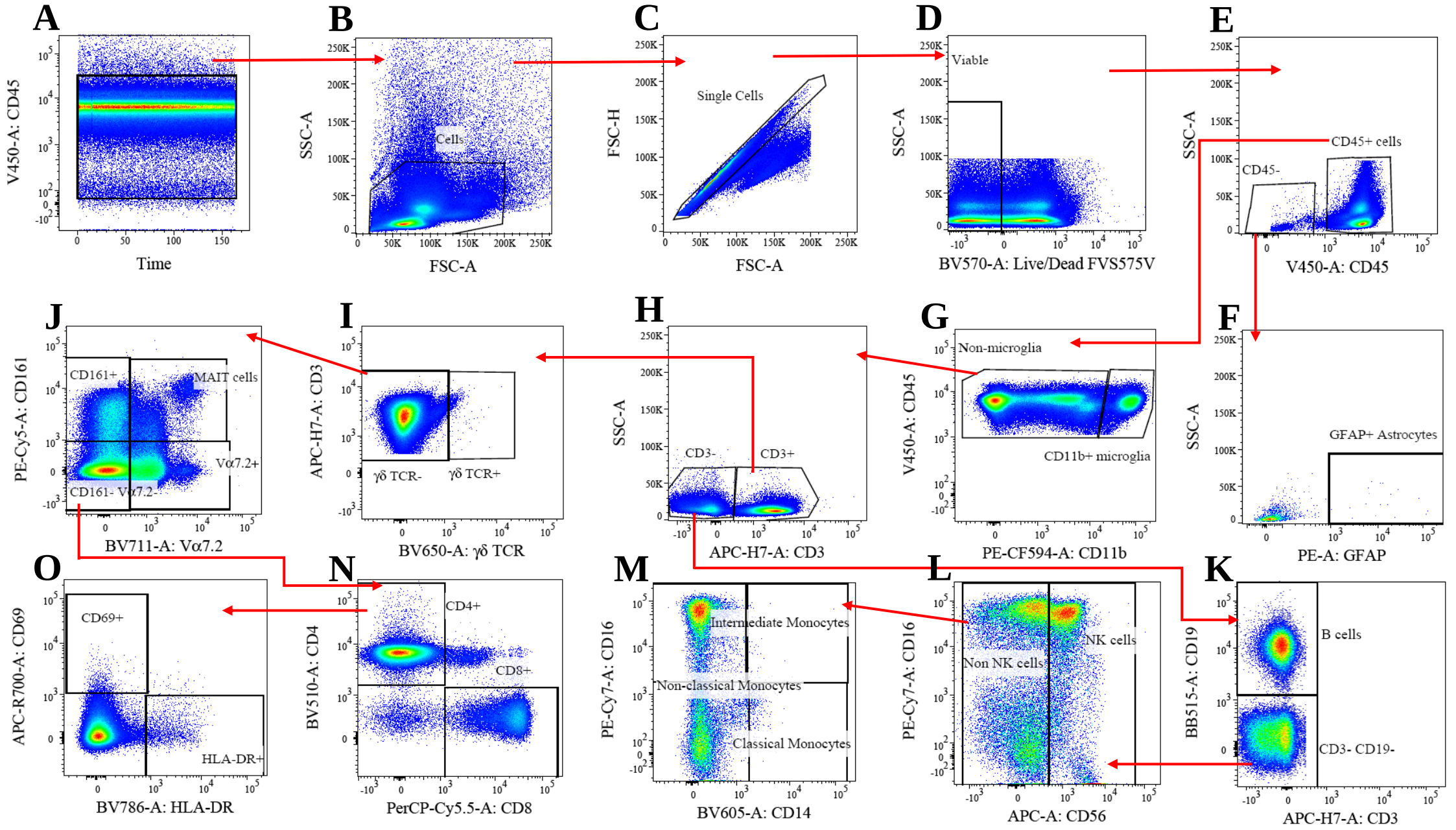

Figure 3: Gating strategy. Uniform fluorescence was selected with the "time" gate, cells were identified with side scatter-area (SSC-A) and forward scatter-area (FSC-A), single- and viable cells were selected by doublet and dye exclusion, respectively. Leukocytes ($CD45^+$), T cells ($CD3^+$), B cells ($CD19^+$), NK cells ($CD16^+$ $CD56^+$), and sub-populations of monocytes ($CD14^+$ & $CD16^+$) were identified. Activation was assessed by HLA-DR and CD69 expression.

1. Comparison of cell percentages across methods

Figure 3 shows an example of the gating strategy. Similar gating strategies were used for all three methods in patient and experimental samples. Uniform fluorescence was selected with the "time" gate (Fig 3A), cells were identified with side scatter- area (SSC-A) and forward scatter-area (FSC-A) (Fig 3B), single- and viable cells were selected by doublet and dye exclusion (Fig 3C&D), respectively. Leukocytes were identified based on $CD45^+$ expression (Fig 3E). Astrocytes were gated from the $CD45^-$ population, and activation was assessed by $GFAP^+$ expression (Fig 3F). Microglia and non-microglia populations were identified based on $CD45^+$ and $CD11b^+$ expression (Fig 3G). From the non-microglia population, T cells ($CD3^+$) were identified (Fig 3H). γδ T cells (γδ TCR^+) were gated from the $CD3^+$ population (Fig 3I). MAIT cells ($CD161^+V\alpha7.2^+$), $CD161^+$ cells and $V\alpha7.2^+$ cells were gated from the γδ TCR^- population (Fig 3J). B cells ($CD19^+$), were gated from the $CD3^-$ population (Fig 3K). NK cells ($CD16^+CD56^+$) were gated from the $CD3^-CD19^-$ population (Fig 3L). Classical monocytes ($CD14^+$ & $CD16^-$), non-classical monocytes ($CD14^-CD16^+$) and intermediate monocytes ($CD14^+CD16^+$), were gated from the $CD16^+CD56^-$ population (Fig 3M) identified. $CD4^+$ and $CD8^+$ T cells were gated from the $CD161^-$ $V\alpha7.2^-$ population (Fig 3N). Activation was assessed by HLA-DR and CD69 expression on the $CD4^+$ population (Fig 3O). Statistically significant differences for the comparison between methods are displayed as heatmap tables (Table 5 & 6). Box-and-whisker plots were used to graphically present the distribution of the data of selected cell populations, showing median and interquartile ranges (Figure 4). Raw data of cell percentages across methods is available in Appendix C and D.

Fresh versus Cryopreservation: No significant differences were found for any of the cell populations or activation markers in patient samples. However, significant differences were found in cell viability (*p=0.05*), $CD11b^{++}$ (*p=0.01*), $CD45^+CD11b^+$ (*p=0.01*) and $CD3^+$ cells (*p=0.02*), when comparing the Fresh and Cryopreservation methods in experimental samples. In some cases, Fresh had higher percentages, in some cases Cryopreservation had higher percentages – Figure 5.

Fresh versus Transfix: Significantly higher percentages of $CD11b^{++}$ (*p=0.01*), $CD4^+$ (*p=0.001*), $CD8^+$ (*p=0.007*), and NK cells (*p=0.04*), as well as $CD69^+$ activation marker (*p=0.001*), were observed in the Fresh method for patient CSF samples. In experimental CSF samples, significantly higher percentages of $CD11b^{++}$ (*p=0.00*), $CD3^+$ (*p=0.00*), γδ TCR^+

(*p=0.01*), CD161^{+} (*p=0.00*), CD4^{+} (*p=0.00*), MAIT (*p=0.007*), NK cells (*p=0.00*), classical and non-classical monocytes (*p=0.00*), as well as CD69^{+} and HLA-DR^{+} activation markers (*p=0.00*), were found in Fresh method. Unlike in Fresh and Cryopreserved CSF, certain cell populations such CD45^{+}CD11b^{+}, Vα7.2^{+}, and B cells could not be clearly distinguished from other cell populations in Transfix-treated CSF as demonstrated in Figure 6. Cell percentages for these sub-populations were, therefore, not included in the analyses. This observation was apparent in both patient and experimental CSF samples.

Summary statistics of cell percentages across methods for patient and experimental samples are included in Table 7 and 8.

Table 5: Comparison of cell percentages across methods in patient samples

	Fresh	Cryopreservation	Transfix
Viable cells			
CD45$^+$ cells			
CD11b^{++} cells			
CD45$^+$CD11b$^+$ cells			X
CD3$^+$ cells			
γδ TCR$^+$ cells			
CD161$^+$ cells			
CD4$^+$ cells			
CD8$^+$ cells			
MAIT cells			
Vα7.2$^+$ cells			X
B cells			X
NK cells			
Classical monocytes			
Non-classical monocytes			
CD69$^+$			
HLA-DR$^+$			
GFAP$^+$ astrocytes			

Cell percentages were compared between Fresh vs Cryopreservation, and Fresh vs Transfix methods in patient samples (n=9). Green boxes signify no statistically significant difference, whereas red boxes signify statistically significant differences relative to Fresh. Boxes demarcated with "X" represent cell population that could not be clearly distinguished from other populations. CD, cluster of differentiation; HLA-DR, human leukocyte antigen-DR; GFAP, glial fibrillary acidic protein; TCR, T cell receptor.

Table 6: Comparison of cell percentages across methods in experimental samples

	Fresh	Cryopreservation	Transfix
Viable cells			
CD45$^+$ cells			
CD11b^{++} cells			
CD45$^+$CD11b$^+$ cells			X
CD3$^+$ cells			
γδ TCR$^+$ cells			
CD161$^+$ cells			
CD4$^+$ cells			
CD8$^+$ cells			
MAIT cells			
Vα7.2$^+$ cells			X
B cells			X
NK cells			
Classical monocytes			
Non-classical monocytes			
CD69$^+$			
HLA-DR$^+$			
GFAP$^+$ astrocytes			

Cell percentages were compared between Fresh vs Cryopreservation, and Fresh vs Transfix methods in experimental samples (n=20). Green boxes signify no statistically significant difference, whereas red boxes signify statistically significant differences relative to Fresh. Boxes demarcated with "X" represent cell population that could not be clearly distinguished from other populations. CD, cluster of differentiation; HLA-DR, human leukocyte antigen-DR; GFAP, glial fibrillary acidic protein; TCR, T cell receptor.

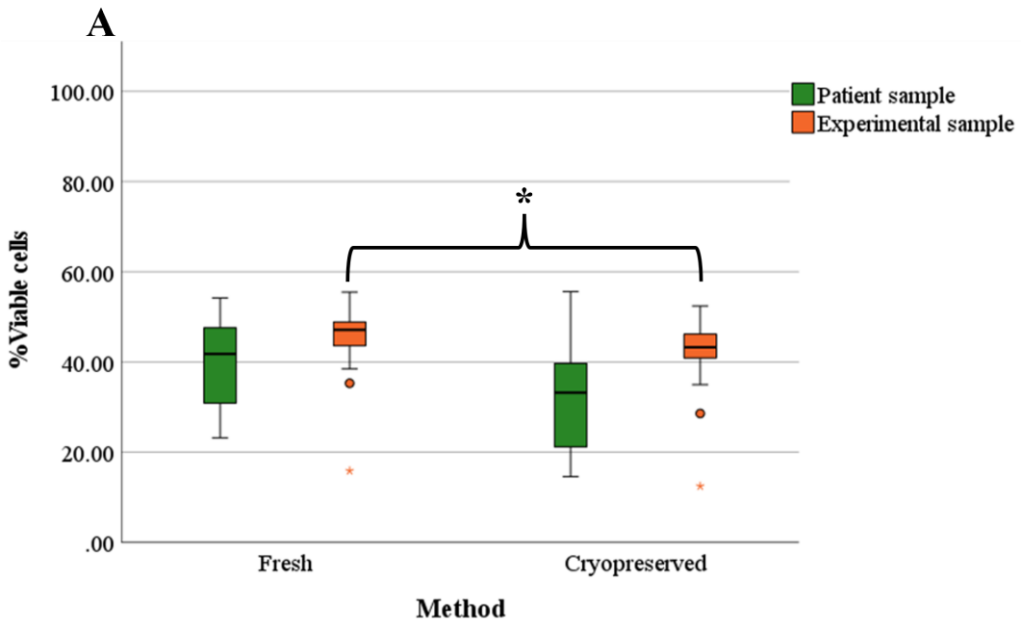
A
100.00
80.00
60.00
40.00
20.00
.00
%Viable cells
Patient sample
Experimental sample
*
Fresh
Cryopreserved
Method

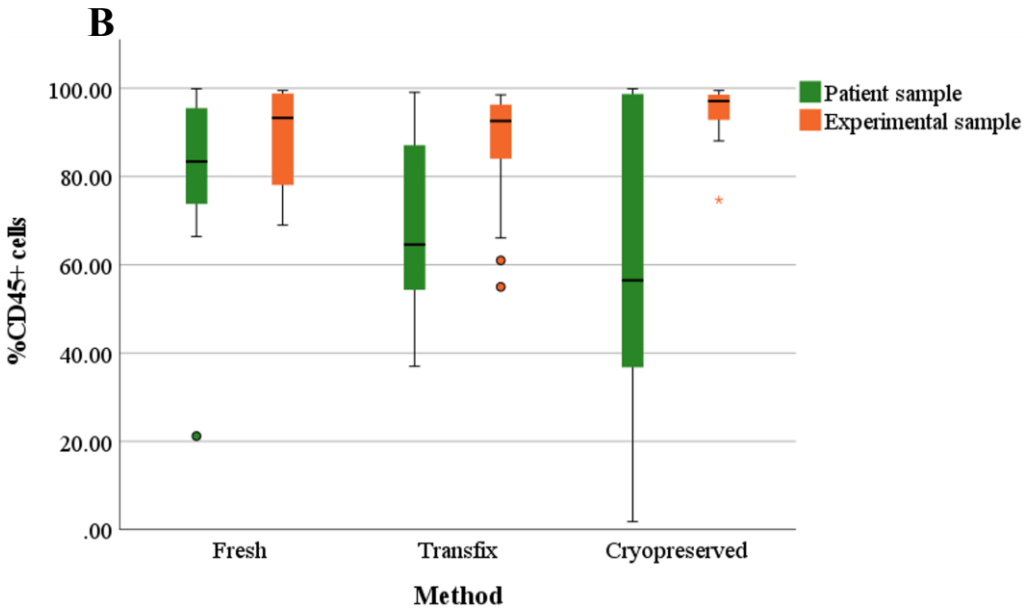
B
100.00
80.00
60.00
40.00
20.00
.00
%CD45+ cells
Patient sample
Experimental sample
Fresh
Transfix
Cryopreserved
Method

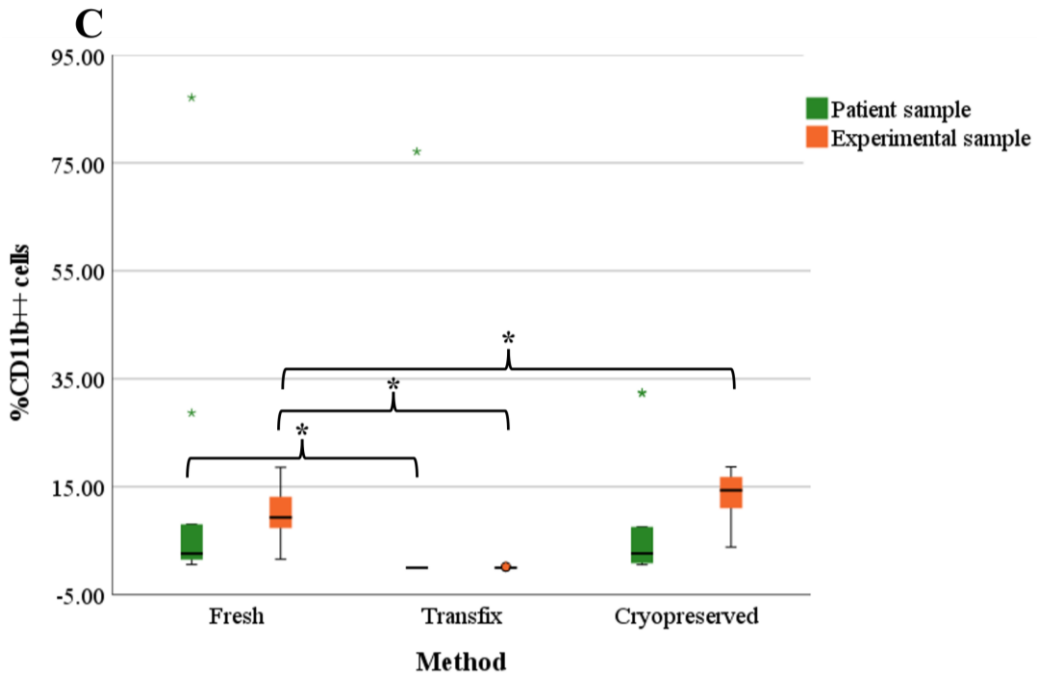
C
95.00
75.00
55.00
35.00
15.00
-5.00
%CD11b++ cells
Patient sample
Experimental sample
*
*
*
Fresh
Transfix
Cryopreserved
Method

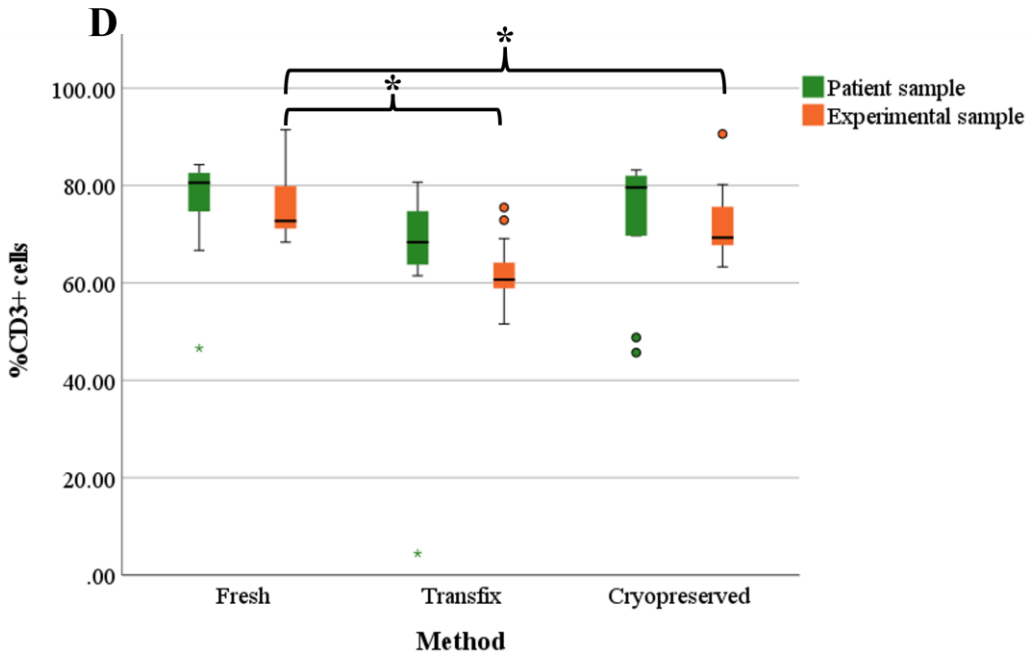

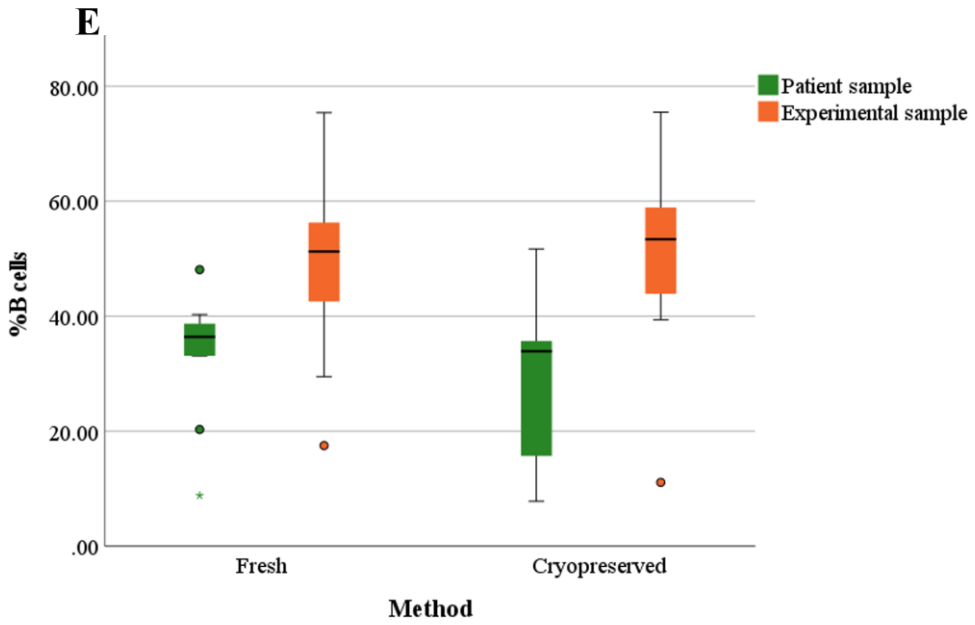

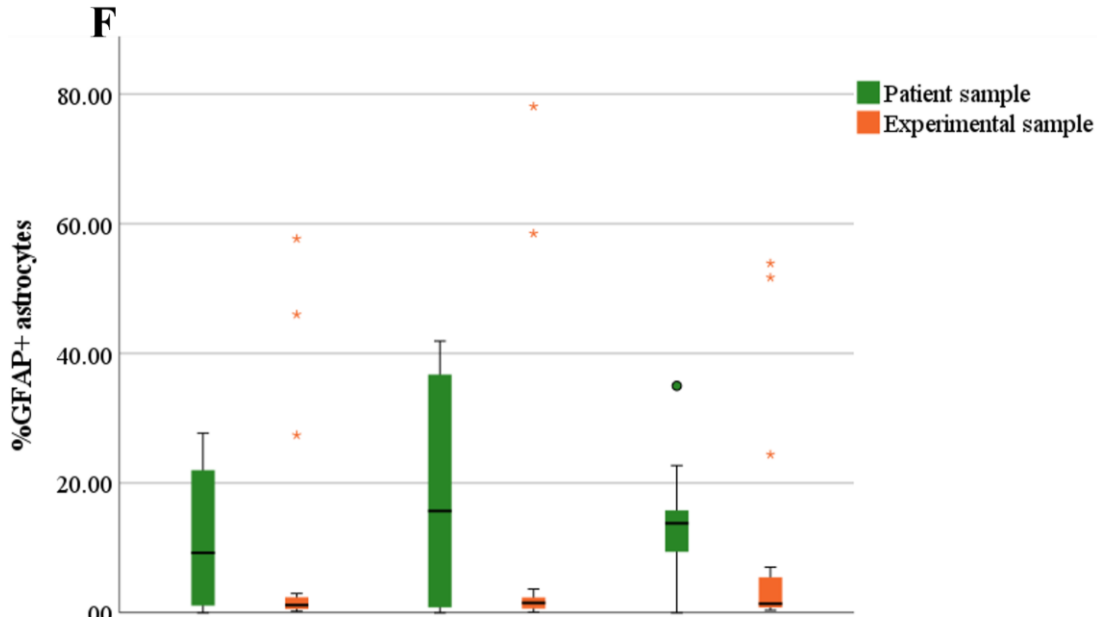

Figure 4: Boxplots comparing cell percentages by method in patient & experimental samples. (A) %viable cells **(B)** %CD45^{+} cells **(C)** %CD11b^{++} **(D)** %CD3^{+} **(E)** %B cells **(F)** %GFAP^{+} astrocytes. Significance ($p<0.05$) indicated by the asterisk (*)

Fresh

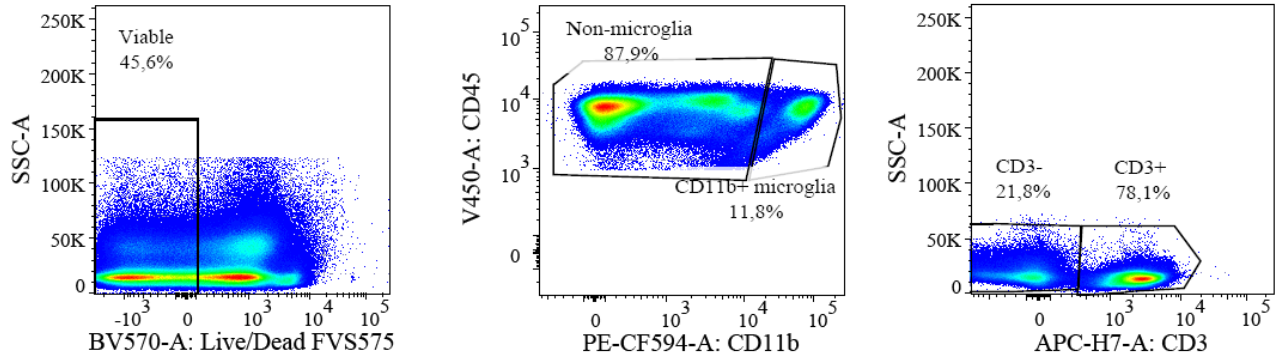

Cryopreservation

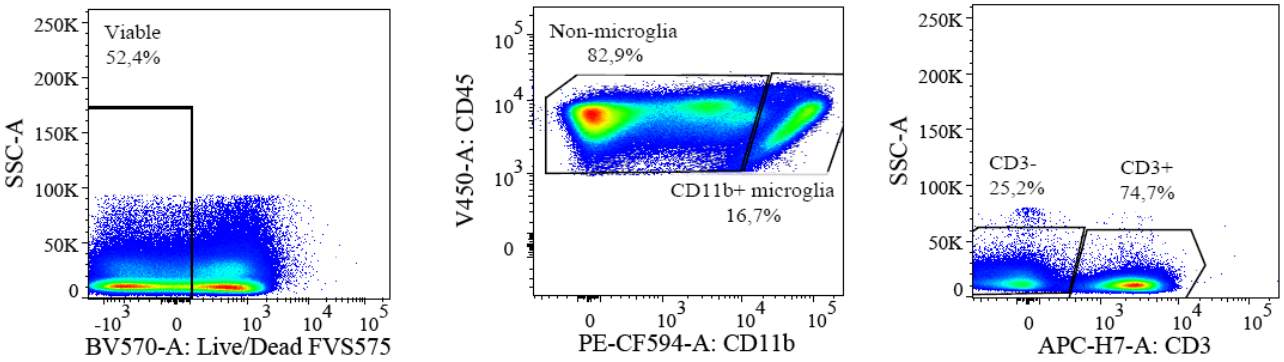

Figure 5: Example of varying cell percentage differences observed in Fresh versus Cryopreservation methods for experimental samples. $CD45^{+}CD11b^{+}$ (non-microglia) and $CD3^{+}$ cell percentages were higher in the Fresh method. Whereas cell viability and $CD11b^{++}$ (microglia) percentages were higher in Cryopreservation method in this example. Data from same sample.

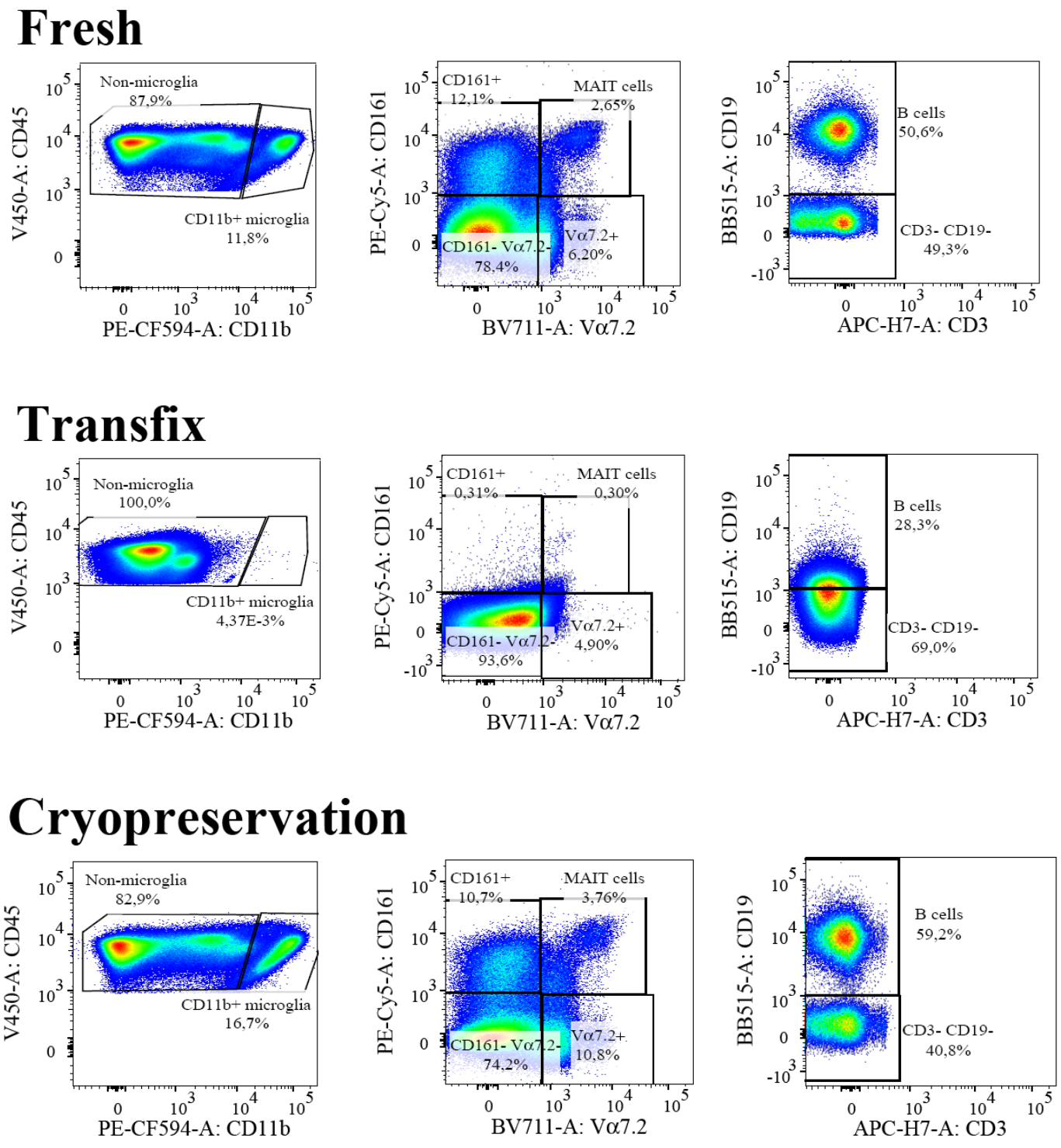

Figure 6: Example of cell populations that were not clearly distinguishable in Transfix compared to Fresh and Cryopreservation methods. $CD45^{+}CD11b^{+}$ (non-microglia), $V\alpha7.2^{+}$, and B cells could not be clearly defined in Transfix. Data from same sample.

Table 7: Summary statistics of cell percentages across methods for patient samples

	Fresh	Transfix	Cryopreservation
Patient samples			
Viable cells	41.8 (30.9-47.6)		33.2 (21.2-39.7)
$CD45^+$ cells	83.4 (73.8-95.5)	64.6 (54.35-87.1)	56.5 (36.8-98.7)
$CD11b^{++}$ cells	2.64 (1.53-8.06)	0.028 (0.01-0.05)	2.68 (0.86-7.58)
$CD45^+CD11b^+$ cells	97.1 (91.6-98.4)		97.1 (92.2-99.1)
$CD3^+$ cells	80.6 (74.7-82.6)	68.4 (63.75-74.75)	79.6 (69.7-82)
γδ TCR^+ cells	1.51 (1.32-2.8)	3.14 (1.85-10.06)	1.25 (0.83-1.54)
$CD161^+$ cells	25.1 (21.5-28.7)	6.22 (5.32-20.99)	23.1 (21.9-27.5)
$CD4^+$ cells	69.1 (648-70.4)	47.7 (39.4-53.7)	68.9 (67-71.5)
$CD8^+$ cells	19.6 (18.4-21.2)	12 (8.83-15.15)	19.8 (17.7-23.1)
MAIT cells	0.88 (0.63-1.71)	0.45 (0.22-3.96)	0.83 (0.71-1.02)
$Vα7.2^+$ cells	8.46 (6.17-12.4)		6.74 (6.4-7.32)
B cells	36.4 (33.1-38.7)		33.9 (15.7-35.7)
NK cells	62.3 (52.3-73.2)	18 (11-23.6)	66.1 (44.9-70.6)
Classical monocytes	2.99 (0.44-4.96)	4.91 (3.5-6.73)	0.96 (0.45-2.68)
Non-classical monocytes	34.2 (24.9-43.2)	0.07 (0.02-0.60)	37.2 (17.3-39.1)
$CD69^+$	41.2 (38.28-43)	3.25 (1.86-12.9)	42.5 (32.3-48.6)
$HLA\text{-}DR^+$	21.7 (17.9-28.4)	9.84 (7.51-25.02)	24.9 (23.1-35.9)
$GFAP^+$ astrocytes	9.24 (1.09-22)	15.7 (0.83-36.75)	13.8 (9.4-15.8)

Note: Transfix data excluded for $CD45^+CD11b^+$, $Vα7.2^+$, and B cells. Values reported as median (interquartile range). Abbreviations: CD, cluster of differentiation; GFAP, glial fibrillary acidic protein; HLA-DR, human leukocyte antigen-DR; MAIT, mucosal associated invariant T cell; NK, natural killer; TCR, T cell receptor.

Table 8: Summary statistics of cell percentages across methods for experimental samples

	Fresh	Transfix	Cryopreservation
Experimental samples			
Viable cells	47.15 (43.8-48.65)		43.3 (40.9-46.05)
$CD45^+$ cells	93.3 (78.9-98.8)	92.6 (84.05-96.3)	97.1 (93.23-98.53)
$CD11b^{++}$ cells	9.34 (7.37-13.03)	0.021 (0.01-0.06)	14.35 (11.06-16.78)
$CD45^+CD11b^+$ cells	91.25 (86.95-92.63)		86.25 (84.25-88.55)
$CD3^+$ cells	72.75 (71.25-79.15)	60.7 (58.9-64.2)	69.3 (67.83-75.13)
γδ TCR^+ cells	0.48 (0.2-1.43)	1.95 (1.28-5.21)	0.38 (0.18-1.01)
$CD161^+$ cells	10.9 (9.13-11.7)	4.27 (1.76-7.56)	11.3 (9.70-12.73)
$CD4^+$ cells	87.1 (72.95-89.53)	47.6 (33.7-53.55)	82.35 (74.23-87)
$CD8^+$ cells	10.37 (7.38-19.28)	13.9 (10.4-21.15)	13.5 (9.58-20.58)
MAIT cells	6.38 (1.41-8.83)	1.39 (0.59-2.23)	5.71 (1.39-7.29)
$Vα7.2^+$ cells	16.75 (11.48-23.2)		13.55 (10.48-21.63)
B cells	51.25 (42.83-55.2)		53.4 (45.2-58.8)
NK cells	32.5 (21.63-41.15)	3.64 (2.73-4.69)	26.75 (16.85-36.9)
Classical monocytes	1.12 (0.80-3.17)	7.75 (5.06-13.2)	1.87 (0.82-3.30)
Non-classical monocytes	58.6 (55.93)	0.69 (0.29-1.35)	60.4 (57.18-63.6)
$CD69^+$	0.98 (0.46-1.87)	0.02 (0.01-0.05)	0.97 (0.01-1.53)
$HLA\text{-}DR^+$	2.21 (1.75-2.71)	0.91 (0.55-1.17)	2.22 (1.53-2.83)
$GFAP^+$ astrocytes	1.17 (0.60-2.32)	1.51 (0.65-2.36)	1.39 (0.81-5.15)

Note: Transfix data excluded for $CD45^+CD11b^+$, $Vα7.2^+$ and B cells. Values reported as median (interquartile range). Abbreviations: CD, cluster of differentiation; GFAP, glial fibrillary acidic protein; HLA-DR, human leukocyte antigen-DR; MAIT, mucosal associated invariant T cell; NK, natural killer; TCR, T cell receptor.

2. Assessing the level of agreement between methods

In the Fresh vs Cryopreservation method comparison, all major cell types were included in the analyses; whereas in the Fresh vs Transfix method comparison, only cell types that could be clearly defined during flow gating were included. Results for patient and experimental samples are illustrated in Figures 7 & 8, and Figures 9 & 10, respectively.

2.1 Patient samples

The estimated level of agreement was greater between Fresh and Cryopreservation (mean of differences=3.19) methods than between Fresh and Transfix methods (mean of differences =14.82). This was further emphasized by the range of the limits of agreement, with Fresh and Cryopreservation having a smaller range (-22.54 to 28.92) compared to Fresh and Transfix methods (-21.68 to 51.33). Both Fresh vs Cryopreservation and Fresh vs Transfix methods had a significant positive correlation of r=0.91 (*p<0.001*) and r=0.81 (*p<0.001*), respectively.

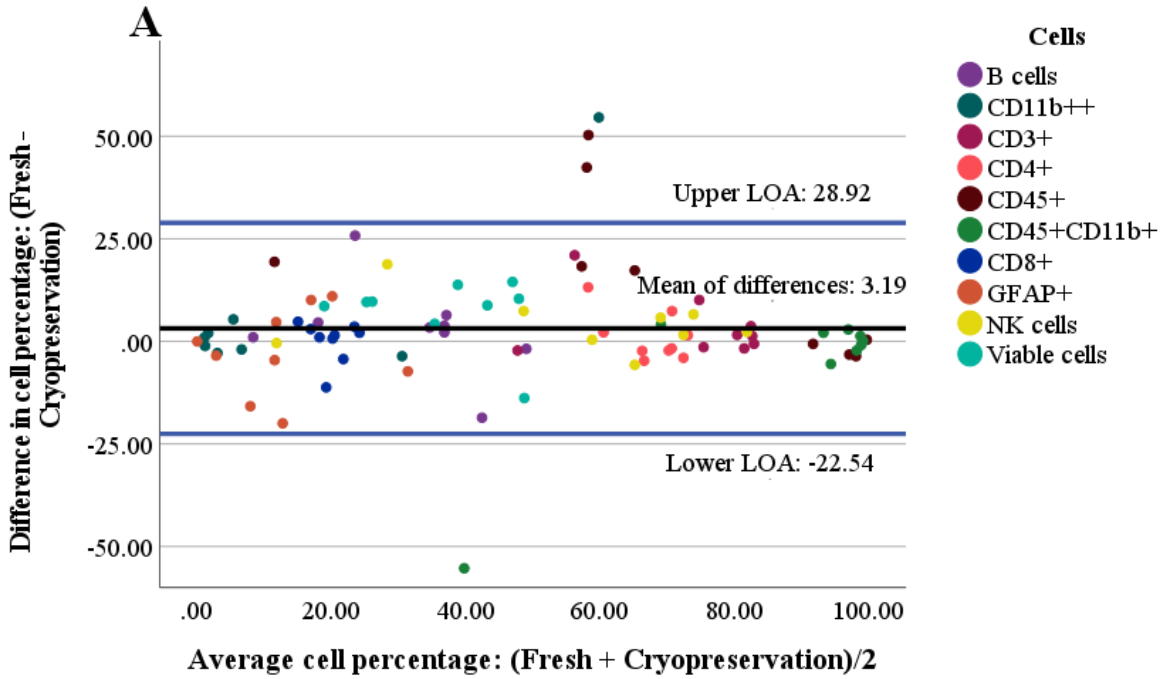

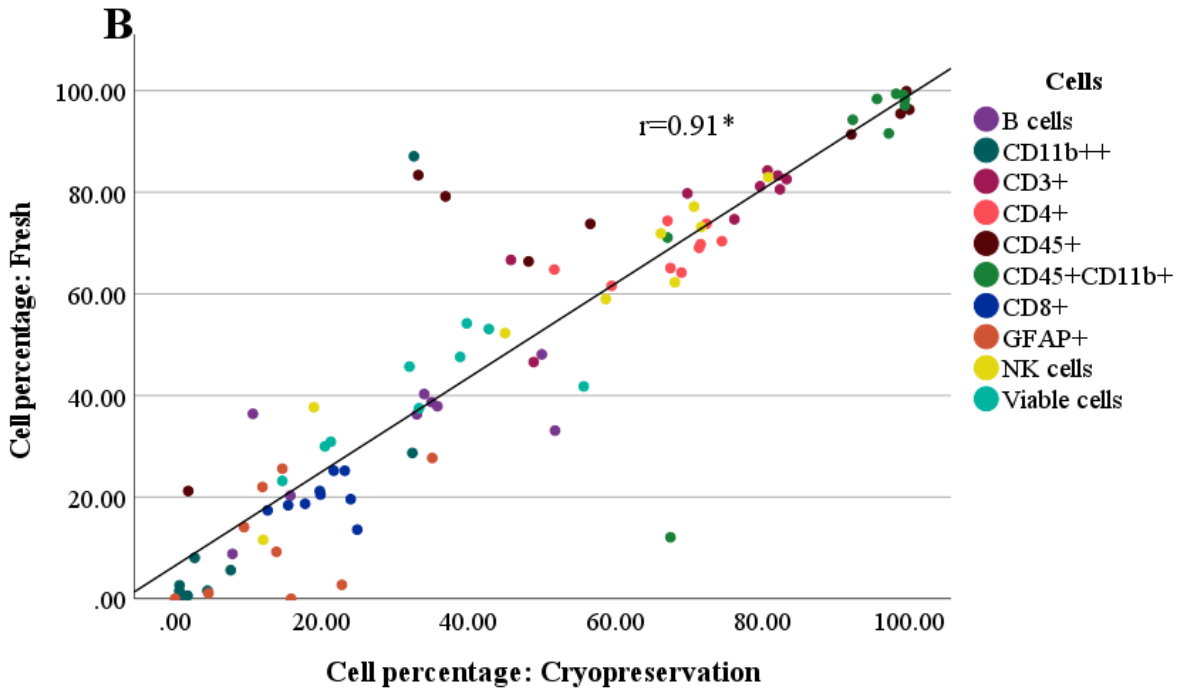

Figure 7: Assessing the level of agreement between Fresh & Cryopreservation methods in patient samples. (A) Bland-Altman plot of the differences in cell percentages between Fresh and Cryopreservation methods vs the average of the two methods. The bias (3.19) is represented by the mean of differences, with the upper-and lower levels of agreement (LOA) displayed as horizontal lines on the plot. **(B)** The correlation scatterplot between Fresh and Cryopreservation methods for all major cell types. A significant positive correlation (r=0.91) between methods was observed. The cell types assessed are colour-coded as represented by the legend.

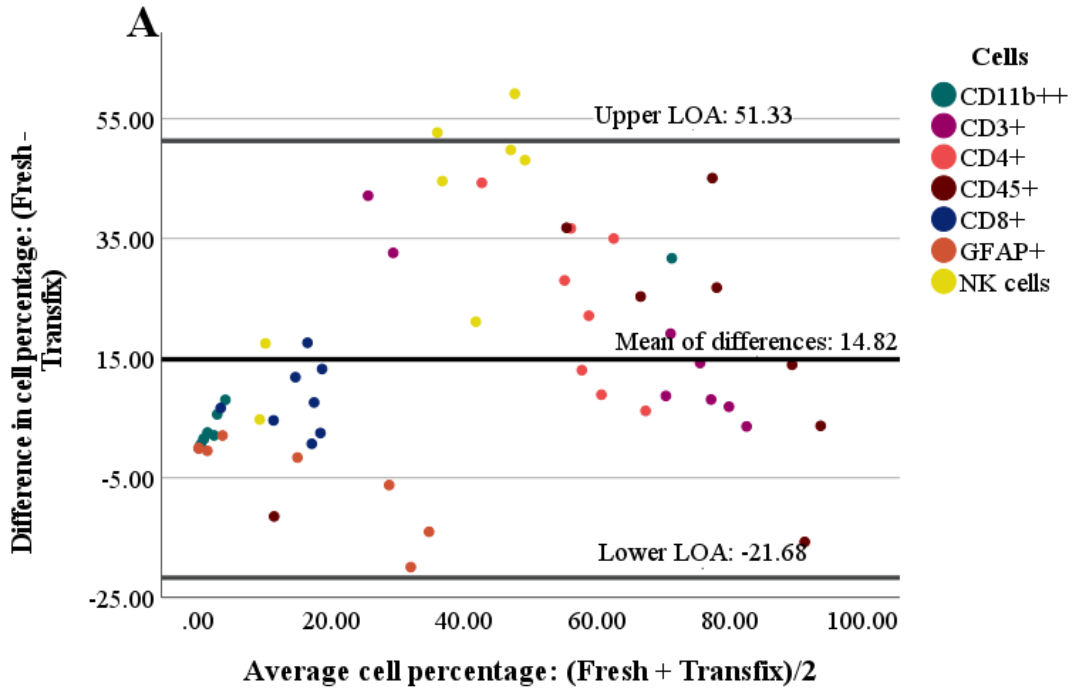

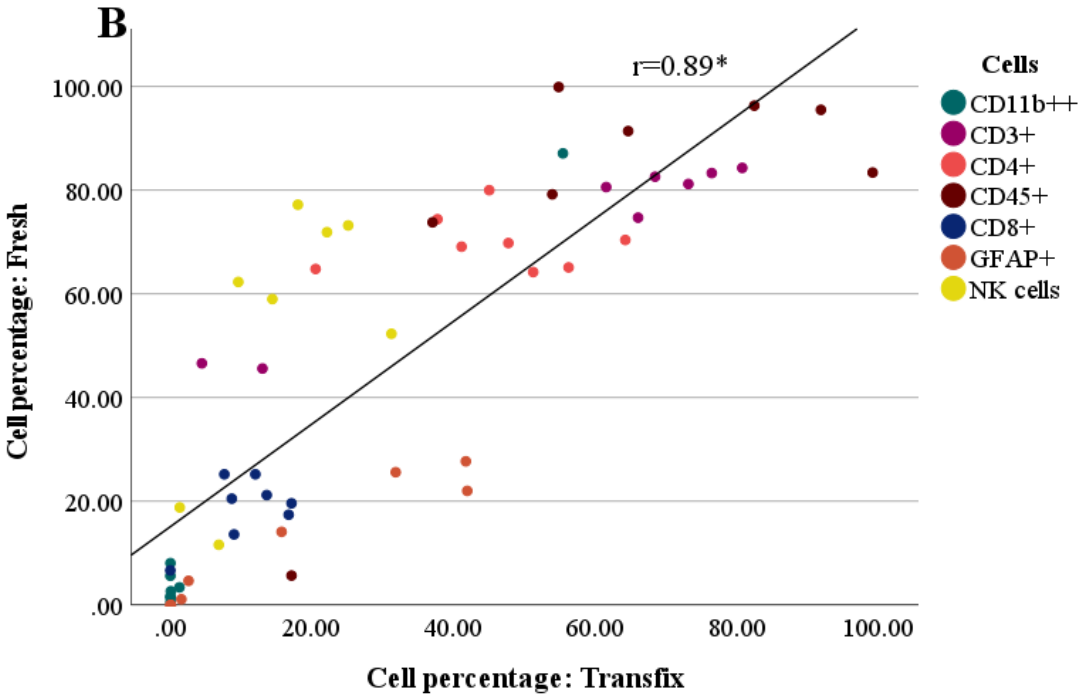

Figure 8: Assessing the level of agreement between Fresh & Transfix methods in patient samples. (A) Bland-Altman plot of the cell percentage differences between Fresh and Transfix methods vs the average of the two methods. The bias (14.82) is represented by the mean of differences, with the upper-and lower levels of agreement (LOA) displayed as horizontal lines on the plot. **(B)** The correlation scatterplot between Fresh and Transfix methods for all major cell types. A significant positive correlation (r=0.89) between methods were observed. The cell types assessed are colour-coded as represented by the legend.

2.2 Experimental samples

Similar to patient samples, Fresh and Cryopreservation methods demonstrated a better level of agreement compared to Fresh and Transfix methods, with the mean of differences being 0.13 and 12.38, respectively. The range of the limits of agreement were also larger between Fresh and Transfix methods (-22.22 to 46.97) than in Fresh and Cryopreservation methods (-14.21 to 14.47). Both sets of methods comparisons showed a significant positive correlation, r=0.97 ($p<0.001$) for Fresh vs Cryopreservation and r=0.81 ($p<0.001$) for Fresh vs Transfix methods.

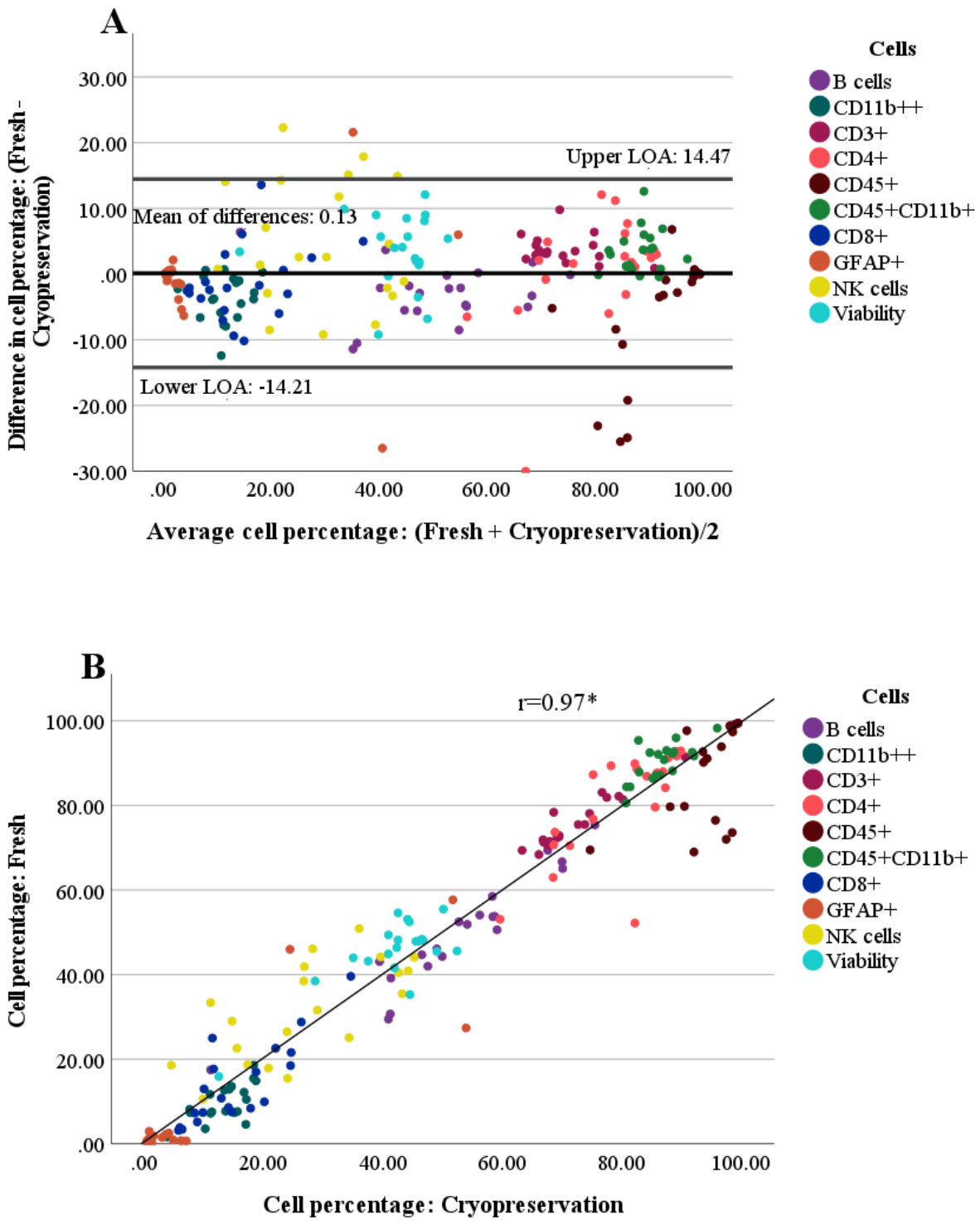

Figure 9: Assessing the level of agreement between Fresh & Cryopreservation methods in experimental samples. (A) Bland-Altman plot of the cell percentage differences between Fresh and Cryopreservation methods vs the average of the two methods. The bias (0.13) is represented by the mean of differences, with the upper-and lower levels of agreement (LOA) displayed as horizontal lines on the plot. **(B)** The correlation scatterplot between Fresh and Cryopreservation methods for all major cell types. A significant positive correlation (r= 0.97) between methods were observed. The cell types assessed are colour-coded as represented by the legend.

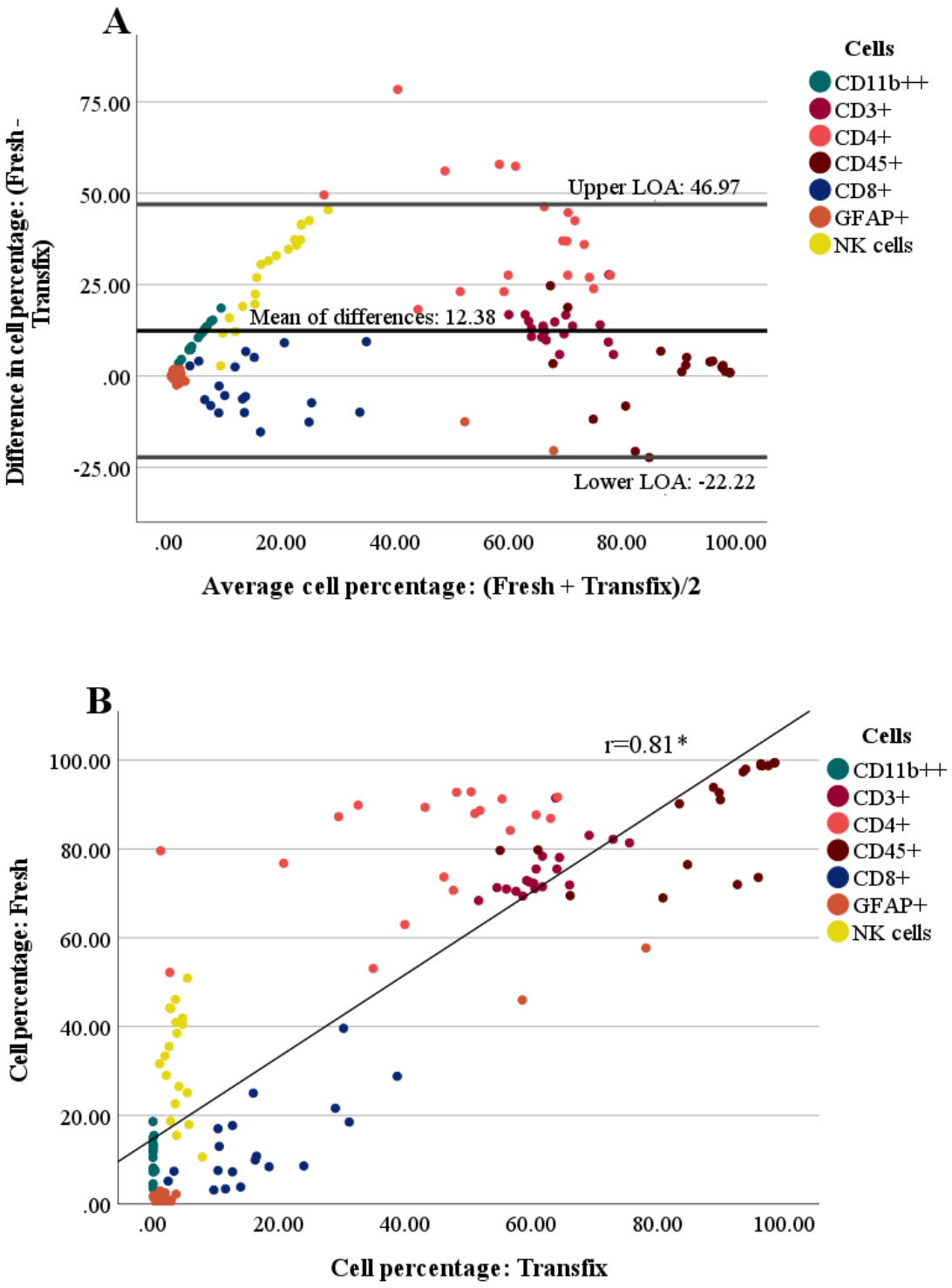

Figure 10: Assessing the level of agreement between Fresh & Transfix methods in experimental samples. (A) Bland-Altman plot of the cell percentage differences between Fresh and Transfix methods vs the average of the two methods. The bias (12.38) is represented by the mean of differences, with the upper-and lower levels of agreement (LOA) displayed as horizontal lines on the plot. **(B)** The correlation scatterplot between Fresh and Transfix methods for all major cell types. A significant positive correlation (r^2= 0.81) between methods were observed. The cell types assessed are colour-coded as represented by the legend.

3. Effects of long-term storage of CSF in Transfix

Certain subsets of cells appeared to be negatively impacted following 2 week storage of CSF in Transfix. Clear separation of populations were not possible in Transfix-treated CSF as compared to freshly processed CSF (Figure 11).

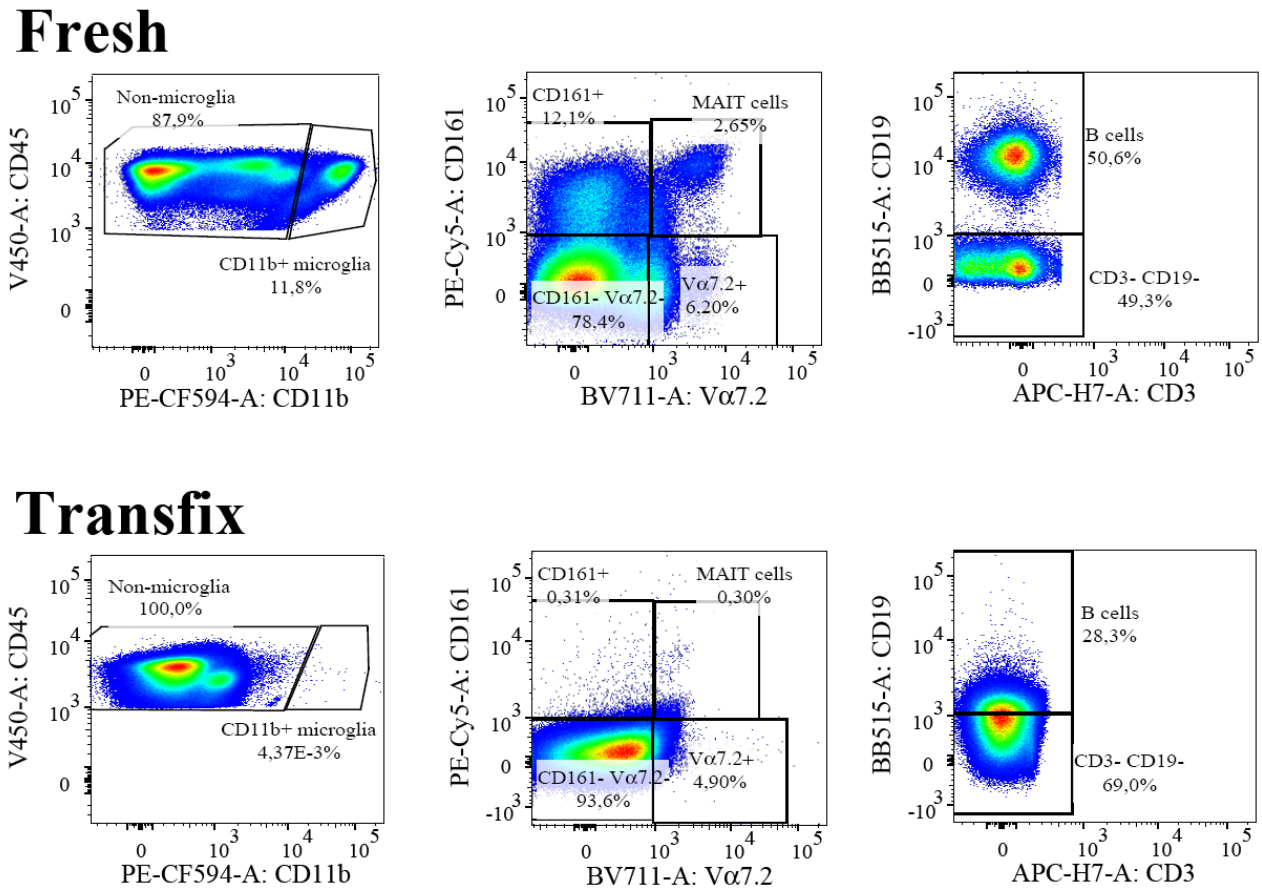

Figure 11: An example of the effects of two week storage of CSF in Transfix. Fluorescent signals of certain cell populations appeared to decrease following two week storage in Transfix compared to Fresh CSF. These observations were apparent in Transfix-treated CSF of both patient and experimental samples.

4. Duration of storage comparison of Transfix-treated experimental CSF samples

Results are displayed in the heatmap table (Table 9). CSF stored in Transfix for 24 hours yielded significantly higher $CD45^{+}$ ($p=0.05$), $CD11b^{++}$ ($p=0.046$), $CD161^{+}$ ($p=0.046$), MAIT ($p=0.05$), and $V\alpha7.2^{+}$ ($p=0.046$) cell percentages compared to the Fresh method. However, in comparison to 1 week and 2 week storage in Transfix, the Fresh method still yielded significantly higher cell percentages. Additionally, for the remaining cell populations and activation marker, the Fresh method yielded significantly higher percentages compared to 24 hours, 1 week, and 2 week storage in Transfix (see Appendix E for *p* values).

Table 9: Duration of storage comparison of cell percentages between Fresh vs Transfix methods

	Fresh	24 hour	1 week	2 week
$CD45^+$ cells				
$CD11b^{++}$ cells				
$CD45^+CD11b^+$ cells			X	X
$CD3^+$ cells				
γδ TCR^+ cells				
$CD161^+$ cells				
$CD4^+$ cells				
$CD8^+$ cells				
MAIT cells				
$Vα7.2^+$ cells			X	X
B cells			X	X
NK cells				
Classical monocytes				
Non-classical monocytes				
$HLA\text{-}DR^+$				
$GFAP^+$ astrocytes				

Cell percentages were compared between fresh CSF and Transfix-treated CSF (n=3) stored for 24 hours, 1 week and 2 weeks. Green boxes signify no statistically significant difference between methods, whereas red boxes signify a statistically significant difference. Boxes demarcated with "X" represent cell populations that could not be accurately distinguished. Statistical significance was set at 0.05. CD, cluster of differentiation; HLA-DR, human leukocyte antigen-DR; GFAP, glial fibrillary acidic protein; TCR, T-cell receptor.

5. Influence on fluorescent signal

Results for patient and experimental samples are illustrated in Figures 12 & 13, respectively.

Fresh versus Cryopreservation: Significantly higher MFIs for $CD19^+$ (*p=0.024*) were observed for the Fresh method in patient samples. In experimental samples, the Fresh method yielded significantly higher MFIs for $CD45^+$ (*p=0.009*) and $CD19^+$ (*0.001*), whereas the Cryopreservation method yielded significantly higher MFI for $CD11b^+$ (*p=0.021*).

Fresh versus Transfix: In patient samples, MFI values for $CD19^+$ (*p=0.01*) and $CD3^+$ (*p=0.001*) markers were significantly higher in the Fresh method. Similar findings were also observed for MFI values of $CD19^+$ (*p=0.00*) and $CD3^+$ (*p=0.00*) markers in experimental samples. In addition, $CD45^+$ (*p=0.009*) and $CD11b^+$ (*p=0.00*) MFIs were significantly higher for the Fresh method in experimental samples.

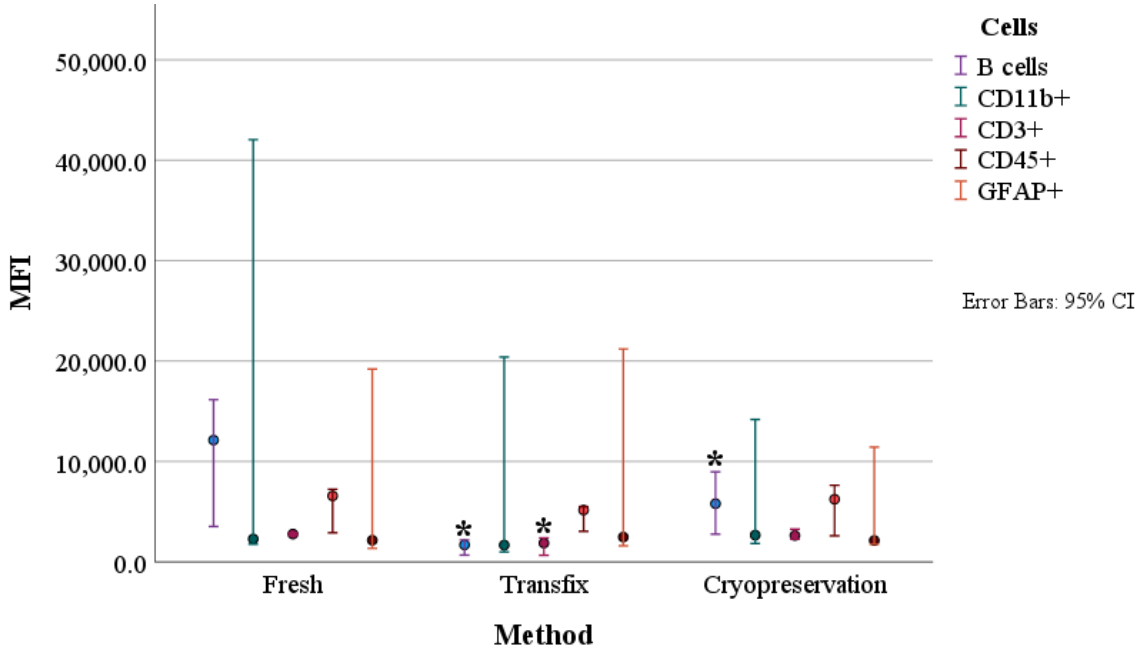

Figure 12: Difference in median fluorescent intensities (MFI) of cell markers between methods in patient samples. $CD19^+$, $CD11b^+$, $CD3^+$, $CD45^+$, and $GFAP^+$ cell markers were assessed. Median MFI values are plotted on the y-axis, with 95% confidence intervals (CI) represented by the error bars. Statistically significant differences in comparison to Fresh are illustrated with an asterisk (*****, $p<0.05$).

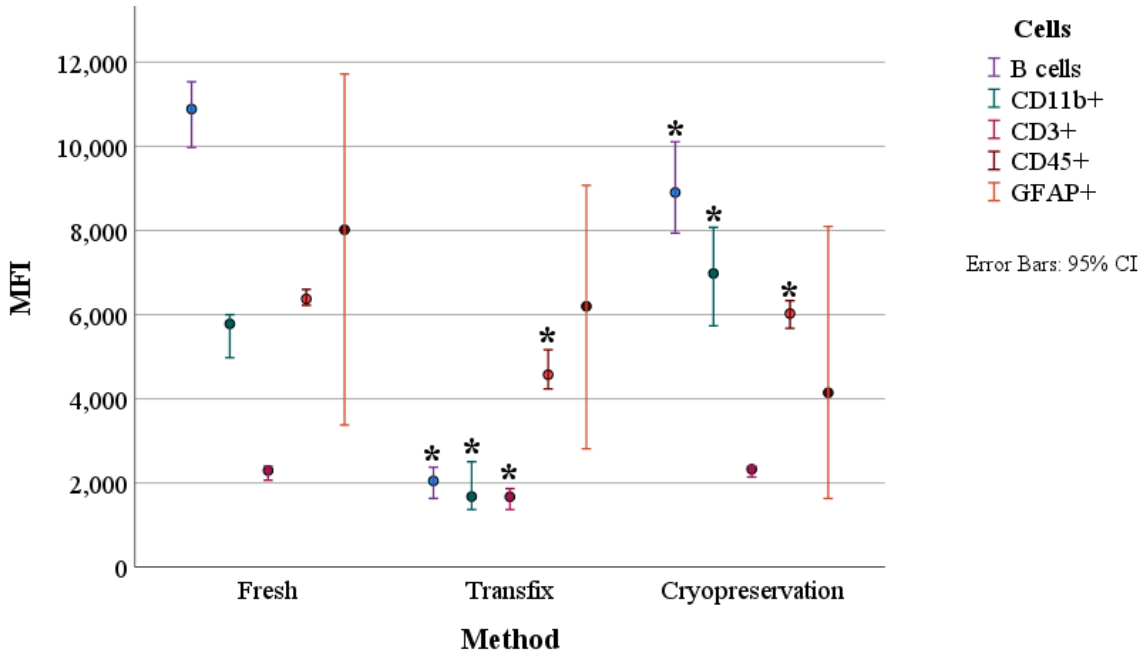

Figure 13: Difference in median fluorescent intensities (MFI) of cell markers between methods in experimental samples. CD19+, CD11b+, CD3+, CD45+, and GFAP+ cell markers were assessed. Median MFI values are plotted on the y-axis, with 95% confidence intervals (CI) represented by the error bars. Statistically significant differences in comparison to Fresh are illustrated with an asterisk (*****, $p<0.05$).

6. Case presentation

Of the 9 cases in the patient cohort, the only time-linked lumbar and ventricular CSF and serial samples obtained were from a 12 year old male patient with TBM. Here we report compartmental differences in percentages of peripheral and brain-derived immune cells observed over the course of their hospital stay. Only one time-linked sample was obtained on admission, additional ventricular and lumbar CSF were collected on Day 2 and Day 3, respectively. Statistical analyses were not performed given the low number of lumbar (n=2) and ventricular (n=2) samples collected from this patient. Percentage $CD45^+$ cells remained stable over time, whereas percentages $CD11b^+$ microglia increased over time. Both $CD45^+$ and $CD11b^+$ percentages were slightly higher in lumbar CSF, similar to the routine white cell count which was 178 000 cells/ml in lumbar CSF and 117 000 cells/ml for ventricular CSF. $GFAP^+$ astrocytes were only found in ventricular CSF with an increase in percentages observed over time. Data shown in Figure 14.

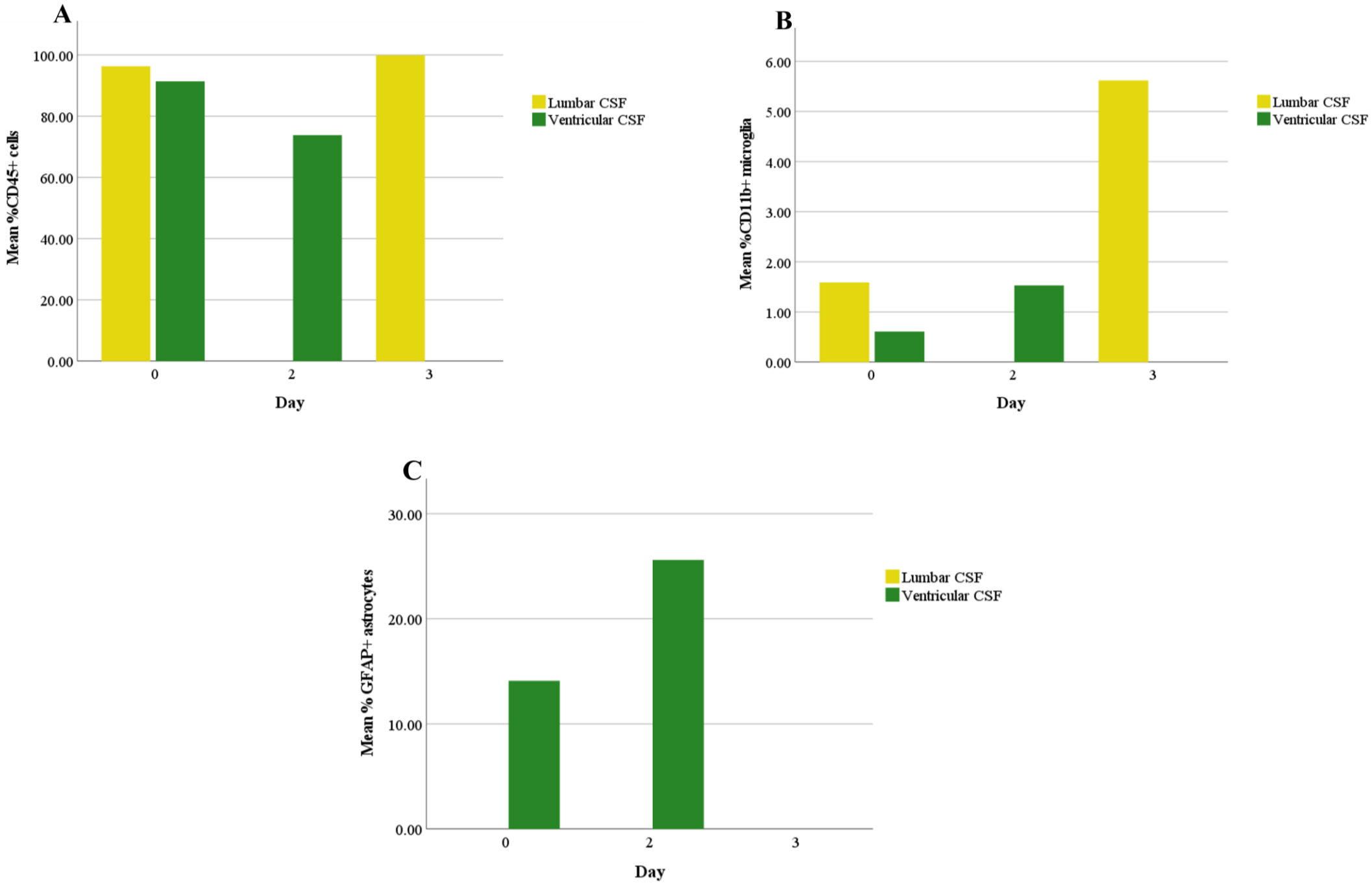

Figure 14: Compartmental differences in cell percentages over time: a case illustration. (A) %CD45^{+} cells **(B)** %CD11b^{+} microglia **(C)** %GFAP^{+} astrocytes. Day 0; admission.

CHAPTER 8: DISCUSSION

Immunophenotyping by flow cytometry has become an increasingly popular technique for the analysis of CSF samples. The application of this technique in clinical research of CNS pathologies would be particularly advantageous given its ability to rapidly assess various cell populations simultaneously and provide valuable information on their phenotypes giving a better understanding of the ongoing immunopathological processes at the site of disease. The highly perishable nature of CSF following sampling, and low baseline cell numbers, are however factors that hinder the use of flow cytometric analysis of these samples. Immediate processing and analysis of CSF samples is impractical, especially in resource-limited settings with no available flow cytometer on site, and in busy clinical environments where sample collection occurs at unpredictable times.

Currently used reagents such as Transfix, and serum-containing media only prevent cell loss for a short period of time. Therefore, finding an alternative method that allows long-term storage of CSF samples, whilst still being able to identify different cell populations with accuracy similar to freshly processed CSF, is highly desirable.

In this study, CSF samples were prospectively collected, and the long-term storage effects of cryopreservation and Transfix on peripheral and brain-derived immune cell percentages and proportions were assessed by flow cytometric analysis and compared to freshly processed CSF (current gold standard).

Cryopreserving CSF

Significant differences in viability, $CD11b^{++}$, $CD45^{+}CD11b^{+}$, and $CD3^{+}$ cell percentages between Fresh and Cryopreservation methods were only observed in experimental samples and not patient samples. Although significant, these differences were small, median values of certain cells were either closely related and, in some cases, higher in Cryopreserved CSF than in Fresh CSF. Furthermore, these cell populations could still be accurately and clearly defined in cryopreserved CSF. Overall, the Cryopreservation method demonstrated highly comparable results to the Fresh method in both patient and experimental samples with small variation in the results and little bias in the variability (respective mean differences of 3.19 and 0.13). In combination these results suggest that cryopreservation may serve as an alternative method to running samples fresh.

Storing CSF in Transfix

Transfix yielded significantly lower percentages of $CD11b^{++}$, $CD4^{+}$, $CD8^{+}$, non-classical monocytes, and NK cells, as well as lower percentages of CD69 activation marker in patient samples. Similar findings were observed in experimental samples, with the exception of $CD8^{+}$ cells. In addition, Transfix also yielded significantly lower percentages of $CD3^{+}$, $CD161^{+}$, MAIT cells, classical monocytes, and HLA-DR activation marker in experimental samples. In both patient and experimental samples, $V\alpha7.2^{+}$, $CD45^{+}CD11b^{+}$, and B cell ($CD19^{+}$) populations could not be clearly identified during gating leading to the exclusion of these cells from the statistical analyses. Transfix showed poor comparability to the Fresh method, with mean differences of 14.82 and 12.38 reported in patient and experimental samples, respectively, suggesting large variation in the results with clear biases in variation for specific cell types from the Transfix method.

The 2 week storage period of CSF in Transfix potentially played a role in the afore-mentioned findings. The maximum storage periods used in previous studies were 18-72 hours[130, 135], and our 24 hour storage of CSF in Transfix yielded significantly higher percentages of $CD45^{+}$, $CD11b^{++}$, $CD161^{+}$, $V\alpha7.2^{+}$ and MAIT cells relative to Fresh CSF. This is similar to the findings of De Jongste *et al* who reported significantly higher absolute counts of lymphocytes in Transfix-treated CSF after 18 hours of storage compared to CSF collected in serum-containing media[130]. Nonetheless, the Fresh method still yielded significantly higher percentages compared to the 24 hour storage time for $CD45^{+}CD11b^{+}$, $V\alpha7.2^{+}$ and B cells, and clear separation of these cells were not possible after 1 week of storage in Transfix. These results suggest that Transfix, even following 24 hour storage, is not a suitable cell stabilizing agent for markers of major cell populations such as B cells, NK cells, and monocytes, and minor cell populations including MAIT cells or activation markers. Additionally due to the fixative in the Transfix, no additional functional assays can be performed on CSF samples.

Influence on fluorescent signal

Significantly lower MFI values were observed in cryopreserved and Transfix-treated CSF, however, the difference in mean ranks between the two separate comparisons was greater in Fresh vs Transfix than in Fresh vs Cryopreservation methods. This could be due to the length of storage time of cells in cryo-solution (1 month) and Transfix (2 weeks), the freeze-thaw cycle in the Cryopreservation method, and the additional wash steps included in both

methods which may have caused a loss of epitopes on the cell. Fixation with formaldehyde, although advantageous, can mask epitopes through crosslinking and make it more difficult for antibodies to bind to their target sites. All three methods included a fixation step, but as shown in a previous study[136], the timing of this step appears to be of significance. The fixation step in both Fresh and Cryopreservation methods was included after antibody staining, the difference in mean ranks was smaller between these methods; whereas in Transfix, fixation occurs immediately once CSF is added to the tube, and a greater difference in mean ranks was observed. Therefore, fixation prior to antibody staining may reduce available epitopes on cell surfaces.

The loss of fluorescent signal in cryopreserved CSF did not, however, appear to negatively impact on determining cell proportions and cell populations could be easily distinguished, unlike in Transfix-treated CSF.

Low cell viability in patient and experimental samples

Low percentages of viable cells were observed in freshly processed and cryopreserved CSF in both patient and experimental samples. This was an unexpected finding, especially for freshly processed CSF seeing as serum-containing media was added immediately after collection and processing occurred within an hour. A possible explanation for this in patient samples could be the presence of exotoxins within CSF. The majority of exotoxins are polypeptides that are produced by pathogenic Gram-positive and Gram-negative bacteria[137]. Exotoxins are responsible for inducing apoptotic and- or necrotic cell death of host immune cells during infection[138]. Thus, the low cell viability observed in patient samples may be a result of cells having undergone cell death prior to CSF sampling and may therefore, not be a reflection of systematic error introduced by the processing methods. The addition of streptomycin/penicillin to media and cryo-solution may improve cell viability, these antibiotics were included in the serum-containing media used by De Graaf et al who reported improved viability in CSF cells[10]. Low cell viability in the experimental samples may have been a result of the multiple freeze thaw cycles the PBMCs underwent; the first occurred when the PBMCs were isolated and cryopreserved for subsequent spiking, and the second was during the Cryopreservation method.

Presence of GFAP$^+$ astrocytes in experimental samples

Low percentages of GFAP$^+$ astrocytes were quantified in experimental CSF samples, which was unexpected given that these samples were spiked with peripheral leukocytes only.

Although the CSF samples were obtained from patients with non-infectious CNS conditions, 85% of this cohort had hydrocephalus. Hydrocephalus is a condition which develops from the excessive accumulation of CSF in the ventricles which increases the intracranial pressure[26]. The increased pressure on the brain tissue can cause significant damage to brain cells and if left untreated can be fatal. Significantly elevated levels of GFAP have been previously found in the CSF of patients with hydrocephalus, which may be indicative of reactive astrogliosis in response to raised pressure, especially in the ependyma (tissue surrounding the ventricles)[139]. The presence of $GFAP^+$ astrocytes in our experimental CSF samples could, therefore, be a result of the brain's response to hydrocephalus.

Patient and experimental samples

Results in experimental samples demonstrated greater differences between CSF processing methods relative to patient samples. There are a few important considerations to interpreting these differences. The sample size of patient samples was smaller (n=9) compared to that of experimental samples (n=20), therefore significant differences in cell percentages in patient samples may have been missed. Although experimental samples contained much higher cell counts (approximately 1 million cells/ml) whereas patient samples had a much lower cell count (127 000 cells/ml), those PBMCs underwent two freeze-thaw cycles which may have contributed to cell death. Importantly, patient samples were obtained from paediatric patients and represent the real world context of CNS infection, in that the cells are part of an ongoing inflammatory disease process. On the contrary, experimental samples represented an artificial environment as the isolated PBMCs used for spiking were drawn from healthy adult volunteers. It is possible that the health status and the known differences in the distribution of cell populations between adults and children[140] may have influenced the results. Given the goal of applying cryopreservation to paediatric CSF to address questions relating to CNS infection, the results from patient samples are promising.

Case presentation

Differences in the composition of ventricular and lumbar CSF, especially in conditions of CNS infection like TBM, have been well established at a protein and molecular level[2, 141]. Ventricular CSF is drawn from the ventricles located in the brain and provides a more robust picture of disease processes occurring at the site of disease in the brain. Lumbar CSF is drawn from the spinal space which is downstream from the brain. Lumbar CSF cellular and analyte concentrations are therefore subject to degradation as they travel down the brain-

spinal axis (e.g., expression levels of GFAP differ depending on the proximity to the injury site, reviewed by Giovannoni and Quintana, 2020; Sofroniew, 2014)[83, 142], to stagnation of CSF flow due to spinal inflammatory exudate, and to the contribution of cells and molecules that represent spinal disease processes. However, the difference in flow cytometric data between these CNS compartments has not, to our knowledge, been investigated.

In TBM brain-derived biomarker concentrations are higher in ventricular CSF and inflammatory biomarkers and cell numbers are higher in lumbar CSF given the presence of concurrent spinal disease[2, 141, 143]. In this study time-linked lumbar and ventricular CSF, and serial CSF samples were obtained in one TBM patient. Although significance could not be tested, differences in cell percentages were observed over time and between lumbar and ventricular compartments. In this study, leukocyte percentages were higher in the lumbar CSF, which mirrors the higher white cell count and inflammatory protein and molecular signatures associated with lumbar CSF. On the other hand, $GFAP^+$ astrocytes were not found in the lumbar compartment but were documented in the ventricular CSF, which is plausible given that ventricular CSF is closer to the site of injury. Furthermore, this patient had evolving basal ganglia infarcts between their admission and follow-up CT scans, which was mirrored by the apparent increase in $GFAP^+$ astrocyte percentages seen in the serial ventricular CSF samples taken over the same timeframe as the CT imaging. At a protein level, elevated levels of GFAP have been associated with larger, more severe brain infarcts[2, 144].

Limitations of the study

While this study is the first to report the effects of cryopreservation on CSF cells, there are certain limiting factors. The small sample size for patient samples may have resulted in significant differences in cell percentages being missed. However, this factor was difficult to control for given that patient recruitment was challenging during the COVID-19 pandemic. Experimental samples represent an artificial environment and the PBMCs used to spike the CSF were drawn from healthy adult volunteers, these cells may differ from paediatric patients that have an ongoing infectious processes. However, the experimental arm was added to compensate for poor patient recruitment and still provided valuable comparative data. Absolute numbers of cell populations were not assessed using true count beads in this study; however, the aim of this study was to assess whether cell proportions and phenotypes could be accurately identified following cryopreservation or Transfix storage, especially given that

cell counts have not demonstrated significant associations with outcomes from CNS infections[143]. CD11b was selected as a marker for microglia but it is not specific to brain-derived microglia, and is expressed by lymphocytes, monocytes, and neutrophils as well, this likely explains why these cells were seen in experimental samples. A more specific marker such as Transmembrane Protein (TMEM) 119, should rather be considered for future studies.

CHAPTER 9: CONCLUSION

Collection and analysis of CSF samples is essential to elucidate CNS disease processes in paediatric patients, therefore the correct and timely storage of these samples is crucial. Various populations of immune (peripheral and brain-derived) cells and their subsets could be reliably quantified in cryopreserved CSF, with different cell proportions well maintained. This study shows that cryopreservation, at the very least, addresses the increasing need of finding an easier and more effective way of long-term storage of CSF samples. Downstream functional assays should be feasible in cryopreserved CSF, unlike Transfix and CSF treated with serum-containing media, seeing as cells are isolated from the supernatant first before the addition of cryo-solution. The development of this method is fundamental in promoting translational research particularly in developing countries faced with high disease burden of CNS infections and limited laboratory resources. Further, it offers valuable opportunities for clinical research across a broad spectrum of CNS conditions beyond infection, examples include traumatic brain injury and brain cancers, and highlights the potential to freeze other surgical specimens for which the application of flow cytometry is currently limited by resource constraints and low cell counts. This method also allows CSF samples to be easily transported between sites in multi-centre studies and shared between research units, promoting collaborations between institutions.

APPENDIX A

Table 1: Calculated antibody titres

Antibody	MFI (-)	rSD (-)	MFI (+)	Stain index[a]	Dilution factor	Volume (µl)
CD3 APC-H7	70	101	6429	31.5	1:120	1.25
CD4 BV510	280	248	11388	22.4	1:120	1.25
CD8 PerCP-Cy5.5	59	42	5154	60.7	1:120	1.25
CD19 BB515	66	77	6265	40.3	1:480	0.31
CD14 BV605	26	24	721	14.5	1:60	2.5
CD16 PE-Cy7	12	97	859	7.3	1:120	1.25
Vα7.2 BV711	96	179	1732	4.6	1:120	1.25
γδ TCR BV 650	60	89	1035	5.5	1:120	1.25
CD45 V450	152	113	7194	31.2	1:120	1.25
HLA-DR BV786	66	137	12351	44.8	1:120	1.25
CD69 APC R700	16	30	219	3.38	1:120	1.25
CD56 APC[b]	9	18	451	12.28	1:60	5
CD161 PE-Cy5[b]	34	50	1065	10.31	1:60	5
GFAP PE	462	308	2388	296604	1:120	1.25
CD11b PE-CF594	140	177	30389	2677037	1:120	1.25

Serial dilutions were made for antibodies using the manufacturers' recommended volume as starting point. All manufacturers' recommended volumes were 5µl, unless stated otherwise. The stain index was calculated in order to obtain the optimal antibody titre which was used to prepare the antibody cocktail. Note: only the dilution factors resulting in the highest stain index are included in the Table. Abbreviations: APC-H, allophycocyanin hillite; BB, brilliant blue; BV, brilliant violet; CD, cluster of differentiation; GFAP, glial fibrillary acidic protein; HLA-DR, human leukocyte antigen-DR isotype; MAIT, mucosal associated invariant T cell; MFI, mean fluorescent intensity; NK, natural killer; PE, phycoerythrin; PerCP, peridinin-chlorophyll-protein complex; rSD, robust standard deviation.

[a] $Stain\ Index = \frac{MFI\ (+)\ population - MFI\ (-) population}{2 \times rSD\ (-)\ population}$

[b] The manufacturers' recommended volume was 10µl.

APPENDIX B

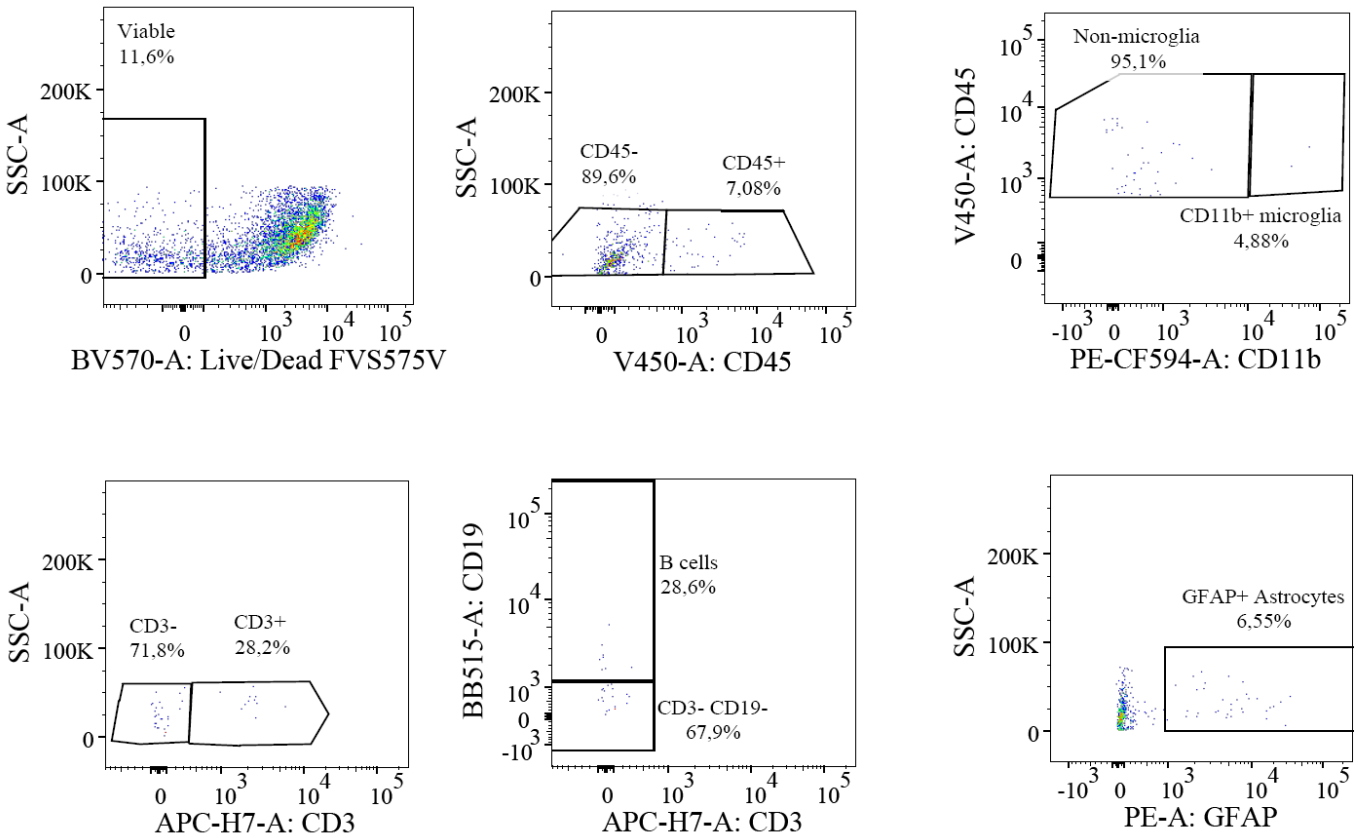

Figure 1: Flow cytometric data of excluded patient. Only major cell populations are shown. Patient was excluded from cohort due to low cell viability and cell percentages of major populations.

APPENDIX C

Table 1: Percentages of major cell populations per method in patient samples

	% Viable cells		% $CD45^+$ cells			% $CD3^+$ cells			% B cells		% $CD11b^+$ microglia			% $GFAP^+$ astrocytes		
Method	**F**	**C**	**F**	**T**	**C**	**F**	**T**	**C**	**F**	**C**	**F**	**T**	**C**	**F**	**T**	**C**
Patient ID																
1.1	37,5	33,2	66,4		48,1	79,8		69,7	20,3	15,7	0,67		0,86	2,74		22,7
2.1	54,2	39,7	95,5	91,8	98,7	74,7	66	76,1	8,83	7,82	2,64	0,064	0,62	27,7	41,7	35
3.1	47,6	38,8	91,4	64,6	92	81,2	73,1	79,6	40,3	33,9	0,61	0,028	1,71	14,1	15,7	9,4
3.2	53,1	42,7	96,3	82,4	99,9	83,3	76,4	82	38,7	34,9	1,59	3,75E-03	4,42	0	0	0
3.3	30	20,4	73,8	37	56,5	82,6	68,4	83,2	37,9	35,7	1,53	0,037	0,59	25,6	31,8	14,6
3.4	30,9	21,2	79,2	53,9	36,8	80,6	61,5	82,3	36,3	32,9	8,06	0,015	2,68	22	41,9	11,9
3.5	45,7	31,9	99,9	54,8	99,5	84,3	80,7	80,6	48,1	49,9	5,62	4,61E-03	7,58	0	0,096	15,8
4.1	23,2	14,6	83,4	99,1	33,1	46,6	4,45	48,8	33,1	51,7	87,1	77,1	32,5	1,09	1,56	4,55
5.1	41,8	55,6	21,2		1,8	66,7		45,7	36,4	10,6	28,7		32,3	9,24		13,8

Note: Patients 1.1 and 5.1 did not have Transfix data, as there was only enough volume of CSF to be divided across two methods, hence the Fresh and Cryopreservation methods were prioritized. F=Fresh; T=Transfix; C=Cryopreservation. Abbreviations: CD, cluster of differentiation; GFAP, glial fibrillary acidic protein; ID, identification.

Table 2: Percentages of T cell sub-populations per method in patient samples

	% γδ TCR$^+$ cells			% CD4$^+$ cells			% CD8$^+$ cells			% CD161$^+$ cells			% Vα7.2$^+$ cells		% MAIT cells		
Method	**F**	**T**	**C**	**F**	**T**	**C**	**F**	**T**	**C**	**F**	**T**	**C**	**F**	**C**	**F**	**T**	**C**
Patient ID																	
1.1	1,34		1,25	73,8		72,3	18,4		15,4	13,1		11,5	6,17	13	0,68		1,02
2.1	4,54	15,3	2,3	70,4	64,2	74,4	17,4	16,7	12,6	44,5	33,1	54,3	8,39	7,32	0,55	6,48	1,84
3.1	1,32	4,85	0,83	64,2	51,2	68,9	25,2	12	21,6	26,4	8,87	27,2	3,75	6,4	0,51	1,44	0,69
3.2	0,77	0,68	0,63	65,1	56,2	67,4	25,2	7,62	23,1	28,7	4,21	27,5	2,92	4,32	0,63	0,1	0,81
3.3	3,35	3,14	1,19	69,1	41,1	71,3	20,5	8,67	19,8	21,5	6,03	22,2	9,52	7,29	1,28	0,45	0,91
3.4	2,8	2,28	1,57	69,8	47,7	71,5	21,2	13,6	19,7	21,6	6,22	21,9	8,46	6,68	0,88	0,27	0,83
3.5	1,18	1,41	0,53	74,4	37,7	67	13,6	8,99	24,8	25,1	4,6	23,1	17,9	3,59	1,91	0,17	0,51
4.1	1,51	57,6	1,54	64,8	20,5	51,6	19,6	17,1	23,9	43,9	44	42,7	12,4	6,74	16,8	15,3	14,4
5.1	1,96		1,4	61,6		59,4	18,7		17,7	9,66		9,96	25,2	19,6	1,71		0,71

Note: Patients 1.1 and 5.1 did not have Transfix data, as there was only enough volume of CSF to be divided across two methods, hence the Fresh and Cryopreservation methods were prioritized. F=Fresh; T=Transfix; C=Cryopreservation. Abbreviations: CD, cluster of differentiation; ID, identification; MAIT, mucosal associated invariant T cell; TCR; T cell receptor.

Table 3: Percentages of non T cell sub-populations per method in patient samples

	% $CD45^+CD11b^+$ cells		% $CD14^+CD16^-$ cells			%$CD14^-CD16^+$ cells			% NK cells			% $CD69^+$			% HLA-DR^+		
Method	**F**	**C**	**F**	**T**	**C**	**F**	**T**	**C**	**F**	**T**	**C**	**F**	**T**	**C**	**F**	**T**	**C**
Patient ID																	
1.1	99,2	99,1	2,99		0	22,4		12,5	83		80,7	42,8		45,1	27,2		35,9
2.1	97,1	99,3	0,7	7,8	0,96	6,08	0	4,79	52,3	31,2	44,9	39,5	23,2	20,1	18,4	5,71	24,9
3.1	99,4	98,1	0,44	4,91	0,86	49,1	0,23	40,1	73,2	25,1	71,6	39,6	3,25	39,9	17,9	9,3	23,5
3.2	98,4	95,5	0,13	5,66	0,33	43,2	0,041	37,2	71,9	22,1	66,1	56,6	2,66	57	13,6	9,94	16,5
3.3	98,4	99,3	5,93	3,25	2,68	42,1	0	34,9	62,3	9,59	68	42,8	1,06	49,2	52,1	40,1	53,2
3.4	91,6	97,1	4,44	2,57	1,78	47,8	0,96	39,1	59	14,4	58,6	43,6	4,6	48,4	53,4	40,5	56,1
3.5	94,3	92,2	0,39	3,75	0,45	34,3	0,071	37,7	77,2	18	70,6	34,4	0,017	30,5	21,7	9,84	23,1
4.1	12,1	67,4	4,96	8,14	12,8	29,9	54,9	17,3	11,6	6,84	12	34,6	21,2	32,9	11,6	4,71	15,9
5.1	71,1	67	11		14,7	24,9		44	37,7		18,9				28,4		33,3

Note: Patients 1.1 and 5.1 did not have Transfix data, as there was only enough volume of CSF to be divided across two methods, hence the Fresh and Cryopreservation methods were prioritized. F=Fresh; T=Transfix; C=Cryopreservation. Abbreviations: CD, cluster of differentiation; HLA-DR; human leukocyte antigen-DR; NK, natural killer; ID, identification.

APPENDIX D

Table 1: Percentages of major cell populations per method in experimental samples

	% Viable cells		% CD45$^+$ cells			% CD3$^+$ cells			% B cells		% CD11b$^+$ microglia			% GFAP$^+$ astrocytes		
Method	**F**	**C**	**F**	**T**	**C**	**F**	**T**	**C**	**F**	**C**	**F**	**T**	**C**	**F**	**T**	**C**
Patient ID																
6.1	44,9	40,9	93,9	88,8	96,7	71,1	60,5	67,9	52,5	52,7	8,18	0,051	7,59	0,53	0,52	1,17
6.2	44	35	92,7	89,7	93,6	75,5	64	73,8	42	47,5	11,7	0,029	11	46	58,5	24,4
6.3	43,2	37,5	90,2	83,4	93,7	75,5	60,7	72,7	46,1	49	15,5	0,17	18,3	57,7	78,1	51,7
7.1	49,4	40,9	72	92,6	97,5	71,3	54,5	66,9	30,7	41,2	14,9	5,01E-03	18,7	2,54	1,93	4,09
7.2	54,6	42,5	73,6	95,9	98,5	68,4	51,6	66,1	29,5	40,9	18,6	5,48E-03	18,3	1,53	1,81	2,98
7.3	15,9	12,5	69,5	66,1	74,7	91,5	63,8	90,6	17,5	11,1	1,10E+01	5,00E-03	1,71E+01	1,92	0,09	1,25
8.1	45,5	49	98	93,9	98,5	83,1	69,1	76,7	43,1	39,4	7,66E+00	1,70E-01	1,56E+01	0,7	1,61	7,02
9.1	45,6	52,4	97,4	93,5	98,6	78,1	64,4	74,6	50,6	59,1	12,2	4,09E-03	16,7	2,24	3,65	3,6
10.1	47,9	45,5	69	80,8	92,1	69,4	58,6	63,3	69,4	67,6	3,58	0,021	10,2	1,38	0,14	0,81
11.1	48,4	46,5	76,5	84,7	95,7	71,9	66	66,8	75,4	75,5	1,62	0,12	3,85	1,86	0,67	1,52
12.1	38,5	28,6	97,7		90,9	81,9		77,5	39,2	41,3	7,36		7,7	27,4		53,9
13.1	47,9	45,9	99,4	98,5	99,4	82,2	72,9	79,5	44,3	49,9	7,37	0,029	15,1	0,96	2,92	4,82
14.1	46,4	42,3	99,5	98,5	99,5	81,4	75,5	80,2	44,7	46,5	12,7	0,014	13,4	0,76	1,51	6,14
15.1	41,6	41,9	91,1	89,9	94,3	71,5	61,7	67,9	51,9	54,1	7,74	0,014	13,6	0,22	2,68	1,26
16.1	48,1	46,7	79,8	61	90,5	70,5	57,5	67,6	66,7	70	7,56	0,35	11,3	0,62	0,89	0,8
16.2	48,2	42,5	79,7	55	88,1	71	56	67,9	65,1	70,1	7,22	0,076	11,1	0,53	0,51	0,38
17.1	52,5	44,4	98,8	96,6	98,1	72,9	59,2	69,5	53,8	58,7	12,9	0,021	14,2	0,47	1,24	0,63
17.2	53,1	44,1	98,8	97,5	98,2	72,3	60,3	69,1	53,7	58,4	13,4	0,023	14,5	0,77	2,04	0,48
18.1	55,5	50,1	98,8	96,3	98,7	72,6	59,6	69,5	54,1	56,2	13,6	0,01	14,6	0,52	0,63	0,74
18.2	35,3	44,5	99,2	96,3	99	78,4	61,7	68,6	58,5	58,3	4,6	0,02	17	2,96	1,15	0,81

Note: No Transfix data available for Patient 12.1, as stock of Transfix tubes were depleted. F= Fresh; T=Transfix; C=Cryopreservation. Abbreviations: CD, cluster of differentiation; GFAP, glial fibrillary acidic protein; ID, identification.

Table 2: Percentages of T cell sub-populations per method in experimental samples

	% γδ TCR$^+$ cells			% CD4$^+$ cells			% CD8$^+$ cells			% CD161$^+$ cells			% Vα7.2$^+$ cells		% MAIT cells		
Method	**F**	**T**	**C**	**F**	**T**	**C**	**F**	**T**	**C**	**F**	**T**	**C**	**F**	**C**	**F**	**T**	**C**
Patient ID																	
6.1	0,79	7,33	2,17	88	51	86,9	7,27	12,6	8,45	12	6,77	11,1	9,26	8,77	1,16	2,59	1,4
6.2	1,58	6,36	0,13	73,7	46,1	68,8	18,5	31,1	24,5	10,3	7,23	9,62	29,8	25,1	8,71	8,12	5,54
6.3	1,4	12,5	0,18	70,7	47,6	68,6	21,6	28,9	24,6	13,8	9,39	12	24,8	23,4	9,32	11,3	6,6
7.1	2,25	1,74	1,43	53,1	34,9	59,6	39,6	30,2	34,6	11,7	7,88	11,5	14,8	16,5	7,82	0,45	7,81
7.2	2,3	8,03	2,7	63	39,9	68,5	28,8	38,7	26,3	11,7	12,6	12,8	24,8	22,8	7,9	4,2	8,46
7.3	78,3	0,87	2,5	52,2	2,66	82,2	25	15,9	11,4	3,46	1,44	11,9	60,2	13	13,3	0,3	1,33
8.1	0,64	2,46	1,26	76,8	20,7	75,2	17	10,3	18,7	11,4	1,74	21,9	24,4	23,4	6,22	1,41	9,63
9.1	0,5	0,3	0,7	79,6	1,22	85,6	17,7	12,6	11,6	11,8	0,45	10,7	6,21	10,8	2,42	0,088	3,07
10.1	1,11	1,23	0,4	87,7	60,7	85,9	7,41	3,33	9,81	10	4,27	8,05	8,35	7,47	0,69	0,58	0,58
11.1	1,52	0,92	0,15	91,3	55,3	87,8	5,18	2,41	8,87	8,79	3,18	4,24	9	6,33	0,69	1,39	0,3
12.1	0,45		0,92	70,5		71,3	22,6		22	11,2		11,1	22,8	22,6	8,32		7,16
13.1	0,1	4,35	0,89	84,2	56,6	87,3	13	10,5	10	9,49	1,75	13	18	21,3	3,14	1,84	6,46
14.1	0,18	1,95	0,36	86,9	63	84,2	10,8	16,4	12,9	11,8	1,59	13,3	18,9	18,3	5,12	1,05	5,21
15.1	0,25	1,91	0,49	91,7	64,1	89,2	3,85	13,9	5,93	7,97	1,77	9,72	12,5	11,1	1,49	0,87	1,53
16.1	0,25	6,07	0,25	92,8	48,1	89,1	3,42	11,5	6,33	5,99	3,9	7,83	11,4	10,4	0,86	1,86	1,25
16.2	0,3	3,19	0,23	92,9	50,4	89,9	3,18	9,65	5,71	6,12	1,91	8,06	11,5	10,7	1,01	0,6	1,34
17.1	0,21	1,54	0,18	89,9	32,5	82,2	7,57	10,3	14,6	11,2	5,75	12,3	17,2	14,1	10,5	1,37	7,89
17.2	0,16	2,75	0,19	88,7	51,8	82,5	8,6	23,9	14,1	10,9	11,9	12,7	17,2	14,2	9,8	2,92	7,66
18.1	0,14	0,52	0,12	87,3	29,4	75,2	9,94	16,2	20,1	10,9	5	10,8	16,3	10,5	9,17	0,35	6,11
18.2	0,16	1,33	0,13	89,4	43,1	78,2	8,41	18,4	17,8	9,24	8,31	13,7	14	10,3	6,53	1,67	5,88

Note: No Transfix data available for Patient 12.1, as stock of Transfix tubes were depleted. F= Fresh; T=Transfix; C=Cryopreservation. Abbreviations: CD, cluster of differentiation; ID, identification; MAIT, mucosal associated invariant T cell; TCR, T cell receptor.

Table 3: Percentages of non T cell sub-populations per method in experimental samples

	% $CD45^+CD11b^+$ cells		% $CD14^+CD16^-$ cells			%$CD14^-CD16^+$ cells			% NK cells			% $CD69^+$			% $HLA\text{-}DR^+$		
Method	**F**	**C**	**F**	**T**	**C**	**F**	**T**	**C**	**F**	**T**	**C**	**F**	**T**	**C**	**F**	**T**	**C**
Patient ID																	
6.1	91,7	92,1	1,04	5,02	3,66	66,5	1,71	66,3	35,5	2,53	43,2	0,92	0,55	1,15	2,15	1,18	2,53
6.2	88,2	88,5	3,44	11,3	4,33	49,4	1,06	48,2	17,9	5,7	20,8	1,08	0,29	0,39	3,49	1,49	3,29
6.3	84,4	81,4	2,26	19,3	2,85	51,2	2,93	55	10,6	7,82	9,82	2,72	1,44	1,09	4,2	2,32	3,87
7.1	84,4	80,8	7,61	3,26	3,19	31,3	0,83	61,8	26,5	4,11	23,9	2,2	0,014	4,45	2,47	1,04	2,71
7.2	80,6	80,7	11,7	7,75	3,65	30,6	8,96	60,4	25,1	5,44	34,3	1,35	0,031	3,5	2,72	1,15	3,18
7.3	90,8	87,1	1,22	1,81	0,44	78	0,016	80,4	33,4	1,89	11,1	2,63	0	2	16,3	0,62	1,31
8.1	93	87,5	1,1	6,92	3,62	57,6	0,34	62,3	38,5	3,79	26,7	0,31	0,014	0,43	2,7	0,91	3,32
9.1	87,9	82,9	1,01	1,1	0,53	48,7	0,011	58	31,6	1,05	29	0,21	0	2,08	0,84	0,75	1,17
10.1	96	89,1	0,42	9,57	1,28	58,5	1,4	66,4	44,2	2,65	39,6	2,94	0,038	2,2	1,4	0,98	2,28
11.1	98,3	96	0,53	5,09	0,6	63,3	0,35	73,9	50,9	5,45	36	1,12	0,02	0,85	1,06	0,38	1,08
12.1	92,6	91,8	3,15		6,2	57,5		62,7	18,6		4,52	0,22		1,37	3,37		3,68
13.1	92,5	84,7	0,61	14,7	1,03	65,9	0,31	60,4	15,5	3,74	24	0,15	0,012	0,47	0,81	0,4	1,59
14.1	87,2	86,4	1,09	4,44	0,87	62,5	0,31	60,7	18,7	2,8	17,3	0,44	0,018	1,25	1,12	0,4	1,31
15.1	92,1	86,1	0,78	7,13	0,92	73,4	1,07	72,1	40,5	4,71	42,6	1,04	0,019	1,09	1,87	1,02	2,15
16.1	92,3	88,5	0,81	15,2	0,45	58,9	2,17	57,3	40,9	3,64	44,2	1,76	0,052	5,07E-03	2,3	1,39	2,55
16.2	92,7	88,7	0,76	11,7	0,66	58,7	1,3	55,1	44,1	2,81	45,2	2,75	0,033	5,74E-03	2,33	1,28	2,55
17.1	87,1	85,7	3,38	14,7	2,48	57,9	0,094	60,4	46,1	3,58	28,2	0,55	0,014	3,40E-03	2,26	0,54	1,98
17.2	86,5	85,3	3,24	15,5	3	58,2	0,69	59,3	41,9	4,67	26,8	0,46	0,055	6,25E-03	2,07	0,69	2,09
18.1	86,4	85,2	2,46	5,6	1,34	61,5	0,13	56,8	29	2,11	14,7	0,72	3,20E-03	1,28E-03	2	0,54	1,4
18.2	95,4	82,8	1,14	11,7	2,39	73,5	0,26	52,6	22,6	3,55	15,5	0,6	0,018	1,23E-03	1,89	0,55	1,57

Note: No Transfix data available for Patient 12.1, as stock of Transfix tubes were depleted. F= Fresh; T=Transfix; C=Cryopreservation. Abbreviations: CD, cluster of differentiation; HLA-DR, human leukocyte antigen-DR; ID, identification: NK, natural killer.

APPENDIX E

Table 1: Duration of storage comparison of cell percentages between Fresh vs Transfix methods

	Fresh	24 hour	1 week	2 week
$CD45^+$ cells		*0.05*		*0.05*
$CD11b^{++}$ cells		*0.046*	*0.046*	*0.046*
$CD45^+CD11b^+$ cells		*0.046*	X	X
$CD3^+$ cells			*0.05*	*0.05*
γδ TCR^+ cells				
$CD161^+$ cells		*0.046*	*0.05*	*0.05*
$CD4^+$ cells			*0.046*	*0.046*
$CD8^+$ cells				
MAIT cells		*0.05*		
Vα7.2^+ cells		*0.046*	X	X
B cells		*0.05*	X	X
NK cells		*0.05*	*0.05*	*0.05*
Classical monocytes		*0.05*	*0.05*	
Non-classical monocytes			*0.05*	*0.05*
$HLA\text{-}DR^+$		*0.05*	*0.046*	*0.046*
$GFAP^+$ astrocytes				

Note: *P* values are indicated where differences were statistically significant as compared to Fresh. Boxes demarcated with "X" refer to populations that could not be clearly distinguished during flow cytometric gating, and therefore were excluded from analyses.

REFERENCES: Harvard British Standard Referencing style

1. GARCÍA-MONCÓ, J.C., POMAR, V. and DOMINGO, P., 2016. *Cns Infections.* Springer.

2. ROHLWINK, U.K., MAUFF, K., WILKINSON, K.A., ENSLIN, N., WEGOYE, E., WILKINSON, R.J. and FIGAJI, A.A., 2017. Biomarkers of cerebral injury and inflammation in pediatric tuberculous meningitis. *Clinical Infectious Diseases,* **65**(8), pp. 1298-1307.

3. BRUZZONE, R., DUBOIS-DALCQ, M., GRAU, G.E., GRIFFIN, D.E. and KRISTENSSON, K., 2009. Infectious diseases of the nervous system and their impact in developing countries. *PLoS pathogens,* **5**(2), pp. e1000199.

4. JOHN, C.C., CARABIN, H., MONTANO, S.M., BANGIRANA, P., ZUNT, J.R. and PETERSON, P.K., 2015. Global research priorities for infections that affect the nervous system. *Nature,* **527**(7578), pp. S178-S186.

5. ROBERTSON, F.C., LEPARD, J.R., MEKARY, R.A., DAVIS, M.C., YUNUSA, I., GORMLEY, W.B., BATICULON, R.E., MAHMUD, M.R., MISRA, B.K. and RATTANI, A., 2018. Epidemiology of central nervous system infectious diseases: a meta-analysis and systematic review with implications for neurosurgeons worldwide. *Journal of neurosurgery,* **130**(4), pp. 1107-1126.

6. PASHENKOV, M., HUANG, Y., KOSTULAS, V., HAGLUND, M., SÖDERSTRÖM, M. and LINK, H., 2001. Two subsets of dendritic cells are present in human cerebrospinal fluid. *Brain,* **124**(3), pp. 480-492.

7. SUBIRÁ, D., CASTAÑÓN, S., ACEITUNO, E., HERNÁNDEZ, J., JIMÉNEZ-GARÓFANO, C., JIMÉNEZ, A., JIMÉNEZ, A.M., ROMÁN, A. and ORFAO, A., 2002. Flow cytometric analysis of cerebrospinal fluid samples and its usefulness in routine clinical practice. *American Journal of Clinical Pathology,* **117**(6), pp. 952-958.

8. FRAGOSO-LOYO, H., RICHAUD-PATIN, Y., OROZCO-NARVÁEZ, A., DÁVILA-MALDONADO, L., ATISHA-FREGOSO, Y., LLORENTE, L. and SÁNCHEZ-GUERRERO, J., 2007. Interleukin-6 and chemokines in the neuropsychiatric manifestations of systemic lupus erythematosus. *Arthritis & Rheumatism,* **56**(4), pp. 1242-1250.

9. VAN LAARHOVEN, A., DIAN, S., VAN DORP, S., PURNAMA, F., KOEKEN, V.A., DIANDINI, E., UTAMI, F., LIVIA, R., APRIANI, L. and ARDIANSYAH, E., 2019. Immune cell characteristics and cytokine responses in adult HIV-negative tuberculous meningitis: an observational cohort study. *Scientific reports,* **9**(1), pp. 1-11.

10. DE GRAAF, M.T., VAN DEN BROEK, PATRICIA DM, KRAAN, J., LUITWIELER, R.L., VAN DEN BENT, MARTIN J, BOONSTRA, J.G., SCHMITZ, P.I., GRATAMA, J.W. and SMITT, P.A.S., 2011. Addition of serum-containing medium to cerebrospinal fluid prevents cellular loss over time. *Journal of neurology,* **258**(8), pp. 1507-1512.

11. NEMES, E., KAGINA, B.M., SMIT, E., AFRICA, H., STEYN, M., HANEKOM, W.A. and SCRIBA, T.J., 2015. Differential leukocyte counting and immunophenotyping in cryopreserved ex vivo whole blood. *Cytometry Part A,* **87**(2), pp. 157-165.

12. DE ROSA, A., DE FRANCESCO, F., TIRINO, V., FERRARO, G.A., DESIDERIO, V., PAINO, F., PIROZZI, G., D'ANDREA, F. and PAPACCIO, G., 2009. A new method for cryopreserving adipose-derived stem cells: an attractive and suitable large-scale and long-term cell banking technology. *Tissue Engineering Part C: Methods*, **15**(4), pp. 659-667.

13. RICHTER, K.S., SHIPLEY, S.K., MCVEARRY, I., TUCKER, M.J. and WIDRA, E.A., 2006. Cryopreserved embryo transfers suggest that endometrial receptivity may contribute to reduced success rates of later developing embryos. *Fertility and sterility*, **86**(4), pp. 862-866.

14. MCGINNITY, D.F., SOARS, M.G., URBANOWICZ, R.A. and RILEY, R.J., 2004. Evaluation of fresh and cryopreserved hepatocytes as in vitro drug metabolism tools for the prediction of metabolic clearance. *Drug metabolism and disposition: the biological fate of chemicals*, **32**(11), pp. 1247-1253.

15. SOMAND, D. and MEURER, W., 2009. Central nervous system infections. *Emergency medicine clinics of North America*, **27**(1), pp. 89-100.

16. BOWERS, K.M. and MUDRAKOLA, V.V., 2020. Neuroinfections: Presentation, Diagnosis, and Treatment of Meningitis and Encephalitis. *Neurology*, .

17. SINGH, G. and PRABHAKAR, S., 2008. The association between central nervous system (CNS) infections and epilepsy: epidemiological approaches and microbiological and epileptological perspectives. *Epilepsia*, **49**, pp. 2-7.

18. MURTHY, J.M., 2010. Tuberculous meningitis: the challenges. *Neurology India*, **58**(5), pp. 716-722.

19. BERMAN, S., KIBEL, M., FOURIE, P. and STREBEL, P., 1992. Childhood tuberculosis and tuberculous meningitis: high incidence rates in the Western Cape of South Africa. *Tubercle and Lung Disease*, **73**(6), pp. 349-355.

20. WOLZAK, N.K., COOKE, M.L., ORTH, H. and VAN TOORN, R., 2012. The changing profile of pediatric meningitis at a referral centre in Cape Town, South Africa. *Journal of tropical pediatrics*, **58**(6), pp. 491-495.

21. HEMINGWAY, C., BERK, M., ANDERSON, S.T., WRIGHT, V.J., HAMILTON, S., ELEFTHEROHORINOU, H., KAFOROU, M., GOLDGOF, G.M., HICKMAN, K. and KAMPMANN, B., 2017. Childhood tuberculosis is associated with decreased abundance of T cell gene transcripts and impaired T cell function. *PLoS One*, **12**(11), pp. e0185973.

22. DANIEL, B.D., GRACE, G.A. and NATRAJAN, M., 2019. Tuberculous meningitis in children: Clinical management & outcome. *The Indian journal of medical research*, **150**(2), pp. 117-130.

23. THWAITES, G.E., VAN TOORN, R. and SCHOEMAN, J., 2013. Tuberculous meningitis: more questions, still too few answers. *The Lancet Neurology*, **12**(10), pp. 999-1010.

24. CHIN, J.H., 2014. Tuberculous meningitis: Diagnostic and therapeutic challenges. *Neurology: Clinical Practice*, **4**(3), pp. 199-205.

25. TÖRÖK, M., 2015. Tuberculous meningitis: advances in diagnosis and treatment. *British medical bulletin,* **113**(1), pp. 117-131.

26. DAVIS, A.G., ROHLWINK, U.K., PROUST, A., FIGAJI, A.A. and WILKINSON, R.J., 2019. The pathogenesis of tuberculous meningitis. *Journal of leukocyte biology,* **105**(2), pp. 267-280.

27. GUTIERREZ-MURGAS, Y. and SNOWDEN, J.N., 2014. Ventricular shunt infections: immunopathogenesis and clinical management. *Journal of neuroimmunology,* **276**(1-2), pp. 1-8.

28. YAKUT, N., SOYSAL, A., KEPENEKLI KADAYIFCI, E., DALGIC, N., YILMAZ CIFTDOGAN, D., KARAASLAN, A., AKKOC, G., OCAL DEMIR, S., CAGAN, E. and CELIKBOYA, E., 2018. Ventriculoperitoneal shunt infections and re-infections in children: a multicentre retrospective study. *British journal of neurosurgery,* **32**(2), pp. 196-200.

29. AL-SHARYDAH, A.M., ABU MELHA, Y.A., AL-SUHIBANI, S.S., ALOJAN, A.A., AL-TAEI, T.H., ALFAWAZ, I.I., ALSHAMMARI, L.T., AL-JUBRAN, S.A. and AMMAR, A.S., 2020. Rates of cerebrospinal fluid infection and the causative organisms following shunt procedures in Saudi Arabia. A retrospective study based on radiological findings. *Saudi medical journal,* **41**(6), pp. 607-613.

30. FARAHMAND, D., HILMARSSON, H., HOGFELDT, M. and TISELL, M., 2009. Perioperative risk factors for short term shunt revisions in adult hydrocephalus patients. *Journal of neurology, neurosurgery, and psychiatry,* **80**(11), pp. 1248-1253.

31. JEELANI, N.U., KULKARNI, A.V., DESILVA, P., THOMPSON, D.N. and HAYWARD, R.D., 2009. Postoperative cerebrospinal fluid wound leakage as a predictor of shunt infection: a prospective analysis of 205 cases. Clinical article. *Journal of neurosurgery.Pediatrics,* **4**(2), pp. 166-169.

32. SINGHI, P. and SAINI, A.G., 2019. Fungal and parasitic CNS infections. *The Indian Journal of Pediatrics,* **86**(1), pp. 83-90.

33. MURTHY, J.M., 2007. Fungal infections of the central nervous system: the clinical syndromes. *Neurology India,* **55**(3), pp. 221-225.

34. PARK, B.J., WANNEMUEHLER, K.A., MARSTON, B.J., GOVENDER, N., PAPPAS, P.G. and CHILLER, T.M., 2009. Estimation of the current global burden of cryptococcal meningitis among persons living with HIV/AIDS. *AIDS (London, England),* **23**(4), pp. 525-530.

35. LUFT, P., OOSTINGH, G.J., GRUIJTHUIJSEN, Y., HOREJS-HOECK, J., LEHMANN, I. and DUSCHL, A., 2008. Patulin influences the expression of Th1/Th2 cytokines by activated peripheral blood mononuclear cells and T cells through depletion of intracellular glutathione. *Environmental toxicology,* **23**(1), pp. 84-95.

36. TSAI, W.T., LO, Y.C., WU, M.S., LI, C.Y., KUO, Y.P., LAI, Y.H., TSAI, Y., CHEN, K.C., CHUANG, T.H., YAO, C.H., LEE, J.C., HSU, L.C., HSU, J.T. and YU, G.Y., 2016. Mycotoxin Patulin Suppresses Innate Immune Responses by Mitochondrial Dysfunction and

p62/Sequestosome-1-dependent Mitophagy. *The Journal of biological chemistry,* **291**(37), pp. 19299-19311.

37. BERNARDO, P.H., BRASCH, N., CHAI, C.L. and WARING, P., 2003. A novel redox mechanism for the glutathione-dependent reversible uptake of a fungal toxin in cells. *Journal of Biological Chemistry,* **278**(47), pp. 46549-46555.

38. TOMEE, J.F. and KAUFFMAN, H.F., 2000. Putative virulence factors of Aspergillus fumigatus. *Clinical and experimental allergy : journal of the British Society for Allergy and Clinical Immunology,* **30**(4), pp. 476-484.

39. SETH, R., XESS, I. and JANA, M., 2019. Diagnosis of Invasive Fungal Infections in Children. *Indian pediatrics,* **56**(3),.

40. LUCKOWITSCH, M., RUDOLPH, H., BOCHENNEK, K., PORTO, L. and LEHRNBECHER, T., 2021. Central Nervous System Mold Infections in Children with Hematological Malignancies: Advances in Diagnosis and Treatment. *Journal of Fungi,* **7**(3), pp. 168.

41. SWANSON II, P.A. and MCGAVERN, D.B., 2015. Viral diseases of the central nervous system. *Current opinion in virology,* **11**, pp. 44-54.

42. DAHM, T., RUDOLPH, H., SCHWERK, C., SCHROTEN, H. and TENENBAUM, T., 2016. Neuroinvasion and inflammation in viral central nervous system infections. *Mediators of inflammation,* **2016**.

43. FURR, S. and MARRIOTT, I., 2012. Viral CNS infections: role of glial pattern recognition receptors in neuroinflammation. *Frontiers in microbiology,* **3**, pp. 201.

44. BERNARDI, L., PERRONE, S. and ESPOSITO, S., 2021. Update on Viral Infections Involving the Central Nervous System in Pediatric Patients. *Children,* **8**(9), pp. 782.

45. SNOW, R.W., GUERRA, C.A., NOOR, A.M., MYINT, H.Y. and HAY, S.I., 2005. The global distribution of clinical episodes of Plasmodium falciparum malaria. *Nature,* **434**(7030), pp. 214-217.

46. LUZOLO, A.L. and NGOYI, D.M., 2019. Cerebral malaria. *Brain research bulletin,* **145**, pp. 53-58.

47. IDRO, R., NDIRITU, M., OGUTU, B., MITHWANI, S., MAITLAND, K., BERKLEY, J., CRAWLEY, J., FEGAN, G., BAUNI, E., PESHU, N., MARSH, K., NEVILLE, B. and NEWTON, C., 2007. Burden, features, and outcome of neurological involvement in acute falciparum malaria in Kenyan children. *Jama,* **297**(20), pp. 2232-2240.

48. WILSON, E.H., WENINGER, W. and HUNTER, C.A., 2010. Trafficking of immune cells in the central nervous system. *The Journal of clinical investigation,* **120**(5), pp. 1368-1379.

49. RANSOHOFF, R.M. and BROWN, M.A., 2012. Innate immunity in the central nervous system. *The Journal of clinical investigation,* **122**(4), pp. 1164-1171.

50. KLEIN, R.S., GARBER, C. and HOWARD, N., 2017. Infectious immunity in the central nervous system and brain function. *Nature immunology,* **18**(2), pp. 132-141.

51. COOPER, M.A., FEHNIGER, T.A. and CALIGIURI, M.A., 2001. The biology of human natural killer-cell subsets. *Trends in immunology,* **22**(11), pp. 633-640.

52. ZIEGLER, S., WEISS, E., SCHMITT, A., SCHLEGEL, J., BURGERT, A., TERPITZ, U., SAUER, M., MORETTA, L., SIVORI, S. and LEONHARDT, I., 2017. CD56 is a pathogen recognition receptor on human natural killer cells. *Scientific reports,* **7**(1), pp. 1-13.

53. LAKSCHEVITZ, F.S., HASSANPOUR, S., RUBIN, A., FINE, N., SUN, C. and GLOGAUER, M., 2016. Identification of neutrophil surface marker changes in health and inflammation using high-throughput screening flow cytometry. *Experimental cell research,* **342**(2), pp. 200-209.

54. FERGUSSON, J.R., SMITH, K.E., FLEMING, V.M., RAJORIYA, N., NEWELL, E.W., SIMMONS, R., MARCHI, E., BJÖRKANDER, S., KANG, Y. and SWADLING, L., 2014. CD161 defines a transcriptional and functional phenotype across distinct human T cell lineages. *Cell reports,* **9**(3), pp. 1075-1088.

55. APPLEBY, L.J., NAUSCH, N., MIDZI, N., MDULUZA, T., ALLEN, J.E. and MUTAPI, F., 2013. Sources of heterogeneity in human monocyte subsets. *Immunology letters,* **152**(1), pp. 32-41.

56. KITCHENS, R.L., 2000. Role of CD14 in cellular recognition of bacterial lipopolysaccharides. *Chem Immunol,* **74**(1), pp. 61-82.

57. KIM, H.J. and CANTOR, H., 2014. CD4 T-cell subsets and tumor immunity: the helpful and the not-so-helpful. *Cancer immunology research,* **2**(2), pp. 91-98.

58. RUDD, C.E., TREVILLYAN, J.M., DASGUPTA, J.D., WONG, L.L. and SCHLOSSMAN, S.F., 1988. The CD4 receptor is complexed in detergent lysates to a protein-tyrosine kinase (pp58) from human T lymphocytes. *Proceedings of the National Academy of Sciences of the United States of America,* **85**(14), pp. 5190-5194.

59. SAXENA, A., MARTIN-BLONDEL, G., MARS, L. and LIBLAU, R., 2011. Role of CD8 T cell subsets in the pathogenesis of multiple sclerosis. *FEBS letters,* **585**(23), pp. 3758-3763.

60. GAO, G.F. and JAKOBSEN, B.K., 2000. Molecular interactions of coreceptor CD8 and MHC class I: the molecular basis for functional coordination with the T-cell receptor. *Immunology today,* **21**(12), pp. 630-636.

61. PANG, D.J., NEVES, J.F., SUMARIA, N. and PENNINGTON, D.J., 2012. Understanding the complexity of γδ T-cell subsets in mouse and human. *Immunology,* **136**(3), pp. 283-290.

62. CHIEN, Y. and BONNEVILLE, M., 2006. Gamma delta T cell receptors. *Cellular and Molecular Life Sciences CMLS,* **63**(18), pp. 2089-2094.

63. GHERARDIN, N.A., SOUTER, M.N., KOAY, H., MANGAS, K.M., SEEMANN, T., STINEAR, T.P., ECKLE, S.B., BERZINS, S.P., D'UDEKEM, Y. and KONSTANTINOV, I.E., 2018. Human blood MAIT cell subsets defined using MR1 tetramers. *Immunology and cell biology,* **96**(5), pp. 507-525.

64. JURGA, A.M., PALECZNA, M. and KUTER, K.Z., 2020. Overview of general and discriminating markers of differential microglia phenotypes. *Frontiers in Cellular Neuroscience,* **14**.

65. HOLMES, N., 2006. CD45: all is not yet crystal clear. *Immunology,* **117**(2), pp. 145-155.

66. BIOLOGICALS, N., 2011. CD11 b Expression, Leukocyte Adhesion and the Innate Immune System. *Nobusbio.com,* .

67. MOLOFSKY, A.V. and DENEEN, B., 2015. Astrocyte development: a guide for the perplexed. *Glia,* **63**(8), pp. 1320-1329.

68. ROESSMANN, U., VELASCO, M.E., SINDELY, S.D. and GAMBETTI, P., 1980. Glial fibrillary acidic protein (GFAP) in ependymal cells during development. An immunocytochemical study. *Brain research,* **200**(1), pp. 13-21.

69. ABDEL-HAQ, R., SCHLACHETZKI, J., GLASS, C.K. and MAZMANIAN, S.K., 2019. Microbiome–microglia connections via the gut–brain axis. *Journal of Experimental Medicine,* **216**(1), pp. 41-59.

70. MARIANI, M.M. and KIELIAN, T., 2009. Microglia in infectious diseases of the central nervous system. *Journal of Neuroimmune Pharmacology,* **4**(4), pp. 448-461.

71. ALOISI, F., 2001. Immune function of microglia. *Glia,* **36**(2), pp. 165-179.

72. BRANDENBURG, L., VAROGA, D., NICOLAEVA, N., LEIB, S.L., WILMS, H., PODSCHUN, R., WRUCK, C.J., SCHRÖDER, J., PUFE, T. and LUCIUS, R., 2008. Role of glial cells in the functional expression of LL-37/rat cathelin-related antimicrobial peptide in meningitis. *Journal of Neuropathology & Experimental Neurology,* **67**(11), pp. 1041-1054.

73. HANISCH, U., 2002. Microglia as a source and target of cytokines. *Glia,* **40**(2), pp. 140-155.

74. LUO, X. and CHEN, S., 2012. The changing phenotype of microglia from homeostasis to disease. *Translational neurodegeneration,* **1**(1), pp. 1-13.

75. CHU, C., ARTIS, D. and CHIU, I.M., 2020. Neuro-immune interactions in the tissues. *Immunity,* **52**(3), pp. 464-474.

76. KOEDEL, U., SCHELD, W.M. and PFISTER, H., 2002. Pathogenesis and pathophysiology of pneumococcal meningitis. *The Lancet infectious diseases,* **2**(12), pp. 721-736.

77. DJUKIC, M., MILDNER, A., SCHMIDT, H., CZESNIK, D., BRÜCK, W., PRILLER, J., NAU, R. and PRINZ, M., 2006. Circulating monocytes engraft in the brain, differentiate into

microglia and contribute to the pathology following meningitis in mice. *Brain,* **129**(9), pp. 2394-2403.

78. TIAN, L., MA, L., KAARELA, T. and LI, Z., 2012. Neuroimmune crosstalk in the central nervous system and its significance for neurological diseases. *Journal of neuroinflammation,* **9**(1), pp. 1-10.

79. HOHLFELD, R., KERSCHENSTEINER, M. and MEINL, E., 2007. Dual role of inflammation in CNS disease. *Neurology,* **68**(22 Suppl 3), pp. S58-63; discussion S91-6.

80. FARINA, C., ALOISI, F. and MEINL, E., 2007. Astrocytes are active players in cerebral innate immunity. *Trends in immunology,* **28**(3), pp. 138-145.

81. TAN, L., GORDON, K.B., MUELLER, J.P., MATIS, L.A. and MILLER, S.D., 1998. Presentation of proteolipid protein epitopes and B7-1-dependent activation of encephalitogenic T cells by IFN-gamma-activated SJL/J astrocytes. *Journal of immunology (Baltimore, Md.: 1950),* **160**(9), pp. 4271-4279.

82. SOOS, J.M., MORROW, J., ASHLEY, T.A., SZENTE, B.E., BIKOFF, E.K. and ZAMVIL, S.S., 1998. Astrocytes express elements of the class II endocytic pathway and process central nervous system autoantigen for presentation to encephalitogenic T cells. *Journal of immunology (Baltimore, Md.: 1950),* **161**(11), pp. 5959-5966.

83. GIOVANNONI, F. and QUINTANA, F.J., 2020. The role of astrocytes in CNS inflammation. *Trends in immunology,* .

84. MARCHETTI, L. and ENGELHARDT, B., 2020. Immune cell trafficking across the blood-brain barrier in the absence and presence of neuroinflammation. *Vascular Biology,* **2**(1), pp. H1-H18.

85. ALVERMANN, S., HENNIG, C., STÜVE, O., WIENDL, H. and STANGEL, M., 2014. Immunophenotyping of cerebrospinal fluid cells in multiple sclerosis: in search of biomarkers. *JAMA neurology,* **71**(7), pp. 905-912.

86. KIVISAKK, P., MAHAD, D.J., CALLAHAN, M.K., TREBST, C., TUCKY, B., WEI, T., WU, L., BAEKKEVOLD, E.S., LASSMANN, H., STAUGAITIS, S.M., CAMPBELL, J.J. and RANSOHOFF, R.M., 2003. Human cerebrospinal fluid central memory CD4+ T cells: evidence for trafficking through choroid plexus and meninges via P-selectin. *Proceedings of the National Academy of Sciences of the United States of America,* **100**(14), pp. 8389-8394.

87. BARTHOLOMÄUS, I., KAWAKAMI, N., ODOARDI, F., SCHLÄGER, C., MILJKOVIC, D., ELLWART, J.W., KLINKERT, W.E., FLÜGEL-KOCH, C., ISSEKUTZ, T.B. and WEKERLE, H., 2009. Effector T cell interactions with meningeal vascular structures in nascent autoimmune CNS lesions. *Nature,* **462**(7269), pp. 94-98.

88. VAJKOCZY, P., LASCHINGER, M. and ENGELHARDT, B., 2001. Alpha4-integrin-VCAM-1 binding mediates G protein-independent capture of encephalitogenic T cell blasts to CNS white matter microvessels. *The Journal of clinical investigation,* **108**(4), pp. 557-565.

89. SPINDLER, K.R. and HSU, T., 2012. Viral disruption of the blood–brain barrier. *Trends in microbiology,* **20**(6), pp. 282-290.

90. BE, N.A., KIM, K.S., BISHAI, W.R. and JAIN, S.K., 2009. Pathogenesis of central nervous system tuberculosis. *Current Molecular Medicine,* **9**(2), pp. 94-99.

91. AMANTEA, D., NAPPI, G., BERNARDI, G., BAGETTA, G. and CORASANITI, M.T., 2009. Post-ischemic brain damage: pathophysiology and role of inflammatory mediators. *The FEBS journal,* **276**(1), pp. 13-26.

92. ALMEIDA-OLIVEIRA, A., SMITH-CARVALHO, M., PORTO, L.C., CARDOSO-OLIVEIRA, J., DOS SANTOS RIBEIRO, A., FALCÃO, R.R., ABDELHAY, E., BOUZAS, L.F., THULER, L.C.S. and ORNELLAS, M.H., 2011. Age-related changes in natural killer cell receptors from childhood through old age. *Human immunology,* **72**(4), pp. 319-329.

93. POLI, A., KMIECIK, J., DOMINGUES, O., HENTGES, F., BLÉRY, M., CHEKENYA, M., BOUCRAUT, J. and ZIMMER, J., 2013. NK cells in central nervous system disorders. *The Journal of Immunology,* **190**(11), pp. 5355-5362.

94. MAYADAS, T.N., CULLERE, X. and LOWELL, C.A., 2014. The multifaceted functions of neutrophils. *Annual Review of Pathology: Mechanisms of Disease,* **9**, pp. 181-218.

95. HAMANN, I., DÖRR, J., GLUMM, R., CHANVILLARD, C., JANSSEN, A., MILLWARD, J.M., PAUL, F., RANSOHOFF, R.M. and INFANTE-DUARTE, C., 2013. Characterization of natural killer cells in paired CSF and blood samples during neuroinflammation. *Journal of neuroimmunology,* **254**(1-2), pp. 165-169.

96. NARANBHAI, V., CHANG, C.C., DURGIAH, R., OMARJEE, S., LIM, A., MOOSA, M.Y., ELLIOT, J.H., NDUNG'U, T., LEWIN, S.R., FRENCH, M.A. and CARR, W.H., 2014. Compartmentalization of innate immune responses in the central nervous system during cryptococcal meningitis/HIV coinfection. *AIDS (London, England),* **28**(5), pp. 657-666.

97. ENZMANN, G., KARGARAN, S. and ENGELHARDT, B., 2018. Ischemia–reperfusion injury in stroke: impact of the brain barriers and brain immune privilege on neutrophil function. *Therapeutic advances in neurological disorders,* **11**, pp. 1756286418794184.

98. GORINA, R., LYCK, R., VESTWEBER, D. and ENGELHARDT, B., 2014. beta2 integrin-mediated crawling on endothelial ICAM-1 and ICAM-2 is a prerequisite for transcellular neutrophil diapedesis across the inflamed blood-brain barrier. *Journal of immunology (Baltimore, Md.: 1950),* **192**(1), pp. 324-337.

99. VAN LAARHOVEN, A., DIAN, S., RUESEN, C., HAYATI, E., DAMEN, M.S., ANNISA, J., CHAIDIR, L., RUSLAMI, R., ACHMAD, T.H. and NETEA, M.G., 2017. Clinical parameters, routine inflammatory markers, and LTA4H genotype as predictors of mortality among 608 patients with tuberculous meningitis in Indonesia. *The Journal of infectious diseases,* **215**(7), pp. 1029-1039.

100. MANDA-HANDZLIK, A. and DEMKOW, U., 2019. The brain entangled: the contribution of neutrophil extracellular traps to the diseases of the central nervous system. *Cells,* **8**(12), pp. 1477.

101. SERBINA, N.V. and PAMER, E.G., 2006. Monocyte emigration from bone marrow during bacterial infection requires signals mediated by chemokine receptor CCR2. *Nature immunology,* **7**(3), pp. 311-317.

102. KOKOVAY, E. and CUNNINGHAM, L.A., 2005. Bone marrow-derived microglia contribute to the neuroinflammatory response and express iNOS in the MPTP mouse model of Parkinson's disease. *Neurobiology of disease,* **19**(3), pp. 471-478.

103. BOYTON, R.J. and OPENSHAW, P.J., 2002. Pulmonary defences to acute respiratory infection. *British medical bulletin,* **61**(1), pp. 1-12.

104. SWAMINATHAN, S., NANDINI, K., HANNA, L., SOMU, N., NARAYANAN, P. and BARNES, P., 2000. T-lymphocyte subpopulation in tuberculosis. *Indian pediatrics,* **37**(5), pp. 489-495.

105. KAUFFMAN, K.D., SALLIN, M.A., HOFT, S.G., SAKAI, S., MOORE, R., WILDER-KOFIE, T., MOORE, I.N., SETTE, A., ARLEHAMN, C.S.L. and BARBER, D.L., 2018. Limited Pulmonary Mucosal-Associated Invariant T Cell Accumulation and Activation during Mycobacterium tuberculosis Infection in Rhesus Macaques. *Infection and immunity,* **86**(12), pp. 10.1128/IAI.00431-18. Print 2018 Dec.

106. HASSERT, M., WOLF, K.J., SCHWETYE, K.E., DIPAOLO, R.J., BRIEN, J.D. and PINTO, A.K., 2018. CD4 T cells mediate protection against Zika associated severe disease in a mouse model of infection. *PLoS pathogens,* **14**(9), pp. e1007237.

107. AGUILAR-VALENZUELA, R., NETLAND, J., SEO, Y., BEVAN, M.J., GRAKOUI, A. and SUTHAR, M.S., 2018. Dynamics of tissue-specific CD8 T cell responses during West Nile virus infection. *Journal of virology,* **92**(10), pp. e00014-18.

108. PHARES, T.W., STOHLMAN, S.A., HINTON, D.R. and BERGMANN, C.C., 2012. Enhanced CD8 T-cell anti-viral function and clinical disease in B7-H1-deficient mice requires CD4 T cells during encephalomyelitis. *Journal of neuroinflammation,* **9**(1), pp. 1-17.

109. TROTTEIN, F. and PAGET, C., 2018. Natural Killer T Cells and Mucosal-Associated Invariant T Cells in Lung Infections. *Frontiers in immunology,* **9**, pp. 1750.

110. XU, B., PIZARRO, J.C., HOLMES, M.A., MCBETH, C., GROH, V., SPIES, T. and STRONG, R.K., 2011. Crystal structure of a gammadelta T-cell receptor specific for the human MHC class I homolog MICA. *Proceedings of the National Academy of Sciences of the United States of America,* **108**(6), pp. 2414-2419.

111. DIELI, F., SIRECI, G., DI SANO, C., CHAMPAGNE, E., FOURNIÈ, J.J., IVANYI, J. and SALERNO, A., 1999. Predominance of V γ 9/V δ 2 T Lymphocytes in the Cerebrospinal Fluid of Children with Tuberculous Meningitis: Reversal after Chemotherapy. *Molecular Medicine,* **5**(5), pp. 301-312.

112. DIANA, J. and LEHUEN, A., 2009. NKT cells: friend or foe during viral infections? *European journal of immunology,* **39**(12), pp. 3283-3291.

113. TANG, X.Z., JO, J., TAN, A.T., SANDALOVA, E., CHIA, A., TAN, K.C., LEE, K.H., GEHRING, A.J., DE LIBERO, G. and BERTOLETTI, A., 2013. IL-7 licenses activation of human liver intrasinusoidal mucosal-associated invariant T cells. *Journal of immunology (Baltimore, Md.: 1950),* **190**(7), pp. 3142-3152.

114. ABRAHAMSSON, S.V., ANGELINI, D.F., DUBINSKY, A.N., MOREL, E., OH, U., JONES, J.L., CARASSITI, D., REYNOLDS, R., SALVETTI, M., CALABRESI, P.A., COLES, A.J., BATTISTINI, L., MARTIN, R., BURT, R.K. and MURARO, P.A., 2013. Non-myeloablative autologous haematopoietic stem cell transplantation expands regulatory cells and depletes IL-17 producing mucosal-associated invariant T cells in multiple sclerosis. *Brain : a journal of neurology,* **136**(Pt 9), pp. 2888-2903.

115. MCKINNON, K.M., 2018. Flow Cytometry: An Overview. *Current protocols in immunology,* **120**, pp. 5.1.1-5.1.11.

116. ADAN, A., ALIZADA, G., KIRAZ, Y., BARAN, Y. and NALBANT, A., 2017. Flow cytometry: basic principles and applications. *Critical reviews in biotechnology,* **37**(2), pp. 163-176.

117. VERNAU, W., VERNAU, K.A. and BAILEY, C.S., 2008. Cerebrospinal fluid. *Clinical biochemistry of domestic animals,* , pp. 769.

118. SHENG, J.G., MRAK, R.E., ROVNAGHI, C.R., KOZLOWSKA, E., VAN ELDIK, L.J. and GRIFFIN, W.S.T., 1996. Human brain S100β and S100β mRNA expression increases with age: pathogenic implications for Alzheimer's disease. *Neurobiology of aging,* **17**(3), pp. 359-363.

119. NYLEN, K., ÖST, M., CSAJBOK, L., NILSSON, I., BLENNOW, K., NELLGÅRD, B. and ROSENGREN, L., 2006. Increased serum-GFAP in patients with severe traumatic brain injury is related to outcome. *Journal of the neurological sciences,* **240**(1-2), pp. 85-91.

120. BERTSCH, T., CASARIN, W., KRETSCHMAR, M., ZIMMER, W., WALTER, S., SOMMER, C., MUEHLHAUSER, F., RAGOSCHKE, A., KUEHL, S. and SCHMIDT, R., 2001. Protein S-100B: a serum marker for ischemic and infectious injury of cerebral tissue.

121. MEDANA, I.M., LINDERT, R., WURSTER, U., HIEN, T.T., DAY, N.P., PHU, N.H., MAI, N.T.H., CHUONG, L.V., CHAU, T.T.H. and TURNER, G.D., 2005. Cerebrospinal fluid levels of markers of brain parenchymal damage in Vietnamese adults with severe malaria. *Transactions of the Royal Society of Tropical Medicine and Hygiene,* **99**(8), pp. 610-617.

122. KRAAN, J., GRATAMA, J.W., HAIOUN, C., ORFAO, A., PLONQUET, A., PORWIT, A., QUIJANO, S., STETLER-STEVENSON, M., SUBIRA, D. and WILSON, W., 2008. Flow cytometric immunophenotyping of cerebrospinal fluid. *Current protocols in cytometry,* **45**(1), pp. 6.25. 1-6.25. 16.

123. DUX, R., KINDLER-RÖHRBORN, A., ANNAS, M., FAUSTMANN, P., LENNARTZ, K. and ZIMMERMANN, C., 1994. A standardized protocol for flow cytometric analysis of cells isolated from cerebrospinal fluid. *Journal of the neurological sciences,* **121**(1), pp. 74-78.

124. QUIJANO, S., LOPEZ, A., MANUEL SANCHO, J., PANIZO, C., DEBEN, G., CASTILLA, C., ANTONIO GARCIA-VELA, J., SALAR, A., ALONSO-VENCE, N., GONZALEZ-BARCA, E., PENALVER, F.J., PLAZA-VILLA, J., MORADO, M., GARCIA-MARCO, J., ARIAS, J., BRIONES, J., FERRER, S., CAPOTE, J., NICOLAS, C., ORFAO, A. and SPANISH GROUP FOR THE STUDY OF CNS DISEASE IN NHL, 2009. Identification of leptomeningeal disease in aggressive B-cell non-Hodgkin's lymphoma: improved sensitivity of flow cytometry. *Journal of clinical oncology : official journal of the American Society of Clinical Oncology,* **27**(9), pp. 1462-1469.

125. STEELE, R.W., MARMER, D.J., O'BRIEN, M.D., TYSON, S.T. and STEELE, C.R., 1986. Leukocyte survival in cerebrospinal fluid. *Journal of clinical microbiology,* **23**(5), pp. 965-966.

126. GREIG, B., STETLER-STEVENSON, M. and LEA, J., 2014. Stabilization media increases recovery in paucicellular cerebrospinal fluid specimens submitted for flow cytometry testing. *Cytometry Part B: Clinical Cytometry,* **86**(2), pp. 135-138.

127. BARNETT, D., GRANGER, V., MAYR, P., FAY, S. and REILLY, J., 1995. Preparation and stabilisation of cells. *Patent No.WO,* **95**, pp. 01796.

128. BENTO, L.C., CORREIA, R.P., ALEXANDRE, A.M., NOSAWA, S.T., PEDRO, E.D.C., VAZ, A.D.C., SCHIMIDELL, D., FERNANDES, G.B.P., DUARTE, C.A.S. and BARROSO, R.D.S., 2018. Detection of central nervous system infiltration by Myeloid and lymphoid hematologic neoplasms Using Flow cytometry analysis: Diagnostic accuracy study. *Frontiers in medicine,* **5**, pp. 70.

129. PAULE, R., DENIS, L., CHAPUIS, N., ROHMER, J., HADJADJ, J., LONDON, J., CHAUVIN, A., BONNET, C., MOUTHON, L. and LE JEUNNE, C., 2021. Lymphocyte immunophenotyping and CD4/CD8 ratio in cerebrospinal fluid for the diagnosis of sarcoidosis-related uveitis. *Ocular immunology and inflammation,* **29**(2), pp. 290-298.

130. DE JONGSTE, A.H., KRAAN, J., VAN DEN BROEK, PATRICIA D, BROOIMANS, R.A., BROMBERG, J.E., VAN MONTFORT, K.A., SMITT, P.A.S. and GRATAMA, J.W., 2014. Use of TransFix™ cerebrospinal fluid storage tubes prevents cellular loss and enhances flow cytometric detection of malignant hematological cells after 18 hours of storage. *Cytometry Part B: Clinical Cytometry,* **86**(4), pp. 272-279.

131. WEINBERG, A., SONG, L., WILKENING, C., SEVIN, A., BLAIS, B., LOUZAO, R., STEIN, D., DEFECHEREUX, P., DURAND, D. and RIEDEL, E., 2009. Optimization and limitations of use of cryopreserved peripheral blood mononuclear cells for functional and phenotypic T-cell characterization. *Clinical and Vaccine Immunology,* **16**(8), pp. 1176-1186.

132. TOMPA, A., NILSSON-BOWERS, A. and FARESJO, M., 2018. Subsets of CD4(+), CD8(+), and CD25(hi) Lymphocytes Are in General Not Influenced by Isolation and Long-

Term Cryopreservation. *Journal of immunology (Baltimore, Md.: 1950),* **201**(6), pp. 1799-1809.

133. COSSARIZZA, A., CHANG, H., RADBRUCH, A., ACS, A., ADAM, D., ADAM-KLAGES, S., AGACE, W.W., AGHAEEPOUR, N., AKDIS, M. and ALLEZ, M., 2019. Guidelines for the use of flow cytometry and cell sorting in immunological studies. *European journal of immunology,* **49**(10), pp. 1457-1973.

134. WHITTAKER, E., NICOL, M., ZAR, H.J. and KAMPMANN, B., 2017. Regulatory T cells and pro-inflammatory responses predominate in children with tuberculosis. *Frontiers in immunology,* **8**, pp. 448.

135. MEIER, L., CARLSON, R., NESSLER, J. and TIPOLD, A., 2020. Stability of canine and feline cerebrospinal fluid samples regarding total cell count and cell populations stored in "TransFix®/EDTA CSF sample storage tubes". *BMC veterinary research,* **16**(1), pp. 1-12.

136. SHANKEY, T.V., FORMAN, M., SCIBELLI, P., COBB, J., SMITH, C.M., MILLS, R., HOLDAWAY, K., BERNAL-HOYOS, E., VAN DER HEIDEN, M. and POPMA, J., 2006. An optimized whole blood method for flow cytometric measurement of ZAP-70 protein expression in chronic lymphocytic leukemia. *Cytometry Part B: Clinical Cytometry: The Journal of the International Society for Analytical Cytology,* **70**(4), pp. 259-269.

137. BARBIERI, J.T., 2009. Exotoxins. In: M. SCHAECHTER, ed, *Encyclopedia of Microbiology (Third Edition).* Oxford: Academic Press, pp. 355-364.

138. LIN, C., CHEN, C., HUANG, W., CHENG, Y., HSIEH, C., WANG, C. and HONG, M., 2010. Different types of cell death induced by enterotoxins. *Toxins,* **2**(8), pp. 2158-2176.

139. BEEMS, T., SIMONS, K., VAN GEEL, W., DE REUS, H., VOS, P. and VERBEEK, M., 2003. Serum-and CSF-concentrations of brain specific proteins in hydrocephalus. *Acta Neurochirurgica,* **145**(1), pp. 37-43.

140. VALIATHAN, R., ASHMAN, M. and ASTHANA, D., 2016. Effects of ageing on the immune system: infants to elderly. *Scandinavian Journal of Immunology,* **83**(4), pp. 255-266.

141. ROHLWINK, U.K., FIGAJI, A., WILKINSON, K.A., HORSWELL, S., SESAY, A.K., DEFFUR, A., ENSLIN, N., SOLOMONS, R., VAN TOORN, R. and ELEY, B., 2019. Tuberculous meningitis in children is characterized by compartmentalized immune responses and neural excitotoxicity. *Nature communications,* **10**(1), pp. 1-8.

142. SOFRONIEW, M.V., 2014. Astrogliosis. *Cold Spring Harbor perspectives in biology,* **7**(2), pp. a020420.

143. ROHLWINK, U.K., DONALD, K., GAVINE, B., PADAYACHY, L., WILMSHURST, J.M., FIEGGEN, G.A. and FIGAJI, A.A., 2016. Clinical characteristics and neurodevelopmental outcomes of children with tuberculous meningitis and hydrocephalus. *Developmental medicine and child neurology,* **58**(5), pp. 461-468.

144. ROSENGREN, L.E., WIKKELSØ, C. and HAGBERG, L., 1994. A sensitive ELISA for glial fibrillary acidic protein: application in CSF of adults. *Journal of neuroscience methods*, **51**(2), pp. 197-204.